Molecular diagnosis and pathogenesis of Marfan syndrome and related heritable diseases associated with thoracic aortic aneurysms and dissections

Von der Naturwissenschaftlichen Fakultät der Gottfried

Wilhelm Leibniz Universität

Hannover

zur Erlangung des Grades

Doktorin der Naturwissenschaften,

Dr.rer.nat

genehmigte Dissertation

von

M.Sc. Ushanthine Kathiravel

geboren am 24.08.1982 in Sri-Lanka

2014

Declaration

I hereby declare that this submission is my own work and to the best of my knowledge and belief, the work contains no materials that has been previously published or written by another person nor material which to a substantial extent has been accepted for the award of any other degree or diploma of this university or other institution of higher degree, except where due acknowledgement has been made in the text. This work has been conducted in the institution of Human Genetics, Medical School of Hannover, in the time from 30.09.2008 to 31.08.2012 and my doctorate supervisor was Prof. Dr. Manfred Stuhrmann.

Hannover, the

(Ushanthine Kathiravel)

Main Referee: Prof. Dr. Manfred Stuhrmann, Institute for Human genetics, Medical school of Hannover, Hannover

Co-referee 1: Prof. Dr. Hans-Jörg Jacobsen, Institution of Genetics of Plants and Plant Technology, University of Gottfried Wilhelm Leibniz, Hannover

Co-referee 2: Prof. Dr. Michael Klintschar, Institution of Legal Medicine, Medical School of Hannover, Hannover

Dedication

This dissertation is dedicated to individuals who are suffering from Marfan syndrome and Marfan-related syndromic and non-syndromic cardiovascular diseases. Many thanks go to living patients with MFS for their volunteering in this study and for allowing us to perform an extensive molecular study in order to improve our understanding on the molecular pathogenesis in MFS and MFS-related diseases and to establish a new molecular sequencing platform, the "MFSTAAD" resequencing array.

Acknowledgement

Foremost, I would like to express my sincere gratitude to my advisor Prof. Dr. Manfred Stuhrmann for his continuous support during my Ph.D study and research, for his patience, motivation, enthusiasm, and immense knowledge in this field. I have learned a lot from him. His guidance and his presence helped in all the time of research and writing of my thesis work. I could not have imagined of having a better advisor and mentor for my Ph.D study. Thank you very much Prof. Manfred Stuhrmann!

Besides my mentor, I would like to thank Prof. Jörg Schmidtke for his financial support and to have allowed me to perform my Ph.D thesis in his institution. Thank you Prof. Jörg Schmidtke!

Further thanks go to Dr. Stephan Waldmüller and Dr. Britta Keyser for their encouragement, insightful comments, for sharing their opinions and experience as scientist with me and for answering my continuous questions!

I would also like to thank all my fellow lab mates and co-workers from the institution of Human Genetics including PD. Dr. Stefanie Schubert, Madeleine Mälzer, Anke Hein, Tatjana Hellwig, from the institution of Cellular and Molecular pathology such as PD. Dr. Doris Steinmann, from CorTag, Dortmund including Melanie Müller and from the institution for Human Genetics, Tübingen such as Dr. Michael Bonin and Sven Poths for their technical support on microarray. Also I would like to thank my colleagues and friends, Edda Kramer, Anna Arnold and Madeleine Mälzer, Anke Hein, and Tatjana Hellwig and the people from my Christian community.

Last but not least, I would like to thank my family, especially my mother for giving me this life and for giving me my priority to decide my own way in this country and for her support throughout my life, even under the condition of different cultures and expectations. And also my gratefulness goes to my doggy, Jezzy, even if she does not understand, but she has given me so much emotional strength to cope with stressful days.

Abstract

Marfan syndrome (MFS) is a systemic genetic disorder of the connective tissue that is inherited as an autosomal dominant trait with major manifestations in the ocular, skeletal and cardiovascular systems. The disease is caused by mutations in the fibrillin-1 (*FBN1*) gene which encodes a major extracellular matrix glycoprotein. Thoracic aortic aneurysms and dissections (TAAD) are the main cardiovascular feature in MFS that are associated with increasing mortality rate. Several other syndromic and non-syndromic overlapping diseases of MFS exists, including Loeys-Dietz syndrome (LDS), vascular type of Ehlers-Danlos syndrome (vEDS), arterial tortuosity syndrome (ATS) and bicuspid aortic valve (BAV) disease where the diagnosis is generally, successfully made using the current Ghent nosology criteria, but about 19% of the TAAD cases have a non-syndromic, *__familial__* TAAD (FTAAD). In worst case these subjects are diagnosed only in the medico-legal autopsies as they do not show outward phenotypic abnormality. Thus, a genetic test would be of benefit to improve the life quality of these subjects and to find close-relatives who may be at-risk of FTAAD. Until date, several genes are described to cause syndromic and non-syndromic TAAD, though an appropriate genetic test for their parallel testing is not yet available. Herein, we describe the novel 117-kb "MFSTAAD" with a custom duplicate resequencing assay that allows the coverage of all the exonic regions of eight candidate genes that are described in association with TAAD; *FBN1*, *TGFBR1*, *TGFBR2*, *COL3A1*, *MYH11*, *ACTA2*, *SLC2A10* and *NOTCH1*. GSEQ and SeqC software were used for data analysis. The analytical sensitivity of the assay was validated by the recognition of 182 known mutations (153 point mutations, 21 deletions, 7 insertions and 1 duplication) and a series of 66 unrelated individuals have been selected to determine the mutation yield, whereby 36 have been previously negative for mutations in the genes *FBN1*, *TGFBR2* and a subset of 18 have been negative for an additional gene *TGFBR1* using conventional Sanger sequencing reaction. The assay showed significantly higher

sensitivity for point mutations (100%) and the largest deletion of 16 bp was detectable through a decline in the hybridization strength. The overall analytical sensitivity was 85%. Mutation testing of 66 unrelated TAAD patients revealed 8 known and 13 possibly pathogenic mutations with a mutation yield of 33%. The MFSTAAD chip is an alternative tool to next generation sequencing that allows parallel analysis of several genes on a single platform. Refinements in the probe design and data analysis software will increase the analytical sensitivity of insertions and deletions making this assay even more applicable for clinical testing. Till date, follow up sequencing methodologies are performed to rule out large sequence alterations in patients negative for mutations using MFSTAAD resequencing assay such as MLPA, a-CGH followed by conventional Sanger sequencing technology. A total of three deletions in the *FBN1* gene were found, a-CGH followed by PCR and bidirectional Sanger sequencing enabled the characterization of the extension of each deletion and the exact deletion breakpoints. Deletions included two large deletions: a 674.351 bp size deletion comprising of the complete *FBN1* gene, and a total of five contiguous genes (*DUT*, *SLC12A1*, *CTXN2*, *MYEF2* and *SLC24A5*) which were located 3' of the *FBN1* gene and a 256.593 bp size deletion consisting of exons 6 to 65 of the *FBN1* gene and the contiguous *DUT* gene, and a small deletion of 9.134 bp consisting of 147 bp of exon 64, intron 64 and the complete exon 65 and 3'UTR of the *FBN1* gene and 7.484 bp of 3' contiguous genomic sequence could be detected. Both, the novel "MFSTAAD" and follow-up analysis with MLPA have been good combination for the detection of all type of mutation described in TAAD. Additionally, an indirect genetic analysis was performed using polymorphic DNA markers for TAAD (*AAT2* on chromosome 5q 13-14; *AAT1* marker on chromosome 11q23.2-24, *TAAD3*/BAV marker on chromosome 15q24-26 and *TAAD*/PDA, *MYH11* on chromosome 16p12.12-13.13 and *TAAD4*, *ACTA2* locus on chromosome 10q22-24) in two families who were negative for mutations using both aforementioned screening methods, but had a positive history for familial TAAD. No correlation was found in family 1. Whereby, a correlation to

Abstract

TAAD3/BAV marker and disease running in family 2 was found, but the disease gene for this marker remains still to be detected. On behalf of this thesis, specific histopathological medial alterations such as cystic medial necrosis (CMN) and elastin fragmentation (EF) in subjects with localized TAAD and age have been tested whether these factors were suggestive for a genetic predisposition to syndromic or familial TAAD. The correlation between both CMN and EF (value of ≥2) and age, independent from each other, versus mutation yield have been tested in a total of 18 decedents who have died of sudden and unexplained TAAD. No significant correlation was found between ≥2 alterations for CMN and EF versus patients with a mutation (p value 0.44). However, a relationship between TAAD occurring at young age (≤55.5 years of age) versus genetic changes could be observed, but the correlation was not significant (p value of 0.15). In summary, this study shows that "MFSTAAD" in combination with MLPA and indirect family segregation study will widen our understanding in the pathogenesis of TAAD and will definitely provide a rapid and accurate diagnosis, especially for patients who are at-risk for TAAD, but do not fulfil the clinical criteria for syndromic forms of TAAD, but show a familial segregation of TAAD. Even, when genetic testing cannot diagnose patients died of sudden TAAD, still close relatives could be helped with this approach, reducing the mortality rate associated with TAAD and improves their quality of life.

Keywords: Marfan syndrome, Thoracic aortic aneurysms and dissections, *FBN1* gene

Zusammenfassung

Marfan-Syndrom (MFS) ist eine ganz-körper betroffende Erkrankung des generelisierten Bindegewebes, bei dem es sich um eine autosomal-dominante Vererbung handelt. Klinische Ausprägungen im Okular, Skelett und kardiovaskuläre System sind bekannt. Die Erkrankung wird durch Mutationen im Fibrillin-1 (*FBN1*) Gen verursacht, das sich im Genort 15q.21.1 befindet. Dieses Gen kodiert für ein extrazelluläres Glykoprotein, dass ubiquitär exprimiert wird. Das Fibrillin- 1 Protein, polymerisiert sich in Mikrofibrillen, welches ein wichtiges Komponent des elastischen und nicht-elastischen Bindegewebes ist. Hohe Mortalitätsrate bei MFS Patienten ist primär assoziert mit der thorakalen Aorten Aneurysma und Dissektion (TAAD). Etliche syndromische und nicht-syndromische Marfan-ähnliche Form existieren, dazu gehört das Loeys-Dietz Syndrom (LDS), der vaskuläre Ehlers-Danlos Syndrom (vEDS) Typ, das Arterial- Tortuosity-Syndrom, genetische Ausprägung der bikuspidalen Aortenklappe, wobei die einzelne Fälle gemäß der Genter Nosologie erfolgreich diagnostiziert werden können. Es wird nur zu einem Problemfall, wenn Patienten keinerlei äußerliche klinische Ausprägungen aufweisen, sie werden nur diagnostiziert, wenn eine lebens- bedrohende TAAD auftretet. Ungefähr 19% dieser Patienten haben mehrere erst-gradige Familienmitglieder, die ähnliche nicht-syndromische TAAD aufweisen, diese Patienten haben ein familiäres TAAD, bei dem die Erkrankung auch autosomal-dominant vererbt wird. Diese Studie sieht es als ein Vorteil genetische Untersuchungen auch bei unsicheren Fällen durchzuführen unabhängig von dem Ergebnis der Genter Nosologie. Bis zum Zeitpunkt der Studie waren acht Gene bekannt die Mutationen tragen, die Ursache eines syndromisches und nicht-syndromisches Marfan-ähnliches Syndrom zurück zu führen sind. Jedoch zur Zeit wird im genetischen Labor, Sanger Sequenzierung einzelner Gene durchgeführt, jenes sehr zeit- und kostenaufwendig ist. Hier in dieser Studie, beschreiben wir „die 117-kb MFSTAAD" Resequenzierungsplatform, welches erlaubt alle kodierende Segmente von acht TAAD Genen

(*FBN1*, *TGFBR1*, *TGFBR2*, *COL3A1*, *MYH11*, *ACTA2*, *SLC2A10* und *NOTCH1*) parallel auf einem Platform zu analysieren. Die analytische Sensitivität des Assays wurde durch die richtige Detektion von 182 bekannte Mutationen (152 Punkt Mutationen, 21 Deletionen, 7 Insertionen und 1 Duplikation) und die Mutationsausbeute wurde bei einer Reihe von 66 nicht-verwandte Individuen untersucht, wobei 36 von den 66 Patienten wurden bereits auf die Gene *FBN1* und *TGFBR2*, und 18 von den 36 Patienten auf ein weiteres Gen *TGFBR1* mit dem koventionellen Sanger Sequenzierung in der Routine Diagnostik untersucht und waren negativ. Dieses Assay zeigte eine sehr hohe Sensitivität für Punkt Mutationen (100%) und die größte 16-bp Deletion wurde aufgrund eines stark abfallende Hybridisierungslinie detektiert. Im Großen und Ganzen hat dieses MFSTAAD Sequenzierungsplatform eine analytische Sensitivität von 85%. Mutation Analyse bei den 66 Patienten konnte 8 bereits bekannte und 13 neue Mutationen aufgedeckt werden, was eine insgesamte Mutationsausbeute von 33% entspricht. Der MFSTAAD Platform ist eine gute alternative zum Next Generation Sequenzierung, der auch ermöglicht mehrere Gene parallel zu untersuchen. Spezielle Verfeinerung im 25-bp Oligonukleotide Design und im Auswertungsprogramm für die Detektion von große Genveränderungen könnte dieser Platform ohne Aufwand in der Routinediagnostik angewendet werden, jedoch zur Zeit ist dies ein Nachteil dieses Assays. In dieser Studie, wurde der MFSTAAD Platform mit zwei nachfolgende genetische Methoden kombiniert, Multiplex-ligation-probe-amplification (MLPA) und eine chipbasierte vergleichender genomischer Hybridisierung (Array-comparative genomic hybridization, a-CGH). Insgesamt wurde mit der MLPA drei Deletionen im *FBN1* Gen gefunden, und a-CGH und eine 3' und 5' gerichtete Polymerase Kettenreaktion wurde durchgeführt, um die exakte Bruchpunkte im *FBN1* Gen zu definieren. Zwei große Deletionen: erste Deletion 674.351 bp groß, jenes das komplette *FBN1* Gen umfasste plus fünf benachbarte Gene (*DUT*, *SLC12A1*, *CTXN2*, *MYEF2* und *SLC24A5*), die sich im 3' Ende auffand und eine zweite Deletion, 256.593 bp lang, die exons 6-65 vom *FBN1* Gen umfasste plus das 3' liegende *DUT* Gen und

eine kleine Deletion, die 9.134 bp lang ist, die 147 bp vom Exon 64, Intron 64 und das komplette Exon 65 und 3'UTR vom *FBN1* Gen und 7.484 bp vom 3' Region des *FBN1* Gens umfasste. Eine kombinierte Analyse mit dem neuen MFSTAAD Platform und MLPA und a-CGH, erlaubte alle Mutationstypen in TAAD abzudecken. Als weitere genetische Untersuchung, wurde ein indirekter Gentest bei zwei nicht-verwandte Familien durchgeführt mit der Benutzung von kurze, nicht-kodierende DNA Markern die mit der TAAD Erkrankung (*AAT2*, 5q13-14; *AAT1*, 11q23.2-24; *TAAD3*/*BAV*, 15q24-26; *MYH11*, 16p12.12-13-13 und *ACTA2*, 10q22-24) assoziiert waren. In Familie 1 wurde keine Korrelation zwischen den oben-erwähnten TAAD Markern und der Erkrankung, die die Ursache in Familie 1 ist, festgestellt werden. Eine positive Korrelation zwischen TAAD3/BAV und die genetische Erkrankung in Familie 2 wurde gefunden, aber das Gen für diesem Marker bleibt bis heute unbekannt. Im weitere Interesse der Studie, wurden charakteristische histopathologische Merkmale wie z.B. Zystische Medial Necrosis (ZMN) und Elastin Fragmentation (EF) und das Alter als distinktive Merkmale für TAAD untersucht. Eine Korrelationsstudie zwischen ZMN und EF (Veränderungswert ≥ 2) und Mutationsausbeute wurde in 18 verstorbene Patienten durchgeführt, und eine statistisch signifikante Korrelation konnte zwischen diesen beiden Gruppen nicht festgelegt werden (p-Wert von 0.44). Jedoch ein Zusammenhang zwischen dem Alter (≤ 55.5 Jahren) und der Mutationsausbeute war zu sehen, aber war statisch nicht signifikant (p-Wert von 0.15). Im Großen und Ganzen kennzeichnet diese Studie, dass eine kombinierte genetische Analyse (MFSTAAD plus MLPA, a-CGH und indirekter Gentest) unser Verständnis über die Pathogenese der komplexen Erkrankung der TAAD erweitert. Eine genetische Untersuchung bzw. Beratung ist vorallem vorteilhaft, bei Patienten die nicht die klinische Bedingung der Genter Nosologie erfüllen und außerlich keine charakteristischen Merkmale eines oben-erwähnten Syndroms aufweisen, jedoch mehrere erst-gradige Familienmitglieder haben, die eine hohe Wahrscheinlichkeit für eine lebens-bedrohliche TAAD prädisposiniert sein können.

Zusammenfassung

Schlagwörter: Marfan Syndrom, Aorten Aneurysma und Dissektion, *FBN1* Gen.

Table of Contents

Table of contents

Abbreviations

%	Percentage
μg	microgram
μL	micro litre
μM	micro molar
μs	microseconds
6-FAM	6-carboxyfluorescein
A	Absorbance
AAD	Aortic Aneurysms and Dissections
AB	Alcian Blue stain
ABACUS	Adaptive Background Genotype Calling Scheme
ACTA2	actin, alpha 2, smooth muscle, aorta
AGCC	Affymetrix GeneChip Command Console
ATS	Arterial Tortuosity Syndrome
BAV	Bicuspid Aortic Valve
BAVD	Bicuspid Aortic Valve Disease
BMAP	Biometric Mutation Analysis Programs
bp	base pair
BSA	Bovine Serum Albumin
c.	codon
cb-	calcium binding
CCD	Charged Coupled Device
CMN	Cystic Medial Necrosis

1

COL3A1	collagen, type III, alpha 1
Cy-	Cyanine
D.r.	Dario rerio
dATP	deoxyadenosine triphosphates
dCTP	deoxycytosine triphosphates
dd-	dideoxy-
dGTP	deoxyguanine triphosphates
DHPLC	Denaturing High Performance Liquid Chromatography
DMSO	Dimethyl sulfoxide
dNTPs	deoxynucleotriphosphates
dsDNA	double stranded Deoxyribonucleic Acid
dTTP	deoxythymine triphosphates
DUT	Deoxyuridine Triphosphatase
ECG	Electrocardiogram
ECM	Extracellular Matrix
EDS	Ehlers Danlos Syndrome
EDTA	Ethylenediaminetetraacetic acid
EF	Elastin Fragmentation
EGF-like	Epidermal growth factor
EtBr	Ethidium Bromide
EVG	Elastic Tissue Fibres-Verhoeff's Van Gieson stain
F	forward
F.c.	Felis catus

FBN1	fibrillin-1
FruitFly	FF
FTAAD	Familial Thoracic Aortic Aneurysms and Dissections
g	gram
G.g.	Gallus gallus
G/S	Glycine/serine
gDNA	genomic DNA
H&E	Hematoxylin and Eosin stain
H.s.	Homo sapiens
HCL	Hydrochloric acid
HGMD	Human Gene Mutation Database
HPLC	High Performance Liquid Chromatography water
kb	kilo base
kDa	kilo Dalton
kV	kilovolts
LAP	Latency associated polypeptide
LDS	Loeys Dietz syndrome
LT BP	Latent TGF-beta binding protein
M	Molar
M.m.	Mus mulatta
M.m.*	Mus musculus
MASS	Mitral valve prolapse, Aortic enlargement, Skin and Skeletal findings syndrome

MB	Megabites
MES	Morpholine-4-ethanesulfonic acid
MFS	Marfan syndrome
Mg_2Cl	Magnesium Chloride
mL	millilitre
MLPA	Multiplex-dependent probe amplification
MMP	Matrix Metalloproteinases
mRNA	messenger RNA
MT	Mutation Taster
MYH11	myosin, heavy chain 11
n-	Neonatal-
Na_2HPO_4	Sodium Phosphate
NaCl	Sodium Chloride
NCBI	National Centre for Biotechnology Information
NetGene 2	NG2
nm	nanometer
NOTCH1	notch-1
-OH	Hydroxyl group
p.	protein
P.t.	Pan troglodytes
PCR	Polymerase Chain Reaction
PD	Prospective Decedent
PDC	Possibly Disease Causing mutation

PL	Prospective Living patient
PM	pMut
PP	PolyPhen
PP2	PolyPhen 2
PTC	Premature Termination Codon
R	reverse
RL	Retrospective Living patient
SAPE	Streptavidin R-phycoerythrin conjugate
SDS-PAGE	Sodium Dodecyl Sulfate Polyacrylamide Gel Electrophoresis
SGS	Shprintzen-Goldberg craniosynthosis syndrome
SLC2A10	Solute Carrier family 2, alpha Actin member 10
SMAD3	Mothers against decapentaplegic homolog 3
SNP	Single Nucleotide Polymorphisms
ssRNA	Single Stranded Ribonucleic acid
STR	Small Tandem Repeats
TAA	Thoracic Aortic Aneurysm
TAAD	Thoracic Aortic aneurysm and dissection
Taq	*Thermus aquaticus*
TBE	Tris-Borate-EDTA buffer
TBE-PAGE	Tris-Borate-EDTA Polyacrylamide Gel Electrophoresis
TE	Tris-EDTA Buffer
TGFBR	transforming growth factor beta receptor
TMAC	Tetramethylammonium chloride solution

Tris   Trishydroxyethylamin

U   Units

UMD   Universal Mutation Database

UV   Ultra Violet

v-   vascular EDS

V   Volts

VNTR   Variable Number of Tandem Repeats

VSMCs   Vascular Smooth Muscle Cells

WMS   Weill-Marchesani syndrome

List of Figures

List of Tables

1. *Introduction*

1.1   **Marfan syndrome**

Marfan syndrome (MFS, MIM 154700) is a multisystem genetic disorder of the connective tissue, with major involvement of the cardiovascular, ocular and skeletal systems and minor involvement of the skin and integument, lung and dura mater. The disorder was first described in 1896 by a French paediatrician, Antoine-Bernard Marfan. He described a 5 year old girl with apparent skeletal manifestation which he termed as hereditary disorder of the connective tissue (Marfan 1896; Loeys *et al*., 2010). The estimated prevalence of MFS is about 1 in 10.000 with no difference among gender, ethnic and race (Pearson 2008; Faivre *et al*., 2007). The disease shows variable intra- and interfamilial phenotypic expression (Judge & Dietz, 2005; William, *et al*, 2008; Ammash, *et al*, 2008). A clear familial cause of MFS has been described in about 75% of MFS cases (Yetman *et al.*, 2003; Yuan & Jing, 2010), and the remaining 25% are sporadic (Keane & Pyeritz, 2008), caused by *de novo* mutations.

1.1.1   **Clinical characteristics of Marfan syndrome**

Patients with MFS are born with this condition, but the disease might not be diagnosed until later in life. Ocular sign include myopia, which is the most common ocular feature, and about 60% of MFS patients manifest with ectopia lentis (EL, Figure 1-1, 1), which is the displacement of the lens from the centre of the pupil and are generally bilateral. These individuals are at highest risk of retinal detachment, glaucoma and early cataract formation. Skeletal manifestations are the predominant cardinal signs of MFS that gain the attention of a physician. The most obvious sign is the tall stature by which the lower segment of the body is greater than the upper segment, thin body habitus with an increase in the arm-span to height, which is fairly equal in the general population. Other obvious signs include joint hyper mobility with long, slender limbs known as dolichostenomelia and long, slender digits, termed as arachnodactyly. Both joint hyper mobility and long fingers allow the patient to fulfil two specific clinic criteria for MFS, such as the Steinberg thumb sign (Figure 1-1, 2), by which the entire thumb nail can protrude beyond the other side of the palm and the positive Walker-Murdoch sign (Figure 1-1, 3), where the thumb and the fifth finger can overlap around the wrist. Furthermore, deformities of the chest caused by overgrowth of the ribs causing the chest to be pushed inwards, pectus excavatum (PE, Figure 1-1, 4) or outwards, pectus carinatum (PC, Figure 1-1, 5), and abnormal curving of the spine known as scoliosis (Yuan & Jing, 2010; Tsipouras & Silverman, 1999) are also frequently described in MFS. Features that are less common include flat foot (pes planus), long and narrow face, flat cheek

bones, and arched palate with crowded teeth. Cardiovascular symptoms are the most serious complications associated with morbidity and early mortality in MFS. Abnormalities include dilatation/aneurysm and dissection at the level of sinus of valsalva of the major aorta. The condition becomes fatal when the aneurysm reach an aortic diameter of >5cm (Karnath & Rangasetty, 2006) which may lead to dissection or rupture at the site of aortic aneurysm. The onset and progression of aortic disease is highly variable, but generally the severeness increase with age, but it is not uncommon in children (Sisk *et al*., 1983; Grimes *et al.,* 2004). Mitral valve prolapse with/without regurgitation can also occur (Brown, *et al*., 1975).

1   2   3

4   5
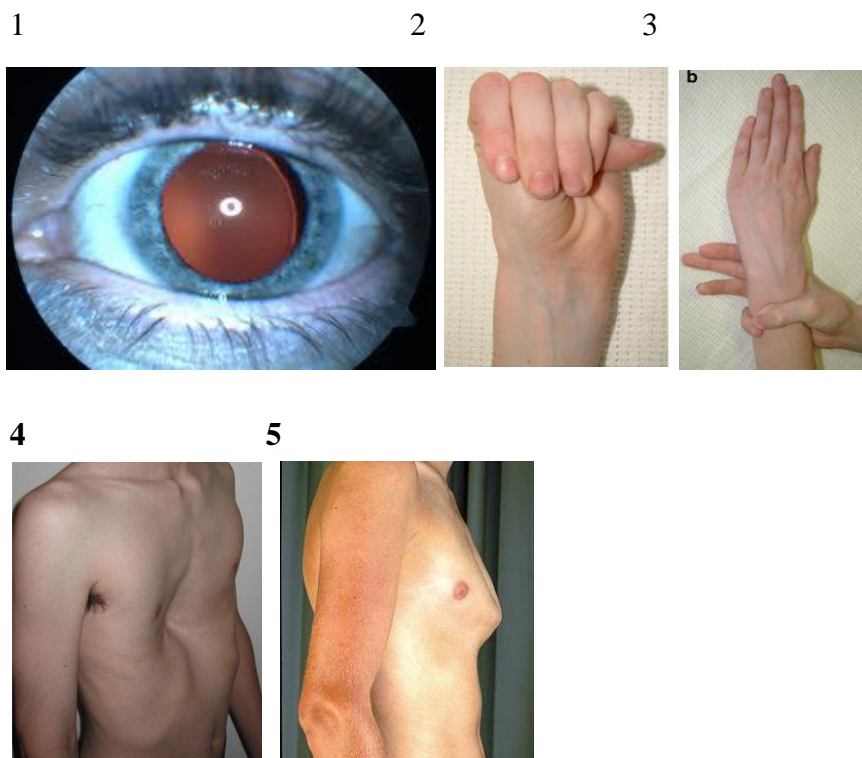
Figure 1-1: Clinic characteristics of Marfan syndrome. 1, Ectopia lentis. 2, The positive Steinberg thumb sign. 3, The positive Walker Murdoch wrist sign. 4, Pectus excavatum. 5, Pectus carinatum.
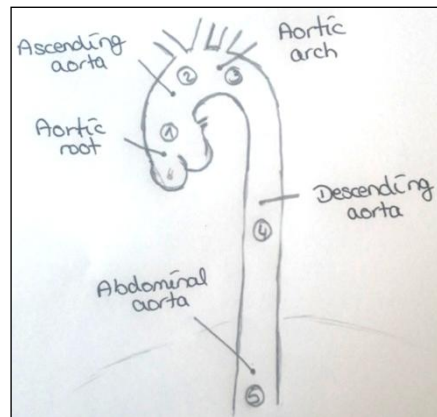
Figure 1-2: **Anatomy of the major aorta.** 1, Aortic root 2, Ascending aorta 3, Aortic arch 4, Descending aorta 5, Abdominal aorta.

1.1.2 Classification of aortic aneurysms and dissections

Aneurysms and dissections (AADs) are major diseases of the aorta and their severity are clinically classified in terms of their anatomical location using the DeBakey system (DeBakey *et al*, 1965) and Stanford classification (Daily *et al*, 1970). The DeBakey system defines the anatomical location of the primary intimal tear or where the dissection has initially occurred (Type I, II, III-Figure 1-3). Type I aortic intimal tear generally locates in the aortic root and intervenes into ascending aorta and aortic arch, and propagates further to the distally located descending aorta. This kind of dissections occur mainly in younger individuals (<65 years of age) (DeBakey *et al*, 1965). Type II dissections originate and remains in the ascending aorta and type III aortic dissections locate in the descending aorta, which rarely extend proximally, but can extend distally, this type of dissection are reported in elderly people who suffer from atherosclerosis or hypertension (DeBakey *et al*, 1965). Sixty-percent of patients with aortic dissections present with Type I dissections (aortic root, ascending aorta, aortic arch and descending aorta), about 10-15% present with type II dissections of the aorta (ascending aorta) and 25-30% have dissections of the descending aorta, type III aortic dissections (Figure 1-2). The Stanford classification (type A and type B- Figure 1-3) are used in the clinical practice to determine whether dissection of the ascending aorta is involved or not, since ascending aortic dissections generally require surgical interventions (DeBakey System I and II), whereby dissections of the descending aorta (DeBakey system III) are generally managed with medical treatment (Daily *et al*, 1970). DeBakey type I and II and Stanford type A dissections are the type of AADs described in MFS and Marfan-related connective tissue diseases.
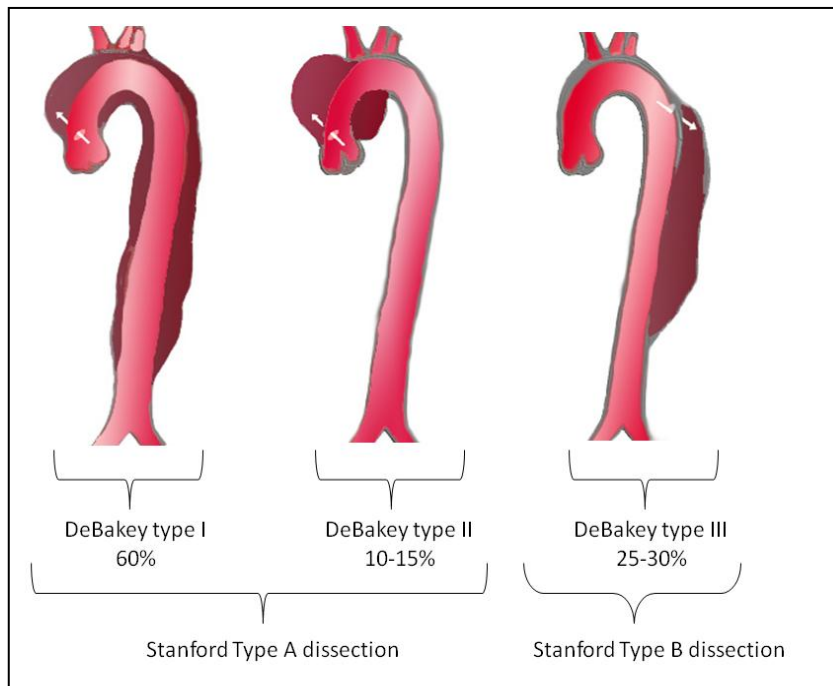
Figure 1-3: **DeBakey system and Stanford classification.** (Information has been derived from Wikipedia (http://en.wikipedia.org/wiki/Aortic_dissection#cite_note-Daily1970-6). The arrow (white) indicates the origin of the intimal tear in the aortic segment. Dark red represent the widening of an aneurysm in the appropriate aortic segment.

1.1.3 Clinical diagnosis of Marfan syndrome

The diagnosis of MFS occurs is based on clinical characteristic of three specific organ systems these include the systems of the cardiovascular, ocular and skeletal organs and the medical history of the patient's family. MFS is a multisystem disorder of the connective tissue, and many of the clinical manifestations of the disease may occur in other heritable diseases. The current revised Ghent nosology criteria (Loeys *et al*, 2010) demonstrates the correct and efficient diagnois of MFS in the clinical setting which is based on the presence of major and minor clinical exhibition of the aforementioned organ systems (Table 1-1), the content in the table was partly adapted from Correlagen Diagnostics, Inc. (https://www.correlagen.com/fields/other/reviews/MFS_CRLGOvw.pdf- Marfan syndrome-an Overview) and from the Review by Canadas V, 2010. Cardinal manifestations include ectopia lentis, aortic root dilatation/dissection, dural ectasia or the presence of at least four skeletal features from the major criteria of MFS. The correct diagnosis of a MFS patient requires major involvement of at least two organ systems with minor involvement of a third organ system. Whereby, in the presence of a mutation in the *FBN1* gene that is known to cause MFS or in the presence of a positive family history for MFS, in such case involvement of one major and one minor clinical characteristic in different organ systems is sufficient to

make a diagnosis. Until date, the Ghent nosology has helped the clinician to diagnose MFS appropriately. Current molecular techniques allow the detection of causative mutations in the *FBN1* gene in 75-93% of MFS patients who meet the Ghent nosology criteria (Loeys *et al*., 2001; Loeys *et al*., 2004). Thus, the diagnostic criteria is highly specific, but the sensitivity of Ghent nosology criteria is rather complex, because the current criteria does not take into account the age-dependent manifestations of some clinical features, making the diagnosis of children more difficult (Faivre *et al*., 2009) and many of the clinical features seen in MFS patients overlap with other MFS-related connective tissue diseases. From the perspective of the differential diagnosis, a more stringent and modification in the current diagnostic criteria is required that implement clinical features of differential diseases of MFS which allow the accurate follow-up, and management guidelines for the various patient groups including children who do not yet meet the clinical criteria but may do in the future (Faivre *et al*., 2009).

Table 1-1 Ghent nosology criteria for Diagnosis of Marfan Syndrome

Minimal requirements of involvement of two major clinical criteria in two organ systems and one minor criteria in a third organ system

Organ system	Major criteria	Minor criteria
Skeletal	at least four of the following clinical presentations: • Pectus carinatum • Pectus excavatum • Reduced upper to lower segment ratio or arm span to height ratio of >1.05 • Wrist and thumb signs • Reduced extension at elbows (>170) • Scoliosis (>20)	at least two manifestations listed under the major criteria, or involvement of one major and two of the following: • Pectus excavatum • Joint hyper mobility • Highly arched palate with crowding of teeth • Facial appearance (dolichocephaly, malar hypoplasia, enophthalamos, retrognathia, down-slanting palpebral fissures)

	• Pes Planus • Protrusio acetabulae	
Ocular	Ectopia lentis	At least two of the following criteria: • Abnormally flat cornea • Increased axial length of the globe • Hypo plastic iris of hypo plastic ciliary muscle, causing decreased miosis
Cardiovascular	At least one of the following: • Dilatation of the ascending aorta involving the sinuses of valsalva • Dissection of the ascending aorta	At least one of the following: • Mitral valve prolapse • Unexplained dilatation of the main pulmonary artery before age of 40 • Calcification of mitral annulus before age of 40 • Dilatation of dissection of descending thoracic or abdominal aorta before age of 50
Nervous	Lumbosacral dural ectasia	
Pulmonary		At least one of the following: • Spontaneous pneumothorax • Apical blebs

Skin and Integument		At least one of the following: • Unexplained striae atrophicae • Recurrent or incisional hernia
Genetics and Family History	At least one of the following: • Mutations in the *FBN1* gene • First degree relative with confirmed diagnosis of MFS	

1.4   Molecular genetics of MFS

MFS is described as an autosomal dominant mendelian disorder characterized by complete penetrance with variable phenotypic expressions within and between families, which means that a person carrying the same mutation do not necessarily present with same clinical features (Judge & Dietz, 2005; William *et al*, 2008; Ammash *et al*, 2008). Classic MFS is generally caused by mutations in the fibrillin-1 (*FBN1*) gene, which is located on the chromosome 15 (15q21.1) (Ammash *et al*, 2008). Fibrillin-1 gene is composed of 65 exons and encodes a large cysteine rich 350kDa structural glycoprotein, a protein that consists of 2871 amino acids. There are three types of fibrillins including fibrillin-1, fibrillin-2, and fibrillin-3. Fibrillin-2 and 3 are highly expressed in embryonic developmental stages, whereby fibrillin-1 is expressed from the gastrula stages throughout the adult life. Both founder proteins of fibrillins share an overall amino acid identity of 61%-69% with fibrillin-1. Fibrillin-1 is found in abundance in the extracellular matrix (ECM) and is important regulators of tissue development and homeostasis. Each fibrillin-1 construct polymerizes with each other to form a complex structure of 10nm-microfibrils. Fibrillin-rich microfibrils are found in a variety of connective tissues which are distributed as elastic (elastic fibres) and as non-elastic microfibrils. These fibrillin-elastic assemblies provide structural rigidity and elasticity to the tissues in combination with another ECM protein, collagen type III (Kielty *et al*., 2002; Ramirez & Dietz, 2007). Five distinct domains and a signal peptide are characteristic for a fibrillin-1 protein (Figure 1-5). The protein is primarily composed of highly repetitive homologous epidermal growth factor (EGF)-like motifs which are found 47

times in fibrillin-1 protein. The EGF-like motifs contain about 45 amino acid residues and are arranged with six highly conserved cysteine residues that together form three disulphide bonds assembled in a specific order (C1-3, 2-4, and 5-6). Forty three of the 47 EGF-like motifs contain conserved calcium-binding sequences which are known as calcium-binding (cbEGF)-like motifs which are homologous to latent transforming growth factor binding protein (LTBP) which binds to TGF-ß protein (Robinson & Booms, 2001). To date, more than 2000 private mutations have been described which are distributed over the entire *FBN1* gene (Keane & Pyeritz, 2008; Ammash *et al*, 2008) which are registered in the UMD-*FBN1* database for MFS and its related heritable diseases. Mutations causing exon skipping have also been described in MFS (Collod-Beroud *et al*., 1998). Premature termination codon (PTC) mutations have been rather described in association with severe skeletal and skin manifestations (Faivre, *et al*., 2007). Boileau *et al*. described a large French family in year 1991, representing with clinical features of both skeletal and cardiovascular system similar to those seen in MFS patients, but none of the family members have met the Ghent nosology criteria. The connective tissue disease in this family was also inherited in an autosomal dominant manner but no mutation in the *FBN1* gene was found (Boileau *et al*., 1993). This condition was referred to as Marfan-like syndrome (Marfan type II, MIM #154705) and the gene harbouring mutations causing Marfan type II syndrome has been later mapped to chromosome 3 (3p24.2-25) (Collod *et al*., 1994). This new disease gene is *TGFBR2* which encode the transforming growth factor beta receptor (TGFBR) type II. TGFBR is a heterodimeric protein composed of type I and II subunits encoded by *TGFBR1* and *TGFBR2* genes, respectively (ten Dijke *et al*., 1996; Wrana *et al*., 1994). Both subunits of the TGF-ß receptor is composed of an extracellular domain, a transmembrane domain and a serine/threonine kinase domain. Another specific domain, a glycine/serine (GS)-rich domain include only for the *TGFBR1*. Signal transduction is initiated through the phosphorylation of the GS domain by the ligand-bound *TGFBR2* (Wieser *et al*., 1995). Mutations in the *TGFBR2* gene have been described in the context of overlapping syndromes of MFS including Marfan type II syndrome, Loeys-Dietz syndrome (LDS) and in FTAAD. Majority of the *TGFBR1* and 2 mutations are missense single nucelotide variants which are generally found in the intracellular kinase domain which affect the receptor signalling. Histologic findings have shown a substantial overactivation of TGF-β (El-Hamamsy & Yacoub, 2009), but the true mechanism of an increased TGF-β signalling remains unclear. TGF-β is a cytokine protein which plays an important role in cell proliferation, differentiation, apoptosis and in maintaining the secretion and function of ECM proteins (Cohen 2003; Derynck *et al*., 2001;

Massague *et al*., 2000). During synthesis, TGF-β, the TGF-β1 form is released into the ECM where it is kept into its inactive state by a large complex protein known as latency-associated polypepetide (LAP) and latent TGF-β binding protein (LTBP) and microfibrils that are found in the ECM (El-Hamamsy & Yacoub, 2009; Gelb 2006; Chaudhri 2007). Once a stimulus is received, proteases release TGF-β1 from the protein complex, enabling its binding to their TGF-β receptors, initiating the process of signal transduction (El-Hamamsy & Yacoub, 2009). Due to the fact that microfibrils are made of fibrillin-1, and hence fibrillin-1 acts as a stabilizer of inactive TGF-β1-LTBP complex in the ECM, this could explain the relationship between abnormal TGF-β signalling and molecular pathogenesis of MFS and severe phenotypes seen in MFS. Since reduced or mutated form of fibrillin-1 may lead to failure of ECM sequestration of the TGF-β1-LTBP complex, leading to excessive TGF-β activation and signalling (El-Hamamsy & Yacoub, 2009). Interestingly, TGF-β missense mutations may manifest with loss of function and overactivation of TGF-β signalling as seen in MFS type II (Mizuguchi *et al*., 2004), LDS and TAAD, another overlapping disease of MFS. For instance, perturbation of the highly conserved amino acid residue at position 460 of TGFBR2 protein, a residue described to be important for structural integrity of the catalytic loop of the *TGFBR2* have been associated with loss-of-function of TGF-ß receptor 2 (Pannu *et al*., 2005), by contrast heterozygous mutations in LDS show an overactivation of the TGF-β signalling, thus bioavailability of one normal allele and one abnormal allele of *TGFBR2* does not necessarily reflect the loss-of-function nature, it has been predicted that the overactivation may be a results of overactivation of wild-tpye TGF-ß receptor 2 to compensate for the loss of mutant allele (Loeys *et al*., 2005).

1.2   Differential Diagnosis

Some of the features and manifestations described in MFS are shared with several other diseases of the connective tissue (Table 1-2). Mutations in the *FBN1* gene are also described in other genetic disorders which share distinct features of MFS which are termed as fibrillinopathies. The explicit overlap of their clinical features and in some extent the progressive nature of their manifestations, mainly the progressive dilatation of the aorta, render differential diagnosis a challenge, and a follow-up investigation and re-evaluation should be highly considered. Information on the main characteristic features of the different Marfan-related syndromes which should be taken into consideration during the differential diagnosis of MFS is summarized in Table 2 (Canadas *et al*., 2010) and in Table 1 (Loeys *et al*., 2010). There are several other disease conditions (non-fibrillinopathies) that also share

overlapping clinical features with MSF where symptoms of all three organ systems (ocular, skeletal and cardiovascular system) and where defects in other genes are described. These include Loeys-Dietz syndrome (LDS), Bicuspid aortic valve (BAV) disease, familial thoracic aortic aneurysm and dissection (FTAAD), vascular form of Ehlers-Danlos syndrome (vEDS), arterial toruosity syndrome (ATS), ectopia lentis syndrome (ELS), Weil-Marchesani syndrome (WMS), Shprintzen-Goldberg syndrome, congenital contractural arachnodactyly, myopia, mitral valve prolapse, aortic root dilatation, skeletal and striae (MASS) disease and mitral valve prolapse syndrome (MVPS).

Table 1-2 Differential diagnosis of Marfan syndrome

Hereditary connective tissue disorders	**Gene**
Fibrillinopathies	
• MASS phenotype	• **FBN1**
• Ectopia lentis syndrome	• **FBN1, LTBP2, ADAMTSL4**
• Weil-Marchesani syndrome	• **FBN1, ADAMTS10**
• Congenital contractual arachnodactyly	• **FBN2**
• Shprintzen-Goldberg syndrome	• **FBN1**
Non-fibrillinopathies	
• Ehlers-Danlos syndrome vascular type	• **COL3A1**
• Loeys-Dietz syndrome	• **TGFBR1/2**
• Arterial tortuosity syndrome	• **SLC2A10**
Non-syndromic familial aortic aneurysms	
• Bicuspid aortic valve disease	• **NOTCH1**
• Familial aortic aneurysms and dissection	• **FBN1, ACTA2, MYH11, TGFBR1/2, AAT1, AAT2, TAAD/BAV**

1.2.1 Loeys-Dietz syndrome

Loeys-Dietz syndrome (LDS) is an autosomal dominant disorder caused by mutations in the genes encoding two subunits 1 and 2 of the transforming growth factor beta receptor (*TGFBR1* and *TGFBR2*). The disease is clinically characterized by hypertelorism (wide

spaced eyes), bifid uvula/cleft palate, and/or arterial tortuosity with aortic aneurysm and/or dissection (AAD) (Loeys *et al*., 2005). Symptoms that distinguish LDS from MFS are craniosynostosis, Chiari malformation, clubfoot deformity, congenital heart disease, cervical spine instability, easy bruising and translucent skin. Importantly, the natural history of LDS patients is significantly worse in respect of cardiovascular complications than those with MFS or vEDS. In LDS, AAD often occur at younger age (mean age of 27 years) or at smaller dimensions (Judge *et al*., 2004). The progression of the vascular lesions is more widespread and not only confined to the major aorta (Finkbohner *et al*., 1995; Nollen *et al*., 2004). Other major cardiac symptoms include patent ductus arteriosus (PDA), BAV, mitral valve prolapse and atrial septal defect occurring at higher frequency than normal. Similar to MFS the disease expression can be highly variable within and between families. Abnormal long bone overgrowth is not always seen in LDS patients, although arachnodactyly may be observed which clinically overlap with MFS, in this case a molecular testing should be strongly considered for differentiation between these two disease groups. Patients who are positive for *TGFBR1/2* mutations, but do not exhibit clinical features of LDS are designated as LDS2, and are thought to have a more aggressive vascular disease (Loeys *et al*., 2006; Mizuguchi *et al*., 2004; Singh *et al*., 2006; Stheneur *et al*., 2008).

1.2.2 Vascular form of Ehlers-Danlos syndrome (vEDS)

The vascular type or type IV of Ehlers-Danlos syndrome is inherited in an autosomal dominant manner and is caused by mutations in *COL3A1* gene which encode the protein type III collagen. The disease is clinically characterized by vascular and tissue fragility. Major symptoms that distinguish vEDS from MFS include translucent skin, easy bruising, dystrophic scarring, and they have a major risk for intestinal and uterine rupture. Typical AAD affect the medium sized arteries and about half of the AAD are confined to the thoracic or abdominal branch arteries (Pepin *et al*., 2000).

1.2.3 Arterial Tortuosity Syndrome (ATS)

Arterial tortuosity syndrome is another vascular autosomal recessive disease which is caused by mutations in the gene *SLC2A10* that encode the protein, solute carrier family (facilitated glucose transporter), type 10 (GLUT10) leading to loss-of-function of the protein to express decorin, which acts as an important extracellular inhibitor of TGF-ß (Couke *et al.,* 2006). Clinically, the disease is characterized by arterial tortuosity, stenosis, and AAD of the major arteries; however, it occurs in lesser extent than LDS.

1.2.4   Non-syndromic familial Thoracic aortic aneurysms and dissections

Familial thoracic aortic aneurysms and dissections (FTAAD) is a major cardiac feature in MFS, but up to 19% of cases with TAAD do not meet the clinical criteria for MFS and have multiple close relatives with similar aortic disease indicating of a strong genetic predisposition (Biddinger *et al*., 1997; Milewicz *et al*., 1998). This condition is known as non-syndromic form of TAAD, or familial TAAD (FTAAD). FTAAD is an autosomal dominant disorder with marked variability in the age of onset and has a decreased penetrance which makes the early identification of these affected individuals difficult (Francke *et al*., 1995). The condition is a genetically heterogeneous disease with three loci and four genes being identified so far including AAT1 at chromosome 11q23.3-q24, AAT2 at chromosome 5q13-q14, TAAD3/BAV at chromosome 15q24-26, *TGFBR2*, *MYH11*, *ACTA2* and *FBN1* (Vaugham *et al*., 2001; Zhu *et al*., 2006; Francke *et al*., 1995; Dietz *et al*., 1995; Hasham *et al*., 2003; Pannu *et al*., 2005; Guo *et al*., 2001; Avidan *et al*., 2010; Guo *et al*., 2007; Hoffjan *et al*., 2011). Pannu and colleagues reported mutations in the *TGFBR2* gene in 4 unrelated families, showing only cardiac malformations (Pannu *et al*., 2005). Guo *et al*. reported a family in combination with or without livedo reticularis and iris flocculi caused by mutations in the smooth muscle alpha-actin (*ACTA2*) gene (Guo *et al*., 2007). TAAD in association with patent ductus arteriosus (PDA) was reported by Zhu and colleagues caused by mutations in the *MYH11* gene. Aneurysms and dissections in these patients were rather confined to intracranial arteries, TAAD were less common. Majority of the mutations affect the C-terminal coiled-coil segment of the smooth muscle heavy chain, a contractile protein of the smooth muscle cells. Studies have reported that heterozygous mutations in the *MYH11* gene, lead to early and severe decrease in the elasticity of the aortic wall, leading to impairment of aortic compliance even with normal aortic size (De Backer *et al*., 2009).

1.2.5   Thoracic aortic aneurysms and dissections in conjunction with bicuspid aortic valve

Bicuspid aortic valve (BAV) affects about 1-2% of the population and it can occur in association with TAAD (Mills *et al*., 1978). The condition results from cystic medial necrosis (CMN), aortic wall abnormality also described in MFS. Patients with BAV have an increased risk for AAD compared to those with normal aortic valves (de Sa *et al*., 1999; Fedak *et al*., 2002). AAD in BAV patients generally locates in the ascending portion of the major aorta, not the aortic root as described in MFS (Hahn *et al*., 1992; De Backer *et al*., 2009). BAV in

association with AAD is also seen in young children (Gurvit *et al*., 2004). Worth knowing, there is a progressive AAD development even after valve replacement, indicating that these patients require life-long follow up, in order to prevent severe lesions. Dietz and colleagues reported results of comprehensive family studies showing BAV in association with AAD, and they have reported a large number of cases where AAD occurred alone, indicating that BAV and AAD are a result of a single gene defect with variable expression. The condition of BAV in family is inherited as an autosomal dominant condition with reduced penetrance. The condition can be sporadic or familial with an estimated frequency of 9.1-17.1% in families (Huntington *et al*., 1997).

1.3   Molecular pathogenesis of TAAD in MFS and MFS-related diseases

TAAD has been defined as a degenerative process characterized by CMN and elastin fragmentation (EF) of unknown cause. The aortic wall is highly dynamic and has a tightly regulated structural composition. Maintenance of aortic wall homeostasis involve strictly regulated interactions between important structural proteins and specific regulatory pathways. The normal arterial wall is composed of three layers including intima, media and adventitia. Each of the layers are separated from each other by two thick layers of elastic fibres (Figure 1-4). The thickness, cell composition and biological properties of the arterial wall do vary along the arterial tree. The main structural and functional property of the aortic wall is maintained by the components in the lamellar unit (Wolinsky & Glagov, 1967). Each lamellar unit is composed of a vascular smooth muscle cell (VSMC) which is located between two layers of elastic fibres, which is composed of microfribrils and proteoglycans that form the ECM. The lamellar unit contains both tensile strength and elastic properties, such that the aorta can withstand the high pressure exerted on the arterial wall and allowing the arterial wall to return back to its normal size. Interaction between proteins of both VSMC and ECM mediates various function of the major aorta, thus dysregulation of one or more of these may lead to TAAD formation.
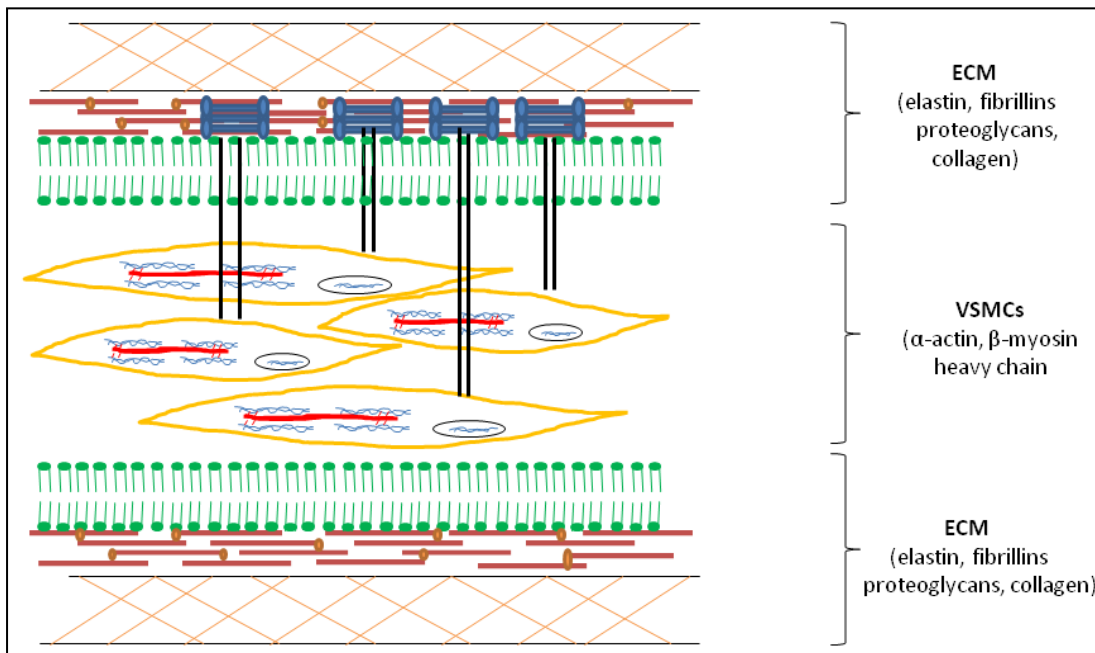
Figure 1-4: **Schematic representation of composition of the aortic medial wall.** ECM is composed of elastin embedded in the fibrillin microfibril scaffold, orange asymmetric bars; fibrillins, brown aligned bars connected with each other that make up microfibrils; proteoglycans, green; collagen, blue rod like structure. VSMCs, vascular smooth muscle cells is composed of α-actin blue chain structure; β-myosin heavy chain (β-MHC) red chain structure. Black bars indicate communication between VSCM and ECM protein collagen through signalling cascades.

1.3.1 VSMCs

VSMC have both contractile and secretory properties, these are interspaced by thin opposite lying elastic fibres (Owens *et al*., 2004) (Figure 1-4). The contractile properties are maintained by the proper interaction between smooth muscle α-actin and β-myosin heavy chain (β-MHC). This actin-myosin complex is found in the cell cytoplasm and are linked to ECM proteins through other proteins such as talin, vinculin, α-actinin and filamin-A. Thus, a cell contraction is a highly organized process and all these proteins are important to maintain aortic wall homeostasis. In addition to contractile properties, VSMCs possess secretory characteristics which facilitate the synthesis and repair of various ECM proteins that maintain the structure of the aortic wall including collagen, elastin, fibrillin and fibulin. Mutations in the contractile proteins, mainly in smooth muscle cell-specific actin encoded by *ACTA2* gene on chromosome 10q23-24 and β-MHC encoded by *MHY11* gene on chromosome 16p12.2-13.3 are involved in the TAA formation possibly as a result of loss of VSMC shape and

alignment, and abnormal synthesis and degradation of ECM proteins. These TAA malformations become evident in the histologic findings as loss of VSMCs and EF. Mutations in the genes *MYH11* and *ACTA2* cause FTAAD.

1.3.2   Collagen

Both the media and the adventitia are abundant in type I and type III collagen (Figure 1-4), and its function is to provide tensile strength and rigidity to the arterial wall (van der Rest & Garrone, 1991). Whereby, type IV collagens are highly enriched in the tunica intima where it mediates the interaction of endothelial cells to the components of the intima. In addition to its structural properties, this protein has functional characteristics and acts as a reservoir for several soluble proteins. Therefore, mutations in genes encoding for collagen fibers can lead to structural and functional abnormalities leading to TAAD formation. Mutations in *COL3A1* gene which encodes the protein type III collagen is a result of vEDS.

1.3.3   Elastin

Elastin is also an ECM protein which is found in abundance in the thoracic aorta (Parks *et al*., 1993) (Figure 1-4), especially in the tunica media. This protein is synthesized by VSMCs during a mechanical movement such as stretch or pressure; it provides recoil properties to the arterial wall. Similar to other proteins, elastin has regulatory properties on the structural component of the arterial wall; it can directly interact with the VSMC and maintain cell proliferation and migration. Elastin fragmentation is not the cause of TAAD; instead it is the loss of functional properties of elastin, leading to abnormal VSMC proliferation.

1.3.4   Fibrillin

Fibrillins are extracellular microfibrils, which are also found in the tunica media which interact with several other ECM proteins such as elastin, collagen, fibronectin and vitronectin (Figure 1-4). Three isoforms of fibrillins exist, fibrillin-1, 2 and 3. Fibrillin-1 is a major structural component in the ECM and provides mechanical strength to the aortic wall. Additionally, this protein plays a role in the sequestration and regulation of growth factors such as TGF-β1 and it can also activate several signaling cascades through its RGD motif. Fibrillin-1 mutations lead to MFS (Ramirez & Dietz, 2007) and FTAAD.

1.4   Today's conflict in clinical and molecular diagnosis of Marfan and Marfan-related cardiovascular diseases

TAAD occurring as a syndromic form as seen in MFS are generally diagnosed clinically using the Ghent nosology criteria because of the presence of skeletal abnormalities, but there are several cases of TAAD where TAAD are often asymptomatic until severe complications or sudden death occurs. In such situations, TAAD can only be diagnosed by careful monitoring of the phenotypic abnormalities, age of death and a family history, since these factors may help to decide whether it relates to a heritable disease of TAAD or not (Loeys *et al.*, 2010; Ripperger *et al.*, 2009; Klintschar *et al.*, 2009). In cases where the deceased provide phenotypic features for MFS, the diagnosis can be made clinically. But about 19% of the TAAD are familial cases and have several relatives with similar aortic disease, where the disease expression and age of onset is highly variable. These cases may only be handled by offering a genetic counselling to the first-degree relatives to make them aware of potential heritable risk of MFS and FTAAD and to offer a molecular testing of all TAAD candidate genes. To date, molecular testing is performed with conventional Sanger sequencing which does not allow the testing of all candidate genes for TAAD in a single experiment, and analysing all candidate genes individually is too expensive and time consuming. Thus, there is a huge demand for a molecular technique which allows the parallel testing of multiple genes, and which is rapid, efficient and cost-effective in order to help the clinician to make an accurate and early diagnosis of TAAD in relatives at-risk who might also be predisposed to severe aortic complications (Bode-Jaenisch *et al.*, 2012; Ripperger *et al.*, 2009; Klintschar *et al.*, 2009).

2. *Aim of this study*

The main intention of this study has been to provide clinicians with a range of appropriate genetic tools which are cost-effective and quick, and provide accurate results that help to identify patients with TAAD who do not fulfil the clinical criteria for MFS, but have a high risk for sudden TAAD, as seen in individuals with FTAAD. We herein, have developed a novel molecular platform, the "MFSTAAD resequencing microarray" which enables the mutation screening of a large panel of genes that have been described in the context of syndromic and non-syndromic familial TAAD in a single experimental run. The study will test its overall performance, its analytical sensitivity in case of how good the novel platform is to detect known and novel DNA variants and finally whether this technology could be used in the clinical setting as a pre-screening method when traditional clinical imaging techniques are negative and in patients who fulfil the clinical criteria for MFS, but do not harbour a mutation in the classically defected *FBN1* gene. Finally, we test a best fitting combination of traditional genetic sequencing technologies which can be used in the clinic in combination with MFSTAAD resequencing assay to cover larger sequence aberrations. As further interest, we will test when a genetic testing should be highly considered in patients with non-syndromic TAAD, this was done firstly, by investigating the correlation between histopathological changes in the thoracic aorta and mutation yield in patients who died of sudden, unexplained TAAD and secondly, by examining the overall mutation yield between two different aged groups ($\leq$ 55.5 years versus $>$ 55.5 years).

3. *Materials and Methods*

3.1 Chemicals and Reagents

Table 3-1 Chemicals and Reagents	
Reagents	**Vendor**
1M Tris-HCL, pH 7.8	Sigma Aldrich, Hannover
10x PCR Buffer II (Mg^{2+})	Qiagen, Hilden
1x TE Buffer (pH 8)	Ambion, Life Technologies, Darmstadt
20x SSPE (3M NaCl; 0.2M NaH_2PO_4, 0.02M EDTA)	Cambrex, Wiesbaden
5M TMAC	Sigma Aldrich, Hannover
5M NaCl, RNase-free, DNase-free	Ambion, Life Technologies, Darmstadt
5x Sequence Buffer	Applied Biosystems, USA
6x Gel Loading Dye Blue	BioLabs, New England
Acetylated BSA (50µg/µL)	Molecular Probes, Life Technologies, Darmstadt
Agarose NEEO, Roti® garose	Carl Roth, Karlsruhe
Boracic Acid	Merck Millipore, Darmstadt
Chloroform	J.T. Baker, Deventer, Netherlands
Denhardt's Solution 50x Concentrate	Sigma Aldrich, Hannover
Destilled Water	Invitrogen, Life Technologies, Darmstadt
DMSO	Sigma Aldrich, Hannover
EDTA	Merck, Darmstadt
Ethanol Absolute	J.T. Baker, Deventer, Netherlands
Ethidium Bromide	Sigma Aldrich, Hannover
Formamide	Applied Biosystems, USA
HPLC Water	J.T. Baker, Deventer, Netherlands
HCL	J.T. Baker, Deventer, Netherlands
Isopropanol	J.T. Baker, Deventer, Netherlands
MES Hydrate	Sigma-Aldrich, Hannover
MES Sodium Salt	Sigma-Aldrich, Hannover

Molecular Biology Grade Water	Cambrex, Wiesbaden
Phenol	Carl Roth, Karlsruhe
Sephadex® G-50	Sigma Aldrich, Hannover
Sodium Acetate	Merck, Darmstadt
SYBR® Gold Nucleic Acid Gel Stain	Molecular Probes, Life technologies, Darmstadt
Tween-20 (10 % solution)	Pierce, Thermo Scientific, Bonn

3.2 Biological Substances and Enzymes

Table 3-2 Biological Substances and Enzymes	
Biological materials	**Vendor**
100 bp DNA Marker	BioLabs, New England
Anti-streptavidin antibody (goat), biotinylated	Vector Labs, England
DNA marker (50-2500 bp)	Cambrex, Wiesbaden
DNA Molecular Weight Marker IV	Roche Applied Science, Mannheim
DNTPs	BioSciences, Amersham
Forward and Reverse Primer	Eurofins MWG Operon, Ebersberg
GeneScan™-500 ROX™ Size Standard	Applied Biosystems, USA
GeneScan™-500 TAMRA™ Size Standard	Applied Biosystems, USA
Herring Sperm DNA	Promega Corporation
IQ-EX Control Primers (20µM)	Affymetrix, UK
IQ-EX Control Template (7.5 kb and 3.5 kb)	Affymetrix, UK
Long Range PCR *Taq* polymerase	Qiagen, Hilden
Proteinase K	Merck Millipore, Darmstadt
SAPE (Streptavidin R-phycoerythrin conjugate)	Molecular Probes, Life Technologies, Darmstadt
Short range PCR *Taq* polymerase (5 U/µL)	Qiagen, Hilden

3.3 Buffer and standard working solutions

10x TBE Buffer

- Mix 0.9M Tris-HCL with 0.9M BoracicAcid and 0.02M EDTA

DNA Gel Electrophoresis (2% or 0.8% agarose gel)

- 100mL of 1x TBE Buffer

2g agarose (for 2 % agarose gel electrophoresis) 0.8g agarose (for 0.8% agarose gel electrophoresis)

Procedure: Dissolve **either** 2g or 0.8g of agarose with 100mL of 1x TE Buffer in a microwave for approx. 3 minutes. Let the solution cool down (hand-warm) before you add 15µL of Ethidium Bromide. Pour gently the mixture in to a gel form containing a 16 or 21 well comb.

Loading Buffer

- 15mL Glycerin, 87%, 28.5 mL HPLC water one small spatula of Bromphen blue, one small spatula of Xylencyanoblue, mix well.

Lysis Buffer

- 50mM Tris, 100mM EDTA, 0.5% (w/v) SDS set to a pH of 8.0.

3.4   Kits and protocols

Table 3-3 Kits and protocols	
Kit	**Vendor**
244K Agilent Human Genome e-microarray	Agilent Technologies, Santa Clara, CA, USA
BigDye Terminator Cycle Sequencing Kit Version 1.1 Kit:	Applied Biosystems, USA
DNA extraction Kit	Qiagen, Hilden
DyeEx 2.0 Spin Kit	Qiagen, Hilden
Expand Long Range, dNTPack	Roche, Mannheim
ExoSAP-IT Kit	Affymetrix, UK
GeneChip Resequencing Assay Kit	Affymetrix, UK
GoTaq Flexi DNA polymerase	Promega, Mannheim
GFX PCR and DNA Gel Band purification kit	Illustra GE Healthcare Life Sciences, Freiburg
KOD XL DNA Polymerase	Merck Millipore, Darmstadt
Qiagen LongRange PCR Kit	Qiagen, Hilden
MRC-Holland-Salsa MLPA kit Syndrome-1(P065) Syndrome-2 (P066)	MRC Holland, The Netherlands
PCR Product Purification Kit	Qiagen, Hilden
Quanti-iT™ PicoGreen® dsDNA Assay kit	Invitrogen, Life Technologies, Darmstadt
GeneChip CustomSeq Resequencing Array protocol	Affymetrix, UK

3.5   Data Analysis Software and custom guide

AGCC software	Affymetrix, UK
GeneMapper	Applied Biosystems, USA
GeneChip Sequence analysis software	Affymetrix, UK
GeneChip CustomSeq Array design guide P/N 701263-revision 4	Affymetrix, UK
Genomic Workbench software	Agilent Technologies, Waldsbrom, Germany
Feature extraction software	Agilent Technologies, Waldsbrom, Germany
Picogreen fluorescence quantification	Magellan software V6.6, Tecan, Crailsheim
Module SeqPilot, SeqC and SeqPatient	JSI, Medical Systems, Germany

3.6   Consumable Materials

Tab3-4 Consumable Materials	
Materials	**Vendor**
Corning® Costar® 96 Well Cell Culture Cluster Flat Bottom Plates with lid	Sigma Aldrich, Hannover
96-well PS Clear black TC plate, flat bottom	Greiner bio-one, Frickenhausen
Combi Tips 0.5 and 5.0Ml	Eppendorf, Hamburg
Microcon YM-30 filters	Millipore, Bitterica, MA, USA
Micro Tube 1.5mL Easy Cap	Sarstedt, Nümbrecht
Multiply®-µL tip Pro-8-strip	Sarstedt, Nümbrecht
Ultra Amp PCR Plates 96-well	Sorenson Biosciences, USA
Falcon Tubes	Greiner bio-one, Frickenhausen
Biosphere Filter Tips (20, 100, 200, 1000, 1250µL)	Sarstedt, Nümbrecht
Gel Casting System 11.14	Whatman, Germany
Sterile Nitrile Powder-free gloves	Kimberley-Clark, Mainz
Disposable Bags	Carl Roth, Karlsruhe
Aluminium Foil	NeoLab, Heidelberg
Parafilm	NeoLab, Heidelberg

Petri Dish	Becton Dickinson, Heidelberg
Pipette Tips (20, 100, 200 and 1000µL	Sarstedt, Nümbrecht
Safe Lock Tube 1.5 and 2.0mL	Eppendorf, Hamburg
Scalpel	Micro-Science
UVette® routine pack disposable cuvettes 50-2000µL	Eppendorf, Hamburg
96-well plates 0.45µM Hydrophilic	Merck Millipore, Darmstadt
Low Protein Binding Durapore Membrane	Merck Millipore, Darmstadt

3.7 Equipments

Table 3-5 Equipments	
Equipments	**Vendor**
ABI Prism™ 3130xl Genetic Analyzer	Applied Biosystems, USA
BioPhotometer plus	Eppendorf, Hamburg
NanoPhotometer	Eppendorf, Hamburg
Centrifuge 5424 (for 96 well plates)	Eppendorf, Hamburg
Centrifuge 5810R (for 1.5-2.0 mL tubes)	Eppendorf, Hamburg
Centrifuge 3200	Eppendorf, Hamburg
Cleanbench	Heraeus Sepatech
Fluorescent 96-well Plate Reader	Tecan, Crailsheim
Gel Electrophoresis Apparatus Horizon 11.14	Bethesda,Research Laboratories, Life Technologies, Darmstadt
Incubator	Heraeus Instruments
Intelligent Heating Block	Biometra, Göttingen
Microwave	Micromat. AEG, Germany
Pipettes (Volumes 0.2-1.0mL)	Gilson Pipetman, USA
Transferpette®-8	Brand
Voltage Supplier, Power Pack 0-250V	Biometra, Göttingen
Weighing machine	Sartorins
Vortex-Gene2	Scientific Industries, USA
Thermostat 5320	Eppendorf, Hamburg
IKA-Vibro-Fix	LabExchange, Burladingen
PCR Thermal machines	

T-Professional Basic Gradient, T-Professional, T3 and T3000	Biometra, Göttingen
Gel Visualization	
Bioprofil -Video System	Vilber, Eberhardzell
Thermal Paper Film Model K 65 HM	Mitsubishi, Germany
UV Transilluminator	Bachofer, LabExchange, Burladingen
Video Copy Processor	Mitsubishi, Germany

3.8 Candidate Gene Reference Accession IDs

Table 3-6 Candidate genes

Protein name	OMIM ID	GenBank transcript ID	Ensembl transcript
actin, alpha 2, smooth muscle, aorta	102620	NM_001613.1	ENST00000224784
collagen, type III, alpha 1	120180	NM_000090.3	ENST00000304636
fibrillin 1	134797	NM_000138.3	ENST00000316623
myosin, heavy chain 11	160745	NM_002474	ENST00000300036
notch 1	190198	NM_017617.3	ENST00000277541
smad type 3	603109	NM_5902.3	ENST00000327367
solute carrier family 2, member 10	606145	NM_030777.3	ENST00000359271
transforming growth factor, beta receptor 1	190181	NM_004612.2	ENST00000374994
transforming growth factor, beta receptor 2	190182	NM_003242.5	ENST00000295754

3.9 In silico programs and commercial Database

Amino Acid Alignment	http://www.ebi.ac.uk/Tools/msa/clustalw2/
Chi-Square Test	http://vassarstats.net/tab2x2.html
Ensembl Genome Browser	http://www.ensembl.org/index.html
Fisher's Exact Test	http://vassarstats.net/tab2x2.html
FruitFly	http://www.fruitfly.org
HGMD Mutation database	http://www.hgmd.cf.ac.uk
Mutation Taster	http://mutationtaster.org
NCBI Public Database	http://www.ncbi.nlm.nih.gov/
NetGene2	http://www.cbs.dtu.dk/services/NetGene2/
PMut	http://mmb.pcb.ub.es/PMut/PMut.jsp
PolyPhen2	http://genetics.bwh.harvard.edu/pph2/

Primer 3 design	http://frodo.wi.mit.edu/primer3/
Protein domains	http://pfam.sanger.ac.uk/
Repeat Masker	http://www.repeatmasker.org/x-bin/webrepeatmasker
SNPCheck3	http://ngrl.manchester.ac.uk/SNPCheckV3/snpcheck.htm
UCSC Genome Browser	http://genome.ucsc.edu/cgi-bin/hgGateway
UMD Mutation database	http://www.umd.be
UniProt	http://www.uniprot.org
UniSTS database	www.ncbi.nlm.gov/unists
Wilson score method	http://faculty.vassar.edu/lowry/prop1.html

3.10 Proband recruitment and group design for the validation of a novel large-scale sequencing microarray

A total of 247 unrelated patients were recruited from the institution of Human Genetics, Medical School of Hannover and from the department of Human Genetics, Ruhr University Bochum and the Heart and Circulation Research, University of Witten/Herdecke. A total of 181 probands were positive controls in this study that either had fulfilled the Ghent nosology criteria for classic MFS and had a mutation in the gene *FBN1* or were positive for LDS with a mutation in the gene *TGFBR1* or *TGFBR2* or have been positive for isolated non-syndromic FTAAD with a mutation in the *ACTA2* gene. The positive cohort represented a total of 182 known disease causing mutations, which included 153 point mutations (missense, nonsense and splice site mutations), 21 deletions (size range: 1 bp-16 bp), 7 insertions (size range: 1 bp—3 bp) and a 15 bp duplication. Other 66 samples were composed of 36 retrospective and 30 prospective samples (Figure 3-1). Retrospective living samples are denoted as "RL" and prospective samples are either denoted as "PL" (prospective living) and as "PD" (prospective decedent) in this study. To note, 20 out of the 30 prospective samples were recruited from the institute for Legal Medicine, Hannover. A medico-legal autopsy was conducted in all 20 decedent, and histopathological examination of these decedents was performed in 18 decedents by Bode-Jaenisch *et al*., 2012, except for one decedent, was examined in the intsitute for Pathology, Hannover. These different cohorts have been selected to design and validate a novel high-density oligonucleotide-based microarray.
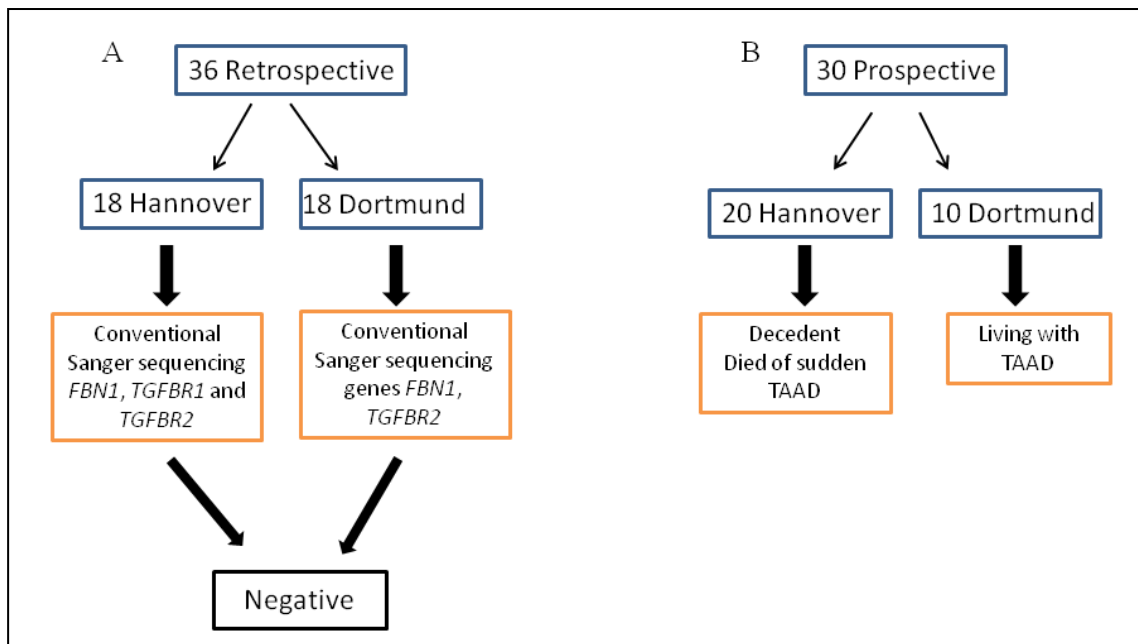
Figure 3-1: **Division of 66 test samples.** (A) Representation of apportion of 36 test probands between Hannover and Dortmund. Subjects in this group are suspected of MFS and/or LDS but are assigned negative for mutations in the genes *FBN1*, *TGFBR1* and *TGFBR2* using conventional Sanger sequencing reaction. (B) Representation of apportion of 30 test prospective test samples. A total of 20 samples were recruited from the Legal Medicine, Medical School of Hannover who died of sudden, unexpected TAAD of unknown cause. The remainder of 10 was living subjects by whom TAAD was suspected without skeletal features suggestive for MFS.

3.10.1 Probands selection for further studies

Three unrelated subjects (designated as P1-P3) were recruited from the institute for Human Genetics, Hannover who had fulfilled the Ghent nosology criteria for MFS with manifestations in the skeletal, cardiovascular and ocular systems. Clinical profiles of two patients were collected from their medical records; please see Appendix 1 for references on clinical symptoms. Clinical history for one patient was not available. Routing molecular genetic testing of these individuals revealed no mutation in the genes *FBN1*, *TGFBR1* and *TGFBR2* using conventional Sanger sequencing reaction and multiplex-ligation-dependent probe amplification (MLPA). Final two individuals were subjects with several members in the family with skeletal features of MFS with or without TAAD. First subject was a patient from the institute for Human Genetics; Hannover (Appendix 2), the other patient was recruited from the department of Clinical Genetics, University of Regional Laboratories, in Lund, Sweden (Appendix 3). In an independent genetic study, Singh *et al*., 2012 identified two non-

synonymous DNA variants in exon 2 of the *TGFBR3* gene (c.44 C>T, p.S15F and c.55 A>G, T19A) in family 1 (Appendix 2) and the variant c.55 A>G, T19A in family 2 (Appendix 3), which was found not to co-segregate with the disease in these two different families (Sing *et al.*, 2012). In addition, during this study, the index patient in family 2 (Appendix 3) was further analyzed in the routine genetic testing and the colleagues from Lund detected a mutation in the *ACTA2* gene (c.977 C>A, p.T326N), however, the mutation did not co-segregate with the disease in family 2.

3.11   Extraction of genomic DNA from whole blood and human tissue

Extraction of genomic DNA from whole blood was performed using the QIAamp DNA Mini kit (Qiagen) under the instructions of the vendor. DNA extraction from human tissue such as aorta or spleen was extracted using the phenol-chloroform extraction technique. This method was first developed by (Chomczynski & Sacchi, 1987) and is used in the molecular biology for the fractionation of proteins and nucleic acids. In brief, a small portion (about 0.1-0.3g) of human tissue was transferred into a 1.5mL safe lock tube containing 500μL of lysis buffer and 35μL proteinase K. The complete extraction was incubated in a compensator overnight at 56ºC. Next day, equal volume of 500μL of phenol (pH of 8.0) was added to the extract. The mixture was vortexed for 2 minutes and centrifuged at 13000rpm for 10 minutes at 4ºC to enable phase fractionation. The aqueous phase or upper phase was cautiously transferred into a clean 1.5mL safe lock tube without transferring content from the interphase (white cloudy substance). As next step, 250μL of phenol and 250μL of chloroform were pipetted to the extract. The mixture was vortexed for 2 minutes and at 13000rpm for 10 minutes at 4ºC. The same procedure was repeated with equal volume of 500μL chloroform following the transfer of aqueous phase into a clean 1.5mL tube. A final volume of 0.2M of sodium acetate (3M) and 500μL of pure ethanol (96-100%) was added to the extract. The mixture was centrifuged at 13000rpm for 10 minutes at 4ºC. After the centrifugation step, the supernatant was gently discarded. The pellet on the bottom edge contain the genomic DNA which was purified with 500μL of 70% ethanol and centrifuged at (13000rpm) for 10 minutes at 4ºC. This step was repeated twice. Following three purification steps with 70% ethanol, the DNA pellet was dried off at 37ºC and resuspended in at least 30μL of HPLC water which was dependent on the size of the DNA pellet.

3.12 Determination of genomic DNA concentration

A spectrophotometer determines the concentration of a substance, as well as its purity in a mixture, by the simple measurement of the light absorbed by the components at a given wavelength. For instance, DNA itself, and most of their contaminants such as guanidium salts and phenol have absorbances in the region 230 to 320nm. Thus, the measurement of the absorbances in this region allows the measurement of DNA concentration and provides general information about the contaminant levels found in the mixture. Four important wavelengths are used for the measurement:

- A_{230}: light absorption by guanidium salts (allowed the DNA binding to silica columns in the DNA preparation) and phenol (used in phenol chloroform DNA extraction)
- A_{260}: light absorption by DNA
- A_{280}: light absorption by proteins such as tyrosine and tryptophan residues
- A_{320}: provides information on the general turbidity of the sample and is subtracted from the value for A_{260}

Nucleic acids such as dsDNA and ssRNA absorb UV light strongly at a wavelength of 260nm because of its nitrogenous base composition (A, G, C and T). At a wavelength of 260nm, the extinction coefficient for double stranded DNA is 0.020 per µg dsDNA per ml of solution per cm of light path, and for single stranded RNA it is 0.025 $(µg/ml)^{-1}$1cm. Thus, an absorbance of 1 at 260nm in a 1cm quartz cuvette corresponds to 50µg/ml solution of double stranded DNA or 40µg/ml solution of a single stranded RNA. Based on this information, the following equation was used to calculate the DNA concentration:

DNA concentration (µg/ml) =   (A_{260} reading- A_{320} reading) x dilution factor (1/20) x 50µg/ml/1

To evaluate the purity of DNA in the sample, the absorbances between 260nm to 320nm are used. The most common purity calculation is the ratio of the absorbance at 260nm divided by the reading at 280nm. Good quality of DNA should have an A260/A280 ratio between 1.7 - 2.0. Following the estimation of DNA concentration, a working solution of 10ng/µL was prepared for downstream applications.

3.13 Separation of nucleic acids by agarose gel electrophoresis

As confirmation, the yielded PCR products were separated according to their molecular weight and size by agarose gel electrophoresis. Agarose is a cross-linked polymer which is made up of disaccharide unit containing D-galactose and 3,6-anhydro-L-galactopyranose.

Agarose in a gel acts as a matrix and is used in molecular biology for the separation of proteins and nucleic acids in size of >100 bp in an electrical field condition. Higher concentrations (e.g. 2%) of agarose were used for the separation of smaller DNA fragments (0.1-3 kb), while lower concentrations (e.g. 0.8%) of agarose were used for larger DNA fragments (0.4-19 kb). In order to follow the migration of nucleic acids during gel electrophoresis, special tracking dyes such as bromophenol blue and xylene cyanol dyes with similar migration rate of nucleic acids were used. The visualization of DNA fragments were enabled by staining the agarose gel with ethidium bromide during gel preparation. EtBr is a fluoroscent dye that intercalates into double stranded DNA and allows the visualization of DNA fragments under UV transilluminator. For the estimation of the size of the amplified fragments, molecular weight markers 1 kb plus (Figure 3-2a) DNA marker and DNA marker IV (Figure 3-2b) were used that was run along with the samples.
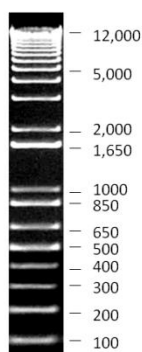
Figure 3-2a: 1 kb (plus) DNA marker. DNA marker used for smaller fragments under 2.0% agarose gel electrophoresis (http://products.invitrogen.com/ivgn /product/10787018).
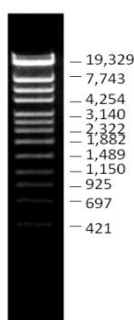
Figure 3-2b: DNA marker IV. DNA marker used for larger fragments using 0.8% agarose gel electrophoresis (http://www.roche-applied science.com/prod data/gpip/3_6_2_5_4_1.html, respectively).

3.14   Short range Polymerase Chain Reaction

For PCR reaction, primer pairs were designed using the online Primer3 input program and were checked for SNPs using SNPCheck3. The Polymerase Chain Reaction is used in molecular biology to generate millions of copies of a specific DNA fragment. This technique was developed in 1983 by (Kary *et al.*, 1983) and relies on a thermal cycling condition, consisting of repeated heating and cooling cycles of the reaction for DNA denaturation and enzymatic amplification of the target DNA. It is called a chain reaction because the generated DNA fragments are re-used as a template for subsequent replication by which the DNA is exponentially amplified. Each cycle include three steps such as denaturation, annealing of primers and extension. Specific short primers (size range 20-27 bp) complementary to the target region and a heat stable DNA polymerase known as *Taq* polymerase, an enzyme isolated from the bacterium *Thermus aquaticus* are the key elements for a selective PCR product amplification. Herein, the *Taq* DNA polymerase from Qiagen was used and the assay was performed according to the instructions provided by the vendor.

3.14.1 PCR Composition and Thermal Conditions of short range PCR

Table 3-7:   **Reaction mix of one 25µL <u>short range</u> PCR reaction**

Component	Volume in Each Reaction (µL)	Final Concentration
PCR Buffer	2.5	1x
dNTPs	2.5	2mM
Primer F	2	0.4µM
Primer R	2	0.4µM
Taq Polymerase	0.3	5U/µL
Template	5	10ng/µL
Q-solution	5	1x
HPLC H_2O	5.7	Total volume of 25µL

Table 3-8:	Thermal Cycling Condition of short range PCR		
Initial Denaturation	95°C	300s	
Denaturation	95°C	30s	
Annealing	58°C	30s	35 cycles
Extension	72°C	30s	
Final extension	72°C	600s	
Holding	4°C	Indefinite	

3.15 Conventional Sanger Sequencing Reaction

Sanger sequencing is a DNA sequencing method and relies on the selective addition of specific chain-terminating di-deoxynucleotides which are incorporated by the DNA polymerase during *in vitro* DNA replication (Figure 3-2). This method was firstly developed by (Sanger, 1977) and was termed as "dideoxy" (dd) or "chain termination" method. A standard chain-termination method requires a single stranded DNA target template, a DNA primer (forward or reverse), a DNA polymerase, the four normal DNA building blocks (dATP, dCTP, dGTP and dTTP) and specific chain terminating nucleotides (dideoxyNTPs; ddATP, ddCTP, ddGTP and ddTTP). These ddNTPs lack a hydroxyl group (-OH) group which is required for the formation of a phosphodiester bond between two nucleotides, therefore it leads to chain termination when one of the ddNTPs is incorporated by the DNA polymerase during DNA extension process. Each of the ddNTPs is labeled with a different fluorescent dye to enable their detection. The incorporation of these ddNTPs takes place on a random basis, thus it leads to the generation of different sized fragments, but the ddNTPs incorporated in one sample remains the same for that position. In the past, DNA sequencing was performed in a four reaction tube by adding all the components listed above plus one of the ddNTPs. Following the DNA extension process, the resulted DNA fragments were denatured and separated by size using gel electrophoresis. The runs were visualized under UV light. The four reactions are run in parallel to allow the decoding of each DNA fragment. In this work, we used ddNTPs which have been labelled with a different fluorescent dye and workflow of a sequencing reaction is illustrated in Figure 3-3. The modification of these ddNTPs enabled the reaction to be done in a single reaction tube which saved time and expense. To decode each DNA sequence, we used the ABI Prism[TM] 3130 Genetic Analyzer which performs an automated size separation by capillary electrophoresis and detects each fragments through the fluorescently labeled ddNTP in each DNA strand. This fluorescence information was used by the software to unravel the DNA sequence and display the data as

fluorescent peak trace chromatogram. Sanger sequencing was performed in this study to confirm true positive mutations found with the MFSTAAD resequencing assay and for the characterization of exact deletion breakpoints found with a-CGH.
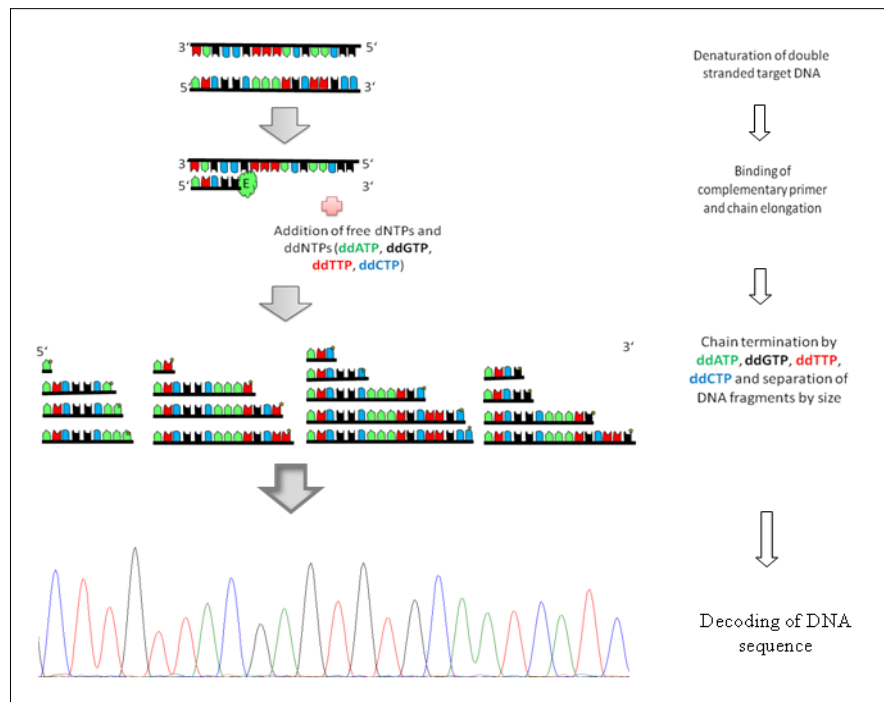
Figure 3-3: **Schematic diagram of conventional Sanger sequence reaction.** First the two DNA strand are denatured. The primer binds to the target DNA. An enzyme known as DNA polymerase binds to the primer and starts copying the target DNA by incorporating free dNTPs that are complementary to the target DNA. The copying of the target DNA strand terminates following the incorporation of a fluorescently labeled ddNTP leading to copies of DNA fragments with varying size. These fragments with fluorescently labeled ddNTPs are then separated by size and are used to read out the original sequence order.

3.15.1 Sequence Set Up and Thermal Cycling Condition

Before the performance of Sanger sequence reaction assay, the PCR products were cleaned up using Exo-SAP-IT kit, the two enzymes contained in this kit enabled the removal of unbound primers and dNTPs that were added in the PCR amplification reaction.

Table 3-9: Mix composition of one Exo-SAP-IT reaction	
PCR Product	5µL
Exo-SAP-IT	2µL

Table 3-10 Thermal Cycling Condition of Exo-SAP-IT reaction		
	37ºC	20 minutes
Enzyme inactivation	80ºC	30 minutes
Addition of 10 µL HPLC water		

Table 3-11: Mix composition of a sequence reaction	
Components	**Volume in Each Reaction**
BigDye Terminator v1.1	1 µL
BigDye Terminator 5x Sequencing Buffer	1.5 µL
Sequence primer (0.5 pmol/ µL)	2.5 µL
ExoSAP-IT clean up products	5 µL

Table 3-12: Thermal Cycling Condition of a sequence reaction			
Initial Denaturation	95ºC	180s	
Denaturation	95ºC	20s	
Annealing	50ºC	30s	**24 cycles**
Extension	60ºC	240s	
Holding	4ºC	∞	
Addition of 10 µL HPLC water			

3.16   Multiplex ligation-dependent probe amplification

Multiplex ligation-dependent probe amplification (MLPA) was initially developed by (Schouten *et al*., 2002). It is a variant of multiplex polymerase chain reaction which allows the detection of abnormal copy numbers of a large number of different genomic DNA or RNA sequences ($\leq$ 50 different copy numbers). MLPA allows the simultaneous analysis of about 96 samples in a single experiment. Presence of partial gene deletions and duplications in most human heritable diseases range from 10% to 30% or even higher which can be covered by this method, thus increasing the overall mutation detections rate, and the molecular diagnosis of many genetic disorders (Aretz *et al*., 2007; Redeker *et al*., 2008; Kanno *et al*., 2007; Aldred *et al*., 2006; Kluwe *et al*., 2005; Michils *et al*., 2005; Furtado *et al*., 2011). MLPA has many advantages for the detection of copy numbers over many other techniques such as conventional sequencing and Denaturing-High-Performance-Liquid-Chromatography (DHPLC) which generally fail to detect copy number aberrations, and including southern blotting which fail to detect smaller copy number changes and are not favored in the routine diagnostics and array-Comparative Genomic Hybridization (a-CGH), another method that allows detection of copy number changes over the whole genome, but it is too expensive and technically far more complicated than MLPA. Although, well characterized gene deletions can be covered by conventional PCR reaction, but the exact deletion breakpoints remains unknown. Moreover, MLPA can be used on purified DNA. The major limitation of the assay is that it cannot be applied for genome-wide screening, but it is a good alternative to array-based technique for many routine applications. Over 300 probe sets are now commercially available. The main principle of this assay is that it is not the sample DNA that is amplified during the PCR reaction, instead the MLPA probes that hybridize to the target sequence. The MLPA consists of four major experimental steps (Figure 3-3) these include:

        1. DNA denaturation and hybridization

        2. Ligation reaction

        3. Exponential PCR amplification reaction

        4. Separation of products by gel electrophoresis

During the first step, the DNA is denatured and incubated overnight with a mixture of MLPA probes. Each of these probe consists of two oligonucleotides, containing a hybridization sequence (depicted in orange) and primer complementary sequence (forward primer (X) or reverse primer (Y), whereby only one of them contain different sized synthetic sequence

known as stuffer sequence (depicted in green). Every probe set hybridize immediately adjacent to each other on their target DNA (Figure 3-4 step 1). Only hybridized oligonucleotides can be ligated during the ligation reaction (Step 2). Similarly, only ligated probes will be exponentially amplified during subsequent PCR reaction (Step 3). To enable the detection of each ligated probes and to distinguish the different samples, one of the universal primer pair is fluorescently labeled (Y-primer) and contain a universal sequence (depicted in green) which varies in size. The relative amount of each probe amplicons is a direct measurement for the relative quantity of probe-target sequence in the reaction sample. To quantify this relation, firstly, the relative signal of each ligated probe is compared to the signal of other ligated probes and then the final quantitation of the overall signals in the test sample are compared to the amount of probe-targets in the reference samples indicating which sequences show abnormal copy numbers. Normally, reference DNA samples are derived from healthy individuals who are negative for mutations in reference genes using conventional sequencing approach
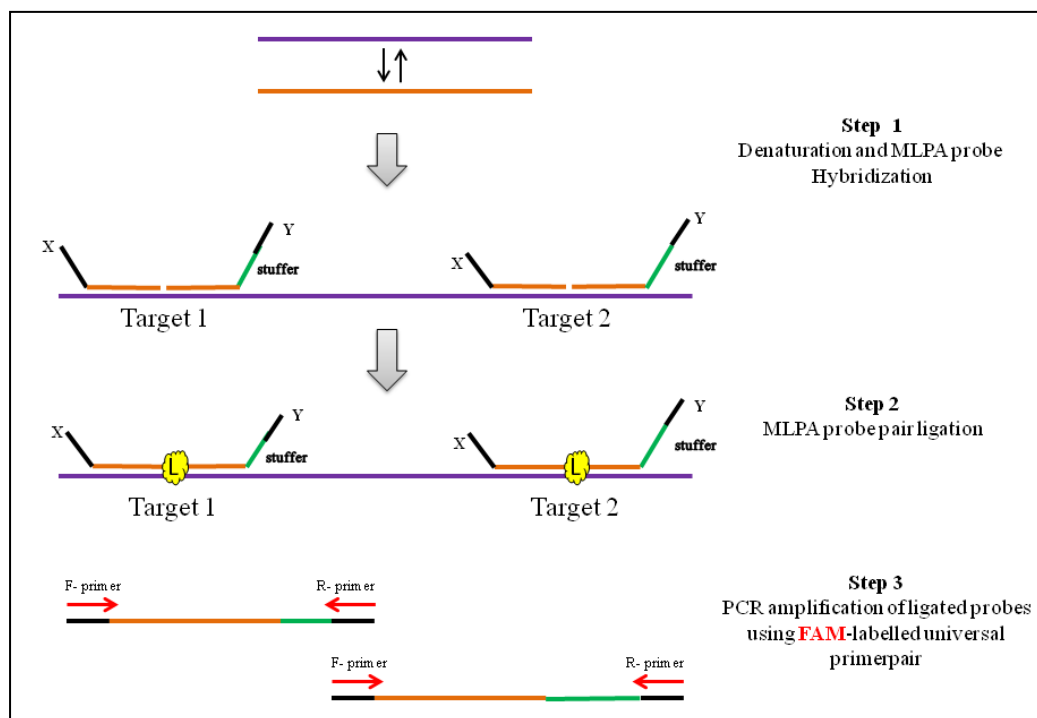
Figure 3-4:   The principle of MLPA.

3.16.1 MLPA assay

MLPA assay was only employed in PD1-20 and in patients P1-P3. We used the commercially available P065 and P06 MLPA kits containing probe mix for 54 exons of the 66 exons of the *FBN1* gene and 7 exons of the *TGFRB2* gene for the detection of copy number aberrations,

such as deletions and duplication. The P065 and P066 did not contain probe mix for *FBN1* exons: 1, 11, 12, 21, 23, 28, 33, 38, 40, 49, 52, 60, and for *TGFBR2* exon 2. DNA template for the MLPA assay was either derived from whole blood or human tissue using the QIAamp DNA Mini Kit and traditional phenol-chloroform extraction kit, respectively. The MLPA assay was performed according to the manufacturer`s instructions. In brief, for each reaction a set of 6 controls were added in each MLPA assay. Noteworthy, DNA from control samples were suggested to come from the same sample type. Two reactions were performed for each test and reference sample (with P065 probe mix and P066 probe mix). First 100ng of genomic DNA from whole blood and from human tissue was extracted and denatured for 10 minutes at 98°C. A total of 3µL of probe mix were added. After brief incubation of 1 minute at 95°C, the probe mixture was allowed to hybridize to their target DNA overnight at 60°C in 8µL complete reaction. The ligation of the primers was performed for 15 minutes at 54°C after adding 32µL of ligase mix. The enzyme was then inactivated at 98°C for 5 minutes. As final step, the ligated MLPA probes were amplified using conventional PCR assay using FAM-labeled universal primer pair. PCR protocol consisted of 1 cycle of 5 mins at 95ºC, 35 cycles of 30s at 95ºC, 30s at 60ºC and 30s at 72ºC, and a final extension cycle of 10 mins at 72ºC. Amplified PCR products from each run were visualized under UV light after gel electrophoresis and then injected into capillary electrophoresis on the ABI Prism® 3130xl Genetic Analyzer. The final fluorescence data of both reference and test samples were compared using sequence data analysis software module SeqMLPA. Deletions and duplications were assigned upon comparing the fluorescent peaks of the reference sample to that of the test sample. A duplication was confirmed when the peak fluorescence ratio was in the upper range (>100%) and a deletion when the peak fluorescence ratio was in the lower range (<100%).

3.17   Refinement of deletion breakpoints using high resolution a-CGH and breakpoint spanning PCR

a-CGH is a high-resolution molecular technique which was introduced by (Solinas-Toldo *et al.*, 1997) to analyze copy number changes in tumour cells and is nowadays also used in the detection of genomic alterations in patients with mental retardation and congenital anomalies. The genome-wide resolution in detection losses and gains depends on the number of probes and the probe spacing. The 244K Agilent Human Genome Microarray contains a total of 244.000 specific 60-mer probe species with a median overall probe spacing of about 7 kb. Herein, the Agilent e-array was used covering the chromosomal region of interest from 46487797 MB to 46547591 MB covering the *FBN1* gene with a probe spacing of 3 probes per

1000 bp. The principle of assay is illustrated in Figure 3-5: test and reference genomic DNA samples are labeled with two different fluorophores, Cy3-UTP and Cy5-UTP, respectively. These dyes are incorporated into the corresponding gDNA using random primers and a mutant form of the Klenow fragment of DNA polymerase I (Exo-Klenow). Labeled products were purified by Microcon YM-30 filters, pooled and hybridized together with 50µg of Human Cot I DNA at 65°C with 20rpm rotation for 40 hours. Washing steps were performed according to the Agilent protocol. Microarray slides were scanned immediately using an Agilent microarray scanner at a resolution of 2µm to measure the fluorescence intensities of each probe-target molecule. The normalized fluorescent ratio of each probe is then plotted against the chromosomal position. Gains or losses across the genome are identified by values increased or decreased from a 1:1 ratio. In a scan image the green fluorescence represents gain of one copy number and red represents loss of one copy number of test DNA for the corresponding target gene. Feature Extraction Software and Genomic Workbench software were used for image analysis and aberration calling.
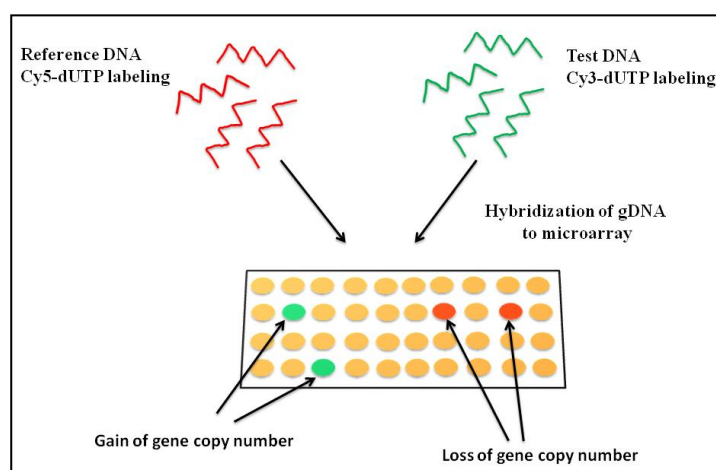
Figure 3-5:   Array Comparative Genomic Hybridization.

3.17.1 a-CGH assay

In this study, two large deletions (exons 1-65 and exons 6-65) and one small deletion (exons 64-65) of the *FBN1* gene which were previously detected using the MLPA assay were analyzed with this assay in order to determine the extension of the three gene deletions in the 3' and/ or 5' direction. The assay was performed with the help of Dr. Doris Steinemann, institute for Cell and Molecular Pathology, Medical School of Hannover following the instructions of the manufacturer. The final data of a-CGH was then used as a reference point to derive genomic sequence of three of 60-mer oligonucleotide probes from the UCSC genome browser. Two of which encompassing the deleted region in the 3' and 5' direction

and one probe positioned on the suspected breaking site of the unique deletion by a-CGH. Probe sequences and their chromosomal locations are listed in tables in the appendix (Appendix tables 12-14). Information of each of these probe chromosomal location was used to design primer pairs for PCR amplification and conventional Sanger sequencing reaction which allowed determining the exact breakpoints.

3.18   Linkage analysis using polymorphic microsatellite markers

Microsatellites, also referred to as short tandem repeats (STRs) or variable number of tandem repeats (VNTRs), are short and simple segments of DNA consisting of two, three or four nucleotides, and can be repeated 3 to 100 times. The majority of these repeats occur predominantly in the non-coding regions, thus varying number of repeats has no influence on the gene function. Among these, $(CA)_n$ nucleotide repeats are the most frequently occurring microsatellites which account for 0.5% of the genome. The number of the repeats can vary between individuals that allows them to be used as genetic markers in the linkage analysis, genetic mapping and in the forensic science.

3.18.1 Indirect DNA marker analysis in two German families

In this work, DNA marker analysis was performed in two unrelated German families (P1 and P2). The first index patient I6 in family 1 (Appendix 2) was a female, with normal stature, but, multiple family members of this subject including her father, two of her brothers and her daughter showed a typical Marfan habitus, and one of her uncle from the paternal side died of abdominal aortic rupture at the age of 65 of unknown cause. Previous marker analysis with MFS markers revealed a disease association with markers for both *TGFBR1* and *TGFBR2* genes, but no mutation could be determined in the Sanger sequencing reaction (data not shown). Furthermore, no mutations were detected in the index patient in the eight TAAD candidate genes (*FBN1*, *TGFBR1*, *TGFBR2*, *COL3A1*, *ACTA2*, *MYH11, SLC2A10* and *NOTCH1*) using the novel MFSTAAD resequencing assay, these subjects were negative for mutations in *SMAD3* gene using conventional Sanger sequencing and MLPA for large deletions and duplications for the genes *FBN1* and *TGFBR2*. Another patient (P2) in family 2 (Appendix 3) was a male with Marfan habitus and had an aortic aneurysm. Both his mother and uncle from the maternal side (Appendix 3, subjects 4 and 5) had a Marfan habitus, whereby aortic aneurysm was only reported in his uncle (Appendix 3, subject 5). The twin sister (Appendix 3, subject 2) of the patient's mother died of an aortic rupture where the cause and age of presentation of aortic complication remained unknown. Routine genetic testing

revealed a probably pathogenic mutation in the *ACTA2* gene (c.977C>A, p.T326N), but did not co-segregate with the disease running in family 2 (Appendix 3). Due to the fact that the family history of both index patients (I6 and I9, respectively) correlate with the disease state of FTAAD, hence that FTAAD occurs without any syndromic features of MFS and MFS-related syndromic diseases, and that FTAAD show a rather reduced penetrance and variable expressivity, we have recruited both healthy and suspected unhealthy family members of I6 and I9 for a indirect DNA markers analysis with FTAAD loci.

3.18.2 Marker selection

To date, three causal loci *AAT2* on chromosome 5q13-14 (Goe *et al.*, 2001; Kakos *et al.*, 2003), *AAT1* on chromosome 11q23-24 (Vaugham *et al.*, 2001), *TAAD3* locus on chromosome 15q24-26 in conjunction with bicuspid aortic valve disease; BAV (Goh *et al.*, 2002; Ellison *et al.*, 2007) and two genes *MYH11* mapping on chromosome 16p12.12-13-13 in association with patent ductus arteriosus; PDA and *ACTA2* mapping on chromosome 10q22-24 (Guo *et al.*, 2007) have been described for the heterogeneous disease TAAD. The haplotypes were ascertained by the number of repeats of each DNA marker. Three microsatellite markers located close to a candidate gene or a marker locus (Figure 3-6) were selected which consisted of variable number of dinucleotide CA_n repeats representing with a high level of heterozygosity (>0.80). Their sequences were taken from previously published papers and primer sequences flanking every genetic marker (Appendix 7) were from the UniSTS database.
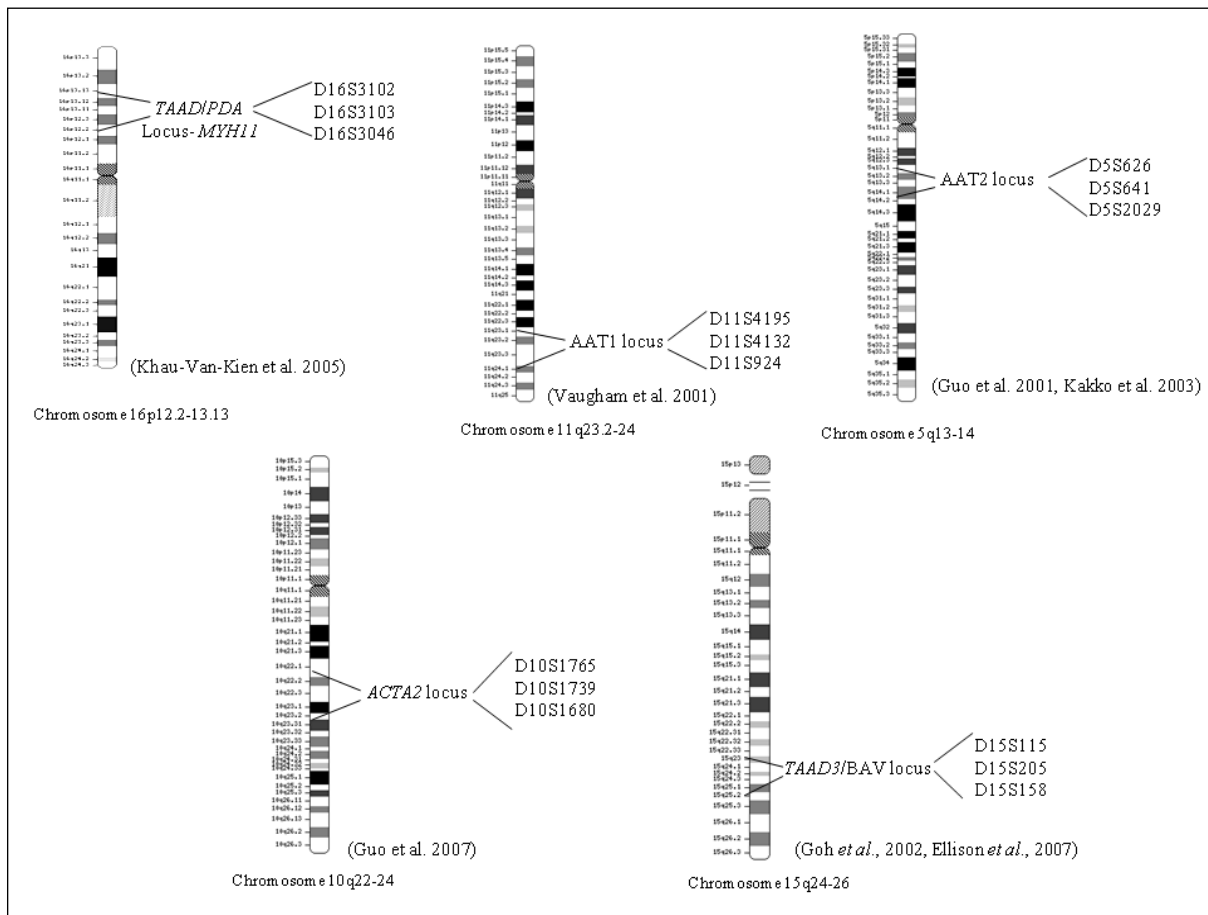
Figure 3-6:   **Chromosomal position of DNA markers for loci linked with TAAD.** Three candidate loci for TAAD; *AAT1* locus (5q13-14), *AAT2* locus (11q23-24) and *TAAD3/BAV* locus (15q24-26) and two candidate genes; *MYH11* (*TAAD/PDA* locus) and *ACTA2* (*TAAD4* locus) are indicated along with their chromosomal location.

3.18.3 Testing and optimization of TAAD DNA markers for linkage analysis

As initial step, primer pairs covering each DNA markers were tested for their optimum annealing temperature and the fragments were generated using short range PCR using DNA *Taq* polymerase. The PCR composition and thermal cycling conditions were the same as described in the section of short range PCR. Each of the STR markers was amplified using 6-carboxyfluorescein fluorescently labeled forward primer and unlabeled reverse primer. The size of the microsatellite fragments ranged from 87 bp to 300 bp (Figure 3-7). Majority of the DNA markers were successfully generated under annealing temperature of 55°C, rest of the DNA amplicons were yielded at 51°C, 58°C and 61°C, respectively (Table 3-13). For marker linkage analysis, a total volume of 0.5μL of PCR product in respect of the band intensity (stronger band intensity: 0.5μL and weaker band intensity: 1.5μL) was added to the corresponding tube containing a cocktail of 0.5μL GeneScan™ 500 TAMRA size standard

and 16 μL Hi-Di^{TM} Formamide. The complete mixture was then denatured for 3 minutes at 95°C and immediately transferred on ice until loading into a genetic analyzer.

Table 3-13: Annealing temperature of primer pair for DNA marker amplification	
Annealing Temperature (T$_a$)	**DNA markers**
51°C	D5S626 (100), D11S924 (119)
55°C	D5S641 (265), D15S158 (81), D15S115 (115), D15S205 (160), D10S1680 (217), D10S1739 (239), D16S3102 (170), D16S3046 (102)
58°C	D16S3103 (233), D10S1765 (180)
61°C	D11S4132 (206), D5S2029 (126), D11S4195 (275), D5S2029 (300)
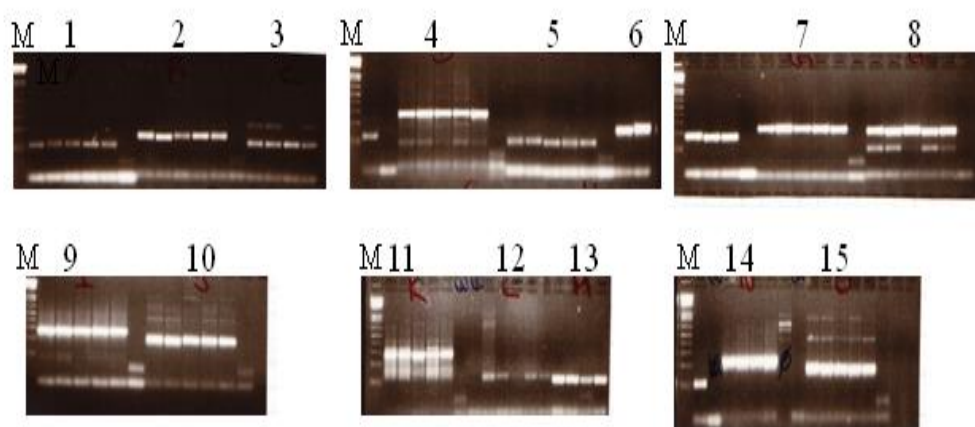
Figure 3-7: PCR products of DNA markers used in segregation analysis. Five controls (wells 1-5) were used for the optimization of DNA markers. (well 6) Blank. (M) 100 bp DNA markers, (1) D16S3046, (2) D15S205, (3) D15S115, (4) D5S641, (5) D15S158, (6) D16S3102, (7) D10S1739, (8) D10S1680, (9) D5S2029, (10) D11S4132, (11) D11S4195, (12) D5S626, (13) D163103, (14) D10S1765, (16) D5S2029.

3.18.4 Sizing and Genotyping of DNA markers

The fluorescence labeling of the forward primer and addition of GeneScan^{TM} 500 TAMRA size standard in each sample allowed the detection and sizing of the fragments using ABI

Prism 3130xl Genetic Analyzer. Both STR and sizing DNA molecules were injected electrokinetically into the capillary by applying a voltage to each sample. During electrophoresis, a high voltage of 15kV for 10 seconds was applied throughout the capillary that enabled the product separation by size based on their molecular charge. The complete fragment analysis was performed at 60°C to prevent the formation of DNA secondary structure (Wenz *et al.*, 1998). Upon size separation, the fragments traveled through a detector window. Two colored system was used to label the products, the internal standard was labeled with a TAMRA fluorephore and the STR alleles with 5'FAM. To note, only the forward strands were incorporated with a fluorescent dye. Thus, under denaturing condition, the labeled forward strands were detected by exciting the dyes using a laser beam. The light emitted by each sample was detected using a CCD camera. Because each dye emitted light at a different wavelength (Table 3-14) when excited by a laser, all colors, and therefore fragments could be detected and distinguished between them.

Table 3-14:   Dye properties

Fluorescence Dye	Color	Excitement maximum (nm)	Emission maximum (nm)
5'FAM	blue	493	522
TAMRA	red	560	583

As part of the initial set of data, the light emitted by each fluorescently labeled fragment was interpreted by applying specific algorithms to the intensity in order to correct the spectral overlap between the dyes and the size of the fragments. After correction, the fluorescence intensities were displayed as peak in the electropherogram based on their color and size. GeneMapper analysis software was used to size and genotype unknown DNA fragments by using the standard curve (Figure 3-8) generated from the fluorescent intensity of the known fragments of the internal size standard. The internal size standard was labeled with a different colored dye so that it could be spectrally distinguished between DNA fragments of unknown size. Under denaturing condition, only the forward 16 labeled DNA fragments of the TAMRA size standard were detected by the genetic analyzer and the 16 different single fragments were displayed as electropherogram peaks (Figure 3-9). The fragment size ranged from 35 to 500 bp. During genotyping analysis, it was made sure that every peak of the known size standard was detected and labeled correctly, before precise sizing and genotyping of each unknown DNA fragment.
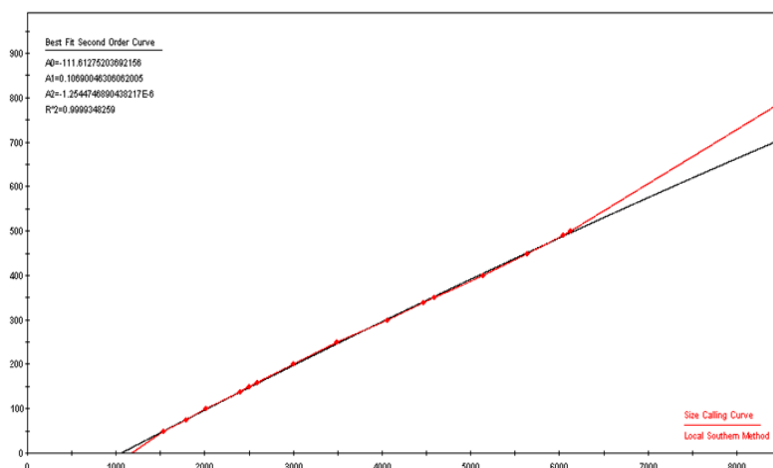
Figure 3-8:   Standard curve of TAMRA internal size standard.
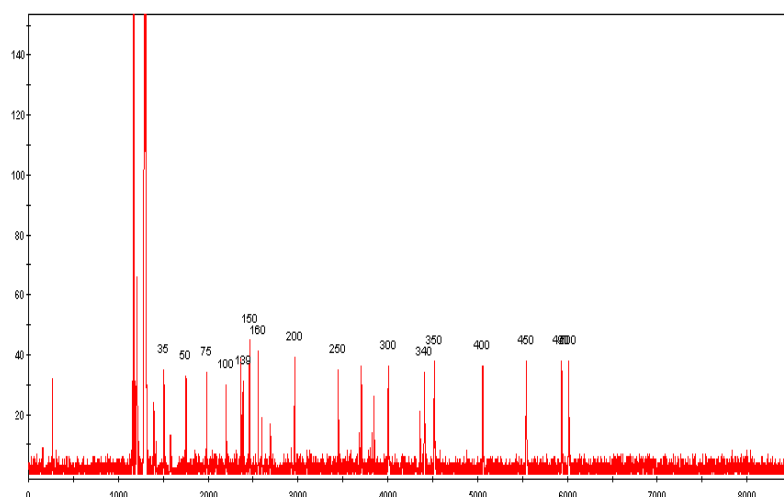
Figure 3-9:   Fluorescence peaks of TAMRA 500 internal size standard. Size range: 35 500 bp (35, 50, 75, 100, .139, 150, 160, 200, 250, 300, 340, 350, 400, 450, 490 and 500). Only one strand is labeled with fluorephore. Thus, the unlabeled strands do not interfere in the peak detection of the labeled fragments when run under denaturing condition. A corrected electropherogram with precise size of each sample was generated upon calibrating the fragment size and detection length between internal size standard and unknown DNA fragments.

One peak allele was observed if a subject was homozygous (Figure 3-9, left) and two peak alleles if heterozygous (Figure 3-9, right) for a STR marker. The number of CA_n repeats of a specific marker in each sample was determined by calculating the difference between the expected product size and *CA* repeats and the product size determined by GeneMapper.
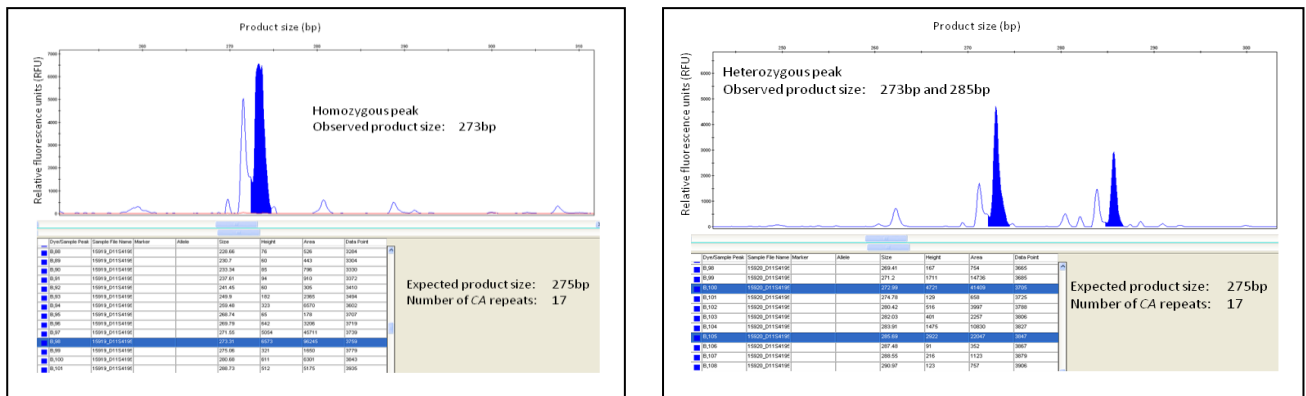
Figure 3-10: Electropherogram of a STR marker. One allele designates homozygous for marker xy and two alleles for heterozygous.

How to calculate the number of *CA* repeats in a subject:

Example: 275 bp (expected product size)   -   273 bp (observed product size)

      =   2 bp (difference)

This means 17 *CA* repeats in 275 bp and 16 *CA* repeats were contained in 273 bp.

3.19   Custom-based high-density MFSTAAD resequencing microarray (Affymetrix)

A novel large-scale microarray technology by Affymetrix allowed the parallel resequencing of multiple genes in a single experiment. The classical resequencing workflow includes eight major steps these include the selection of genomic target DNA, amplification of target sequence, quantitation and pooling, fragmentation and end-labelling, hybridization of target fragments to the array, washing steps and data analysis (Figure 3-11). Each step will be particularized in the next sections. A resequencing array consist of million copies of unique probe species, each containing of many copies of a 25 bp long probe of defined sequence. For each base interrogation, a total of eight probe species were required (four probes for each DNA strand; each of them were identical except for the middle nucleotide that was replaced by A, C; G or T, to allow interrogation of every DNA variant) (Figure 3-12).
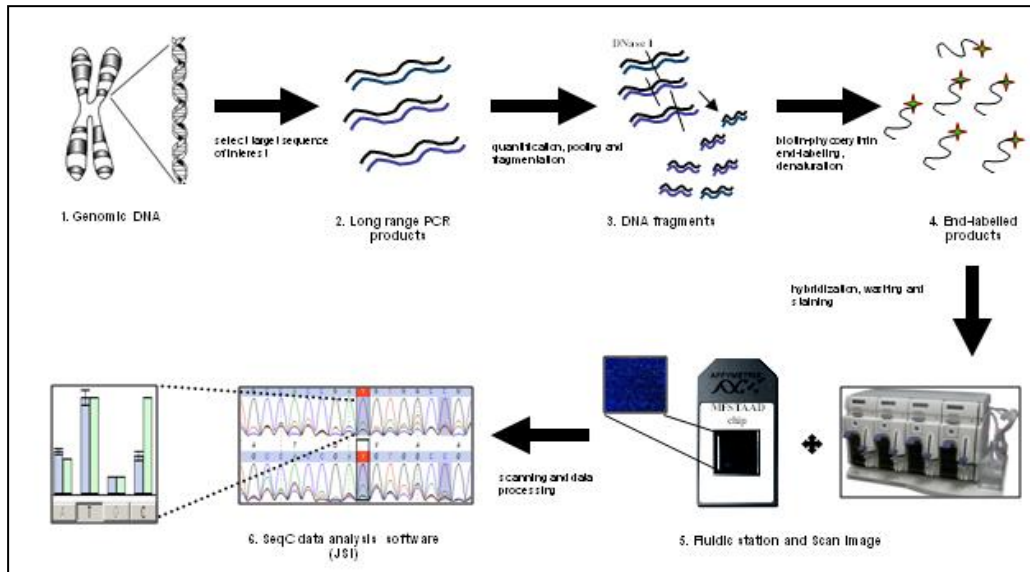
Figure 3-11: General resequencing workflow.
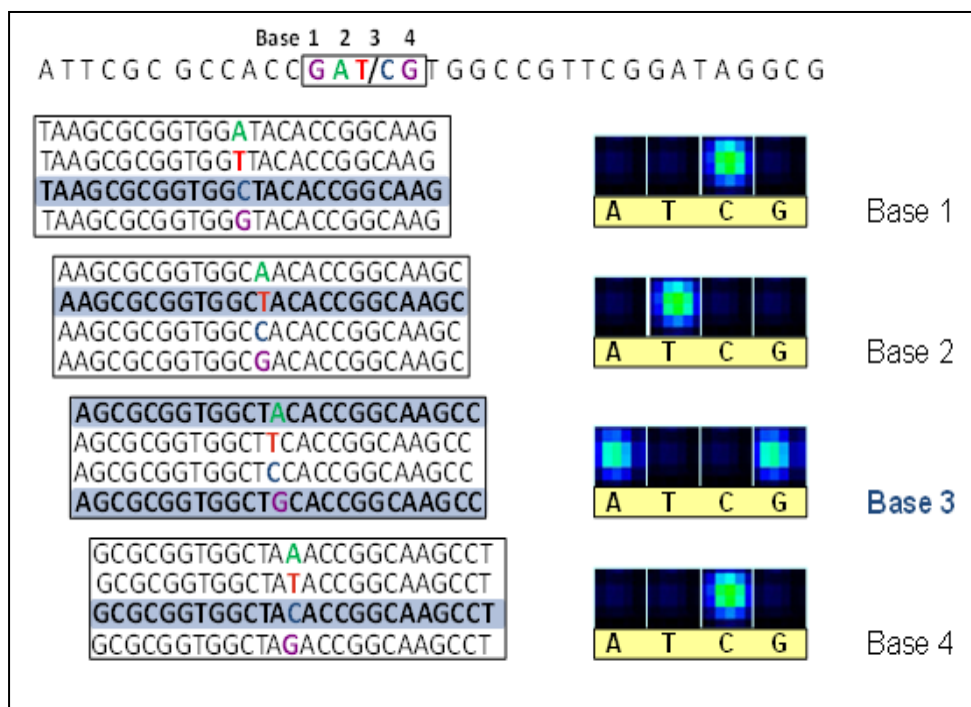
Figure 3-12: Array- based resequencing strategy. During hybridization, each base of the reference sequence (top row) is interrogated with one perfect match probe (bolded letter in highlighted in blue, left) and three mismatch probes. Four different 25-mer probes are required to resequence one base of a single stranded DNA; they are identical except for the central position where A, G, C or T is incorporated to enable efficient detection of all possible substitutions. Fluorescent signals of four probe species are depicted for each of the four

46

interrogated bases (right panel) using sequence analysis software provided by Affymetrix which will be in later sections. Two fluorescent signals of similar intensity indicate a heterozygous change of base 3.

3.19.1 MFSTAAD microarrays

A total of 88 arrays were provided by Affymetrix for a 100-kb format microarray, 17 of these arrays were used for the validation of analytical sensitivity and its results reproducibility and the remaining 66 arrays were apportioned between two different laboratories, Hannover and Dortmund, 38 and 28 arrays, respectively (Figure 3-12). Initial steps including target selection and amplification, and quantitation, pooling and purification was performed in the main labs, pre-hybridization steps such as fragmentation and end-labelling of the DNA fragments and target hybridization to the array was solely performed in the department for Medical Genetics, MFT Services in Tübingen where the microarrays have been designed. Partial quantitation of PCR amplicons for 25 Hannover arrays were performed in CorTag, Dortmund, and the remainder were quantified in the institute of Immunology, MHH, Hannover, in order to reduced the potential effect of transporting and frequent freezing and thawing on the overall DNA quality.
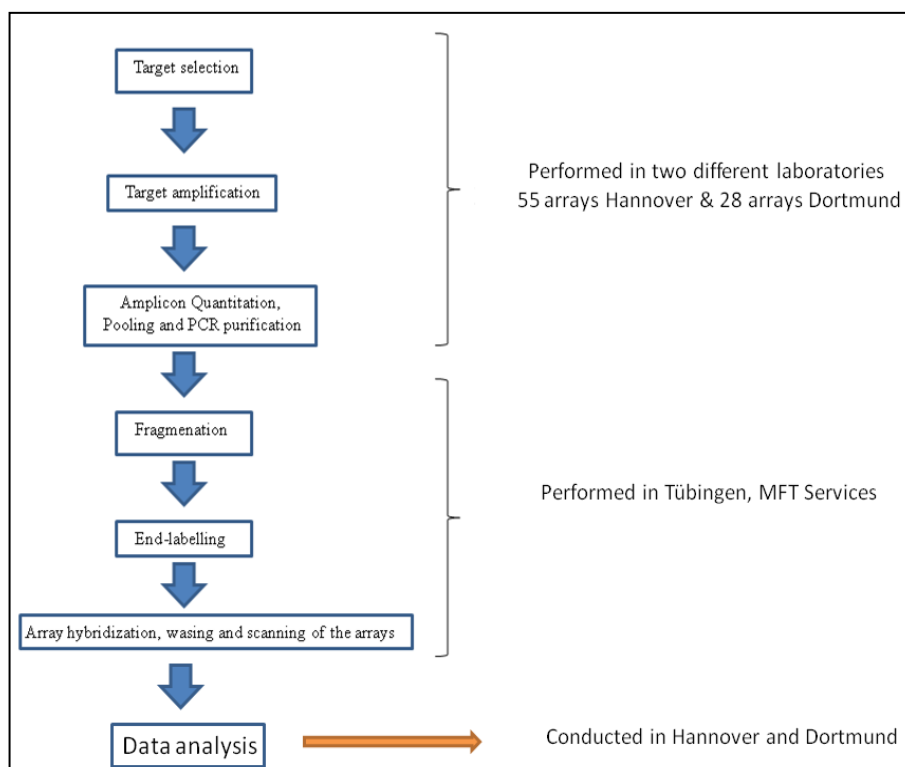
Figure 3-13: Workflow of MFSTAAD resequencing microarray.

3.19.2 Target sequence and probe selection

A 100-format (117-kb) Affymetrix resequencing array platform was used to design and construct a customized resequencing chip, the MFSTAAD array. According to the custom array design guide, the sequences of interest of eight genes (*FBN1* (fibrillin-1), *TGFBR1* (transforming growth factor, beta receptor 1), *TGFBR2* (transforming growth factor, beta receptor 2), *MYH11* (myosin, heavy chain 11), *ACTA2* (actin, alpha 2, smooth muscle, aorta); *COL3A1* (collagen, type III, alpha 1), *SLC2A10* (solute carrier family 2, member 10) and *NOTCH1* (notch 1) were identified and downloaded from the Ensembl database and converted into FASTA format and quality checked (Figure 3-11, step 1). Specific sequence regions such as repetitive elements, internal duplications that may have an impact of the hybridization process were checked using RepeatMasker. No repeats and internal duplications were found. The final reference sequences were then used for probe and primer selection. The sequences comprised of a total of 222 coding exons plus 43 bp of each flanking intronic region (each exon-intron boundaries) (Table 3-15), which included a total of 106.322 bp of target sequence. For the interrogation of each base of the target sequence a total of 425.288 different probe species was synthesized on the array. The MFSTAAD array was a duplicate design, thus the 425.288 different probe species were synthesized on two defined field. As a positive control, the 7.5kb IQ-EX control template was used.

3.19.3 Long range PCR assay

Long range PCR assay has a high fidelity for the amplification of larger DNA fragments, which also reduces the number of PCR reaction when compared to conventional short range PCR methods.

Table 3-15 Candidate genes of TAAD for array design				
Gene	Number of exons	Number of bases sequenced	Total Number of 25-mer probe (8 probes/base)	PCR reactions
ACTA2	9	1993	15944	2
COL3A1	51	8959	71672	5
FBN1	65	14650	117200	17
MYH11	41	9433	75464	12
SLC2A10	5	2326	18608	3
TGFBR1	9	2382	19056	3

TGFBR2	8	2708	21664	4
NOTCH1	34	10710	85680	8
Total	222	53161	425288	54
plus 43 bp of each exon-intron boundary				

3.19.3.1 Testing of long range PCR assay kit

Several long range PCR kits are available on the market, to get the best kit for this thesis work, several long range PCR kits (KOD-XL DNA polymerase (*Novagen*), Expand Long Range dNTPack (*Roche*), GoTaq Flexi DNA polymerase (*Promega*) and Qiagen LongRange (*Qiagen*)) were tested for their efficient and accurate amplification of 222 coding exons plus 43 bases of each exon-intron boundaries covering all the genes *FBN1*, *TGFBR1*, *TGFBR2*, *COL3A1*, *ACTA2*, *MYH11*, *SLC2A10* and *NOTCH1* in order to get the best fit kit for MFSTAAD target DNA amplification (Figure 3-11, step 2). Primer sequences, composition and thermal cycling conditions of each long range PCR assay kits are listed in the appendix (Appendix 8-12). As preliminary testing, the 65 exonic regions of the *FBN1* gene were used for the selection of a suitable kit which was cost-effective and required minimum optimization steps followed by the amplification of the exons of the remaining 7 genes. The correct composition of each target PCR was verified using bi-directional Sanger sequencing reaction. Two different size range and three different annealing temperatures for fragments < 8kb and > 8kb were applied. To determine the efficacy of amplification long-range PCR enzyme, we used three controls. A total amount of 100ng genomic DNA have been used for the PCR assay and the final product sizes were in the range between 850 bp to 11.500 bp.

3.19.4 PicoGreen quantification, pooling and purification of PCR amplicons

Application of equimolar concentration of each target amplicons in the hybridization process was necessary in oder to get a good quality and reliable amount of sequence information from the MFSTAAD resequencing array 8Figure 3-11, step 2-3). For larger number of samples, the quantification of PCR amplicons was performed using the PicoGreen quantification method. The PicoGreen quantitation reagent is a ultra-sensitive fluorochrome that binds selectively to double-stranded (ds) DNA. This dye emits light at its maximum when it is chelated to dsDNA. Procedures on quantitation was performed according to the instructions by Affymetrix and the following worksheets were downloaded from Affymetrix homepage:

- PicoGreen Quantitation Protocol
- PicoGreen Quantitation Raw Data
- PicoGreen Quantitation Standard Curve
- PicoGreen Quantitation PCR Product Pooling

3.19.4.1 Quantitation and pooling of PCR amplicons

Briefly, at first picogreen working solution was prepared and kept in the dark until use. The DNA standard curve was prepared by adding 3.84µL (100 ng/µL) of lambda DNA to 296.16 µL of 1x TE buffer in a safe lock micro-centrifuge tube. The mixture was gently vortexed and centrifuged. The total mixture of 300µL was added to well C12 of a transparent 96-well plate. A two-fold serial dilution was made by transferring 150µL of DNA standard into each subsequent well until a concentration of 0.04ng/µL was reached (D12 to H12). The remaining wells were filled with 298µL of 1x TE buffer and 2µL of each PCR product was added to an empty well. The plate with the samples was shaken for 5 minutes at 900rpm and was gently centrifuged. A light protective 96-well plate was used for the DNA quantity measurement. 100µL of PicoGreen was added to all wells that were required for the measurement and the wells C12-H12 was also filled with 100µL PicoGreen for the DNA standard curve. The fluorescence intensity of PicoGreen was measured using a microplate reader and the final data was extracted using a user specified method with Magellan data analysis software.

Custom Settings for Magellan microplate reader:

Wavelength	Excitation at 485nm
	Emission at 535nm
Reads	3
Integration time	40µs
Gain setting	manual 69 (any overflow should be diluted with TE and the measurement has to be repeated for that particular sample)

At first, a blank reading was obtained. After blank reading, a total of 150µL of each sample was added into the corresponding wells containing PicoGreen and the measurement of the target samples was started. The raw data of blank and the raw data of the samples were entered in the appropriate worksheet (PG protocol) to generate a standard curve (Figure 3-14). The standard curve was used to calculate the amount of each DNA sample required for pooling. Equimolar amounts of each 54 PCR amplicons from each patients sample were pooled at a concentration of 150 picomolar per PCR fragment for a 100-array format. The

amount of sample required from each amplicon was generated from the Affymetrix PicoGreen Quantitation worksheet. Pooled PCR products were then purified using QIAquick PCR purification kit according to the protocol of the vendor.
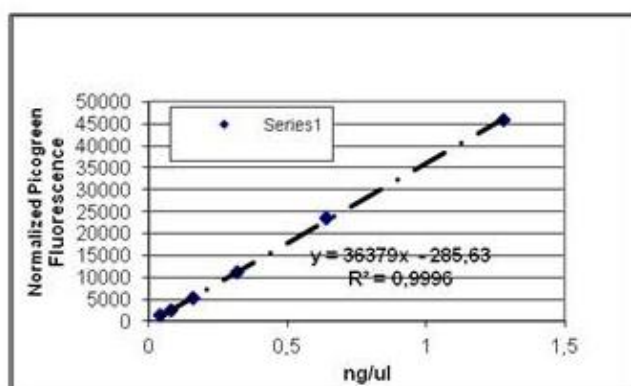
Figure 3-14: Standard curve of PicoGreen. The standard curve is automatically generated based on the values entered in the PG raw data input. The pooling of amplicons was continued when the standard curve was linear and the value for R^2 was >0.9, the reading was repeated if the value of R^2 was below 0.9.

3.19.5 Fragmentation

The samples were then subjected to DNA fragmentation (Figure 3-11, step 3) using fragmentation reagents from the Affymetrix resequencing assay kit. The set up of fragmentation reaction and the thermal condition for the fragmentation has employed as described in the GeneChip® CustomSeq® Resequencing array protocol. The fragmentation reaction was performed in a reaction volume of 28µL at 37°C for 35 minutes with 0.015U of fragmentation DNAase enzyme per microgram DNA and was inactivated at 95°C for 15 minutes. Successful fragmentation was checked on a 20% TBE PAGE gel followed by staining with SYBR Gold nucleic acid staining. Proper fragmented DNA products were in the range 20 to 200 bp (Figure 3-15). Under or over-fragmented DNA samples were repeated.

Lane 1=	Ladder
Lane 2=	Over-fragmentation
Lane 3=	Correct fragmentation
Lane 4=	Under-fragmentation
Lane 5=	Ladder
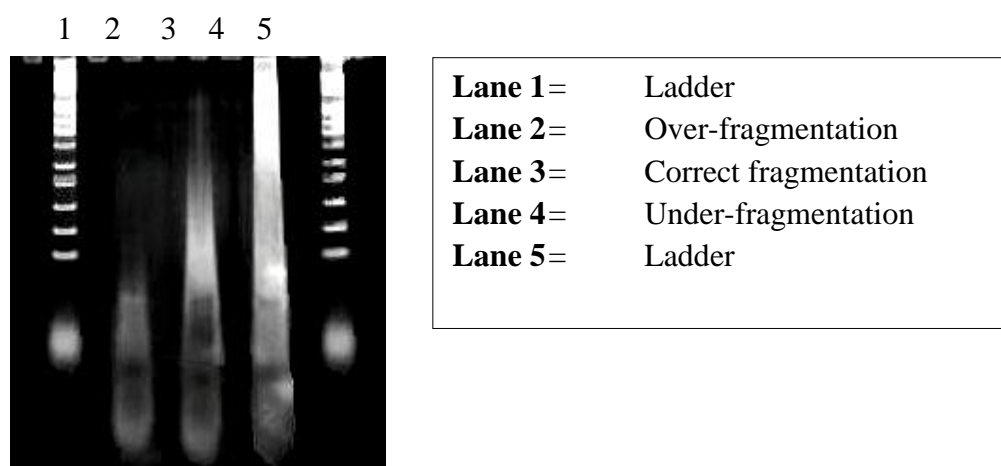
Figure 3-15:   Correct fragmentation of Target amplicon. Correct fragmented amplicons should appear as a smear in the range from 20 to 200 bp (lane 3). Both over-fragmentation (lane 2) and under-fragmentation (lane 4) have an impact on the performance of the array (adapted from GeneChip® CustomSeq® Array protocol).

3.19.6 Labeling and Hybridization

Fragmented DNA samples were end-labeled using DNA-labeling reagent biotin (Figure 3-11, step 4), which was included in the Custom array resequencing assay kit. Labeling was performed following the array protocol. The oligonucleotide control reagent included in the same kit contains a gridding control which serves as hybridization control.

3.19.7 Washing, staining and data scanning

The washing, staining and data scanning of the arrays were performed under fluidic stations following the manufacturer's protocol (Figure 3-11, step 5). In order to increase the detection of end-labeled biotinylated probe-fragment assemblies, an additional amplification step with anti-streptavidin biotinylated antibody was performed which is illustrated in (Figure 3-16). On the left are the steps which illustrate the double streptavidin-biotinylated antibody amplification. Following the hybridization of target samples on the microarray, the arrays were scanned using the GeneChip® 3000 scanner (Figure 3-11, step 6).
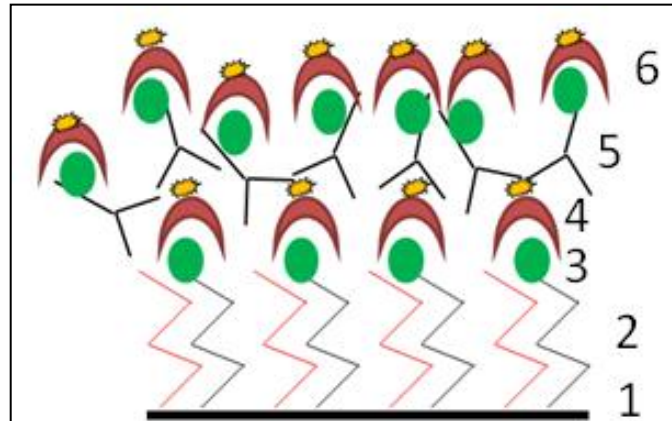
Figure 3-16: Streptavidin-Phycoerythrin staining with double streptavidin-biotinylated antibody amplification. (1) Array, (2) Target-probe hybrid, (3) Biotin binding to the target-probe hybrid, (4) adding of Streptavidin-phycoerythrin complex which bind to biotin, (5) adding of Antistreptavidin biotinylated antibody, (6) second amplification of streptavidin-phycoerythrin.

3.19.8 Data acquisition and sequence data analysis

The final data was generated and analyzed using GeneChip® Resequencing Analysis software, version 4.0. Current base calling relies on the adaptive background genotype calling scheme (ABACUS) which has been developed by (Cutler *et al.*, 2001) (Figure 3-11, step 6). This algorithm allows the detection of homozygous and heterozygous single nucleotide DNA variations such as A, C, G, T and AC, AG, AT; CG, CT, GT, respectively and "no call" if none of the models listed above match with the probe-target hybridization for a particular DNA position. The base-calling scheme calculates the likelihood of a specific model from the fluorescent intensities of forward probe-target and reverse probe target species, and these data are then used to determine the overall likelihood of a model for a given nucleotide position. The call rates were improved by analyzing a minimum of 15 arrays as a batch. Additionally, a commercially available data analysis software SeqC JSI Medical Systems was also employed.

3.20   Characterization of novel DNA variants

DNA variants were defined as novel sequence changes when they were absent in the dbSNP databank, in the 1000 genome project and in the literature. The degree of pathogenicity of each novel DNA variant were characterized using *in silico* biometric mutational analysis programs (BMAPs) which will be discussed in the next section. Furthermore, a co-segregation of known and novel DNA variants was performed in family members where ever

it was possible to evaluate whether the detected variant co-segregated with the disease in that particular family.

3.20.1 *in silico* biometric verification of DNA variants

A series of BMAPs, Mutation taster (MT); PMut (PMut); PolyPhen 2 (PP2), NetGene2 (NG2), and FruitFly (FF) were introduced to evaluate the potential pathogenic effects of all novel mutations found with the "MFSTAAD" array. The p-scores provided by each BMAP were used to define the severity of a specific sequence alteration. A sequence variant was assigned as possibly disease-causing (PDC) if one these biometric programs listed above provided a p-score close to 1. To note, these scores provided here did not refer to "probability of error" but to "probability of prediction", for instance a p-score close to 1 indicated a high certainty that the prediction was reliable. In addition to the p-score, PMut provided an r-value for every requested sequence alteration. The r-value was used for definite reliability of the prediction 0 (low reliability) and 9 (high reliability).

4. *Results*

4.1 Selection of different cohorts

In this work, we have selected a large panel of subjects, the prime group consisted of subjects by whom MFS and/ or LDS has been suspected but were no carriers of mutations causing syndromic forms of TAAD, the other group were composed of probands who have been diagnosed for TAAD, and the remaining subset of group were subjects who died of sudden rupture of the thoracic aorta of unknown cause. Majority of the cases were male subjects both in retrospective and prospective cohorts and the age of the probands ranged from 11 years to 58 years of age and 26 years to 81 years of age in the retrospective and prospective cohorts, respectively. The composition of a diverse cohorts should allow us to examine the distribution of disease causing mutations and type of mutation in a preselected population by which TAAD occur as a syndromic feature or as an isolated non-syndromic disease by using various molecular technology approach.

4.2 Results of the custom-based MFSTAAD microarray

Various factors in the pre-(yield of high DNA quality and quantity) and in the post PCR reactions such as quantitation and pooling, fragmentation and labelling have been carefully monitored in order to achieve a maximum quality of sequence information by high-density MFSTAAD resequencing microarray.

4.2.1 Results of Long- Range PCR assays

Long range PCR assay has substantially reduced the number of PCR reactions that was required to amplify a total of 222 coding exons plus exon-intron boundaries of eight target genes associated with syndromic and non-syndromic cardiovascular diseases of the thoracic aorta. In order to find the best long range PCR kit with minimum optimization steps required, we selected various long range PCR kits and compared the yield and quality of PCR amplicons generated from these selected PCR kits. For reliability and specificity of correct amplification of target DNA sequence, we have selected two control DNA samples of two unrelated subjects. Herein, the results of only one subject were shown, since the results were identical.

4.2.1.1 KOD XL DNA polymerase Long Range PCR kit, Novagen

KOD XL kit showed irregularity in the amplification of products <8 kb (Figure 4-1), the best result was obtained at 62°C with 3% DMSO, whereby optimization was required for

fragments of exon 1 (lane 1), exons 4-5 (lane 3), exons 34-39 (lane 6) and exons 45-49 (lane 7) of the *FBN1* gene which did not work under any of these conditions. The same result was obtained for *FBN1* fragments >8 kb (Figure 4-2), two of the fragments with the primer pairs for the exons 06-08 (lane 10) and 09-13 (lane 11) worked best at 64°C, and the primer pair for fragment covering exons 60-65 (lane 15) worked best at 62°C. The remaining primer pairs for exons 14-18 (12) and exons 30-33 (13) required optimization.
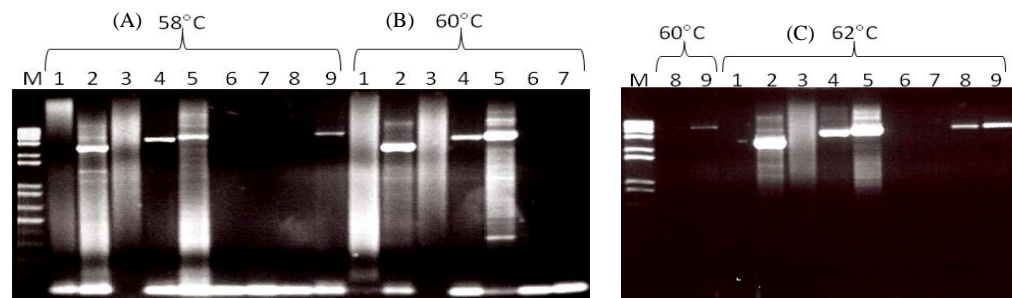
Figure 4-1: **Amplification results of fragments <8 kb of the *FBN1* gene using the KOD XL Long Range DNA polymerase.** PCR products were run on 2% agarose gel electrophoresis along with 1kb (+) DNA marker (M). (1) *FBN1*-Exon 01: 837 bp (2) *FBN1*-Exon 02-03: 2.788 bp , (3) *FBN1*-Exon 04-05: 4.333 bp, (4) *FBN1*-Exon 19-23: 4.018 bp, (5) *FBN1*-Exon 24-29: 4.833 bp, (6) *FBN1*-Exon 34-39: 7.337 bp, (7) *FBN1*-Exon 45-49: 7.614 bp, (8) *FBN1*-Exon 50-54: 5.297 bp and (9) *FBN1*-Exon 55-59: 5.860 bp. Top row A-C show the various annealing temperatures used in the corresponding PCR cycling condition.
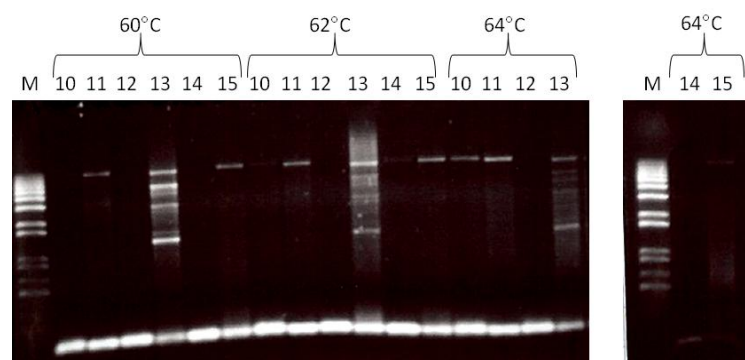
Figure 4-2: **Amplification results of fragments >8kb of the *FBN1* gene using The KOD XL Long-range DNA polymerase.** PCR products were run on a 0.8% agarose gel electrophoresis along with 1 kb (+) DNA marker (M). (10) *FBN1*-Exon 06-08: 11.950 bp (11) *FBN1*-Exon 09-13: 10.955 bp, (12) *FBN1*-Exon 14-18: 11.636 bp, (13) *FBN1*-Exon 30-33: 10.108 bp, (14) *FBN1*-Exon 40-44: 11-792 bp, (15) *FBN1*-Exon 60-65: 11.424 bp, Top row

A-C show the various annealing temperatures used in the corresponding PCR cycling condition.

4.2.1.2 GoTaq Flexi DNA polymerase Long Range PCR kit, Promega

For the testing of GoTaq Flexi LongRange PCR kit, a total of nine amplicons of the *FBN1* gene with a size <8 kb and six amplicons >8 kb were selected. The reaction was performed under two different annealing temperatures. Amplicons <8 kb were run at 58°C and 62°C annealing temperature and amplicons >8 kb were run at 60°C and 62°C. GoTaq Flexi failed to amplify fragments using primer pairs of the exon 01 (lane 1), exons 04-05 (lane 3), exons 34-39 (lane 6) and exons 45-49 (lane 7) under annealing temperatures of 58°C and 60°C. Lane 2 represents the amplification of exon 02-03 which worked best at 58°C. Successful amplification of fragments was observed for exons 19-23 using any annealing temperature, whereby lane 8-9 worked best at 62°C. Two bands was observed in the lane 5 using primer pair for the fragment 24-29, whereby the upper band was the expected PCR amplicon. This kit was not efficient for the amplification of fragments >8 kb (data not shown).
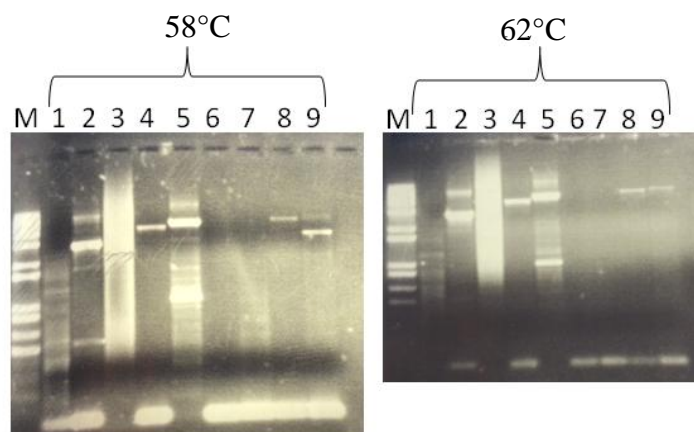
Figure 4-3: Amplification results of fragments <8 kb of the *FBN1* gene using the GoTaq® Flexi DNA polymerase. PCR products were run on 2% agarose gel electrophoresis along with 1 kb (+) DNA marker (M). (1) *FBN1*-Exon 01: 837 bp (2) *FBN1*-Exon 02-03: 2.788 bp , (3) *FBN1*-Exon 04-05: 4.333 bp, (4) *FBN1*-Exon 19-23: 4.018 bp, (5) *FBN1*-Exon 24-29: 4.833 bp, (6) *FBN1*-Exon 34-39: 7.337 bp, (7) *FBN1*-Exon 45-49: 7.614 bp, (8) *FBN1*-Exon 50-54: 5.297 bp and (9) *FBN1*-Exon 55-59: 5.860 bp. Top row (A) Primer annealing temperature at 58°C and (B) at 62°C.

4.2.1.3 Expand LongRange dNTPack Long Range PCR kit, Roche

In the preliminary testing of Expand dNTPack LongRange PCR kit, all amplicons of the *FBN1* gene were selected and were performed under the conditions and reagent composition

as instructed in the vendor's protocol, without optimization, no successful amplification was achieved. For optimization purpose, we have selected three amplicons with a size of <8 kp and three amplicons >8 kp of the *FBN1* gene were selected. Amplicons with a size of <8 kb were run at 58°C, 60°C, and at 62°C and amplicons >8 kb were run at 60°C, 62°C and 64°C. A positive target amplification result was achieved after addition of 3mM of Magnesium chloride ($MgCl_2$), but only amplicons <8 kb were successfully amplified under all three annealing temperatures (58°C, 60°C, 62°C). No results were obtained for PCR fragments >8 kb in size (data not shown).
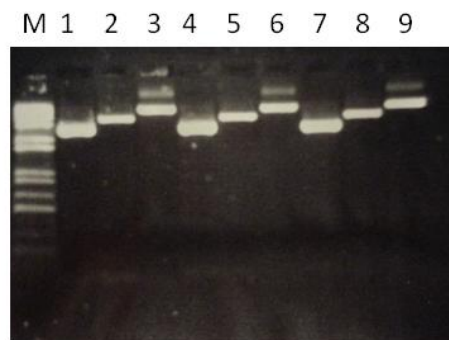
Figure 4-4:   Amplification results of fragments <8 kb of the *FBN1* gene using the Expand LongRange DNA polymerase kit. PCR products were run on 2% agarose gel electrophoresis along with 1 kb (+) DNA marker (M). (1) *FBN1*-Exon 02-03: 2.788 bp (2) *FBN1*-Exon 19-23: 4.018 bp and (3) *FBN1*-Exon 45-49: 7.614 bp at 58°C annealing temperature. Lanes 4-6 same amplicons as above under annealing temperature of 60°C and lanes 7-9 same amplicons as above under annealing temperature of 62°C.

4.2.1.4 Qiagen LongRange PCR kit, Qiagen

Under standard amplification step, the generation of amplicons of fragments <8 kb was successful, except for amplicon covering exons 45-49 of the *FBN1* gene was not generated under all annealing temperatures (58°C, 60°C, 62°C) (Figure 4-5, lanes 3, 6, 9). And amplicons >8 kb were successful for fragments covering exons 30-33 and exons 60-65 of the *FBN1* gene, but only under annealing temperature of 62°C. However, the complete exons of the *FBN1* gene was successfully amplified by changing the range of amplicon size for the smaller amplicons to <5 kb, and by adding Q-solution, and by amplifying larger amplicons >5 kb with three amplification cycling step with time increment of 20s in each amplification cycle in the third cycling step (Appendix 12) (Figure 4-6, optimization was repeated with five control subjects).
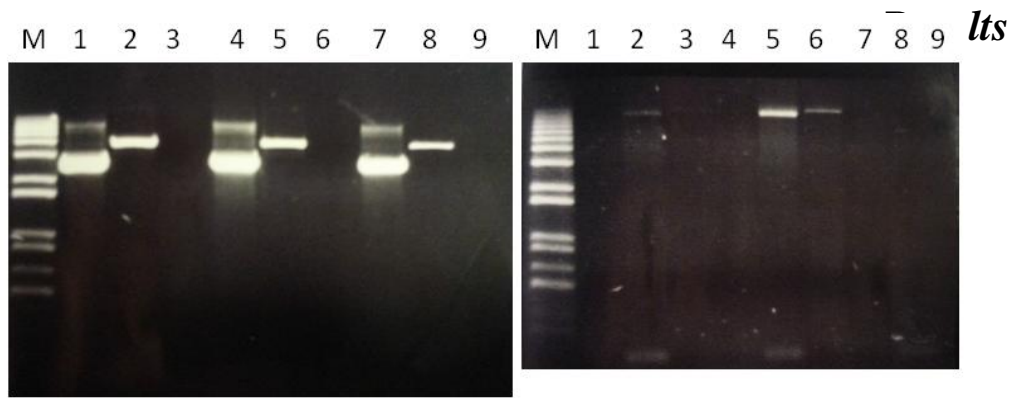
Figure 4-5: **Primary amplification of fragments of the *FBN1* gene using Qiagen LongRange PCR kit.** PCR products were run on 2% agarose gel electrophoresis along with 1 kb (+) DNA marker (M). **Left gel picture:** (1) *FBN1*-Exon 02-03: 2.788 bp (2) *FBN1*-Exon 19-23: 4.018 bp and (3) *FBN1*-Exon 45-49: 7.614 bp at 58°C annealing temperature. Lanes 4-6 same amplicons as above under annealing temperature of 60°C and lanes 7-9 same amplicons as above under annealing temperature of 62°C. **Right gel picture:** (1) *FBN1*-Exon 06-08: 11.950 bp (2) *FBN1*-Exon 30-33: 10.108 bp and (3) *FBN1*-Exon 60-65: 11.424 bp at 60°C annealing temperature. lanes 4-6 same amplicons as above under annealing temperature of 62°C and lanes 7-9 same amplicons as above under annealing temperature of 64°C.
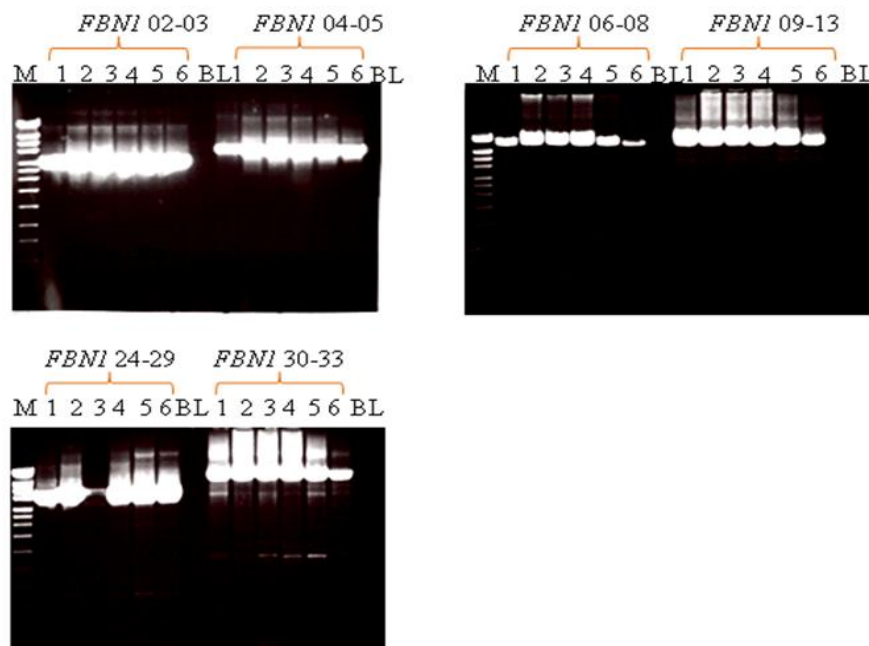
Figure 4-6: **Final optimization of Qiagen LongRange DNA polymerase.** Results of fragments of the *FBN1* gene <5 kb, without Q-solution (fragments >5 kb) and larger fragments >5kb under a three thermal cycling condition. Pictures on top row left and bottom row left first 1-6 lanes represent the amplification of fragments <5 kb: *FBN1* 02-03, 2.788 bp; *FBN*1 04-05, 4.333 bp; and *FBN1* 24-29, 4.833 bp and bottom row left last 6 lanes top row

right represent the amplification of PCR products >5 kb: *FBN1* 30-33, 10.108 bp; *FBN1* 06-08, 11.950 bp; *FBN1* 09-13, 10.955 bp.

4.2.1.5   **Final selection of a LongRange PCR kit for further analysis**

Among the serial long range PCR kits that have been tested in this study, the Qiagen LongRange PCR polymerase kit was the most efficient and reliable. This PCR kit had successfully generated all the amplicons of the *FBN1* gene and the remaining amplicons of the seven other target genes in this study (Figure 4-7). As final step of optimization of the long-range PCR assay, the amplified products were verified for their specificity by sequencing in the 5' and 3' direction using conventional Sanger sequencing reaction.

Lanes 1-16	*FBN1*-02-03 (3329), 04-05 (4362), 06-08 (11950), 09-13 (10955), 14-18 (11964), 19-23 (4083), 24-29 (4834), 30-33 (10109), 34-35 (3163), 36-39 (3605), 40-44 (11793), 50-54 (5298), 55-59 (5860), 60-65 (11424), *TGFBR1*-[¥]02-03 (4691), 04-09()
Lanes 17-32	*TGFBR2*-01 (779), 02-03 (6016), 04-05 (3534), 06-07 (3573), *ACTA2*-[¥]01-03 (5707), 04-09 (8982), *SLC2A10*-02 (2051), 03-05 (7528), *NOTCH1*-[¥]03-04 (1771), [¥]05-09 (2809), [¥]10-13 (2035), [¥]14-17 (3276), [¥]18-24 (3771), 25-30 (5233), [¥]31-34 (5327), *COL3A1*-[¥]01 (724)
Lanes 33-48	*COL3A1*-02-21 (10885), 22-40 (9602), 41-44 (2354), 45-51 (4772), *MYH11*-[¥]01 (654), [¥]02 (752), [¥]03 (614), [¥]04 (275), 05-09 (11165), 10-13 (12569), [¥]14-16 (5014), [¥]17-20 (3163), 21-27 (10217), 28-32 (8818), 33-41 (8703), 42-43 (5163)
Lanes 49-54	*NOTCH1*-[¥§]01, *TGFBR1*-[¥§]01, *FBN1*-[¥§]00-01, *SLC2A10*-[¥§]01

Figure 4-7 and Table 4-1:   Coverage of 222 exons in 54 PCR products using Qiagen Long-range PCR kit. [¥]Addition of 1x *Q*-solution in the amplification reaction. [$]Fragments run at 58°C under normal cycling condition. [§] Primer pair for exon 01-02 of the *NOTCH1* gene generated product at 64°C, the remaining fragments (lanes 1-16, 18-20, 22-24, 30, 33-36, 41-42, 45-48, 53-54) were run at 62°C under three cycling conditions by which the third cycle was performed with 20s time increment in each additional cycle.

4.2.2   Analytical sensitivity of the custom-based MFSTAAD resequencing microarray

The overall analytical sensitivity of the microarray was 85% (154/182), while the sensitivity of the assay in respect to single nucleotide DNA variants was 100% (153/153) in both the initial experiment and in its replicate (Table 4-2). In contrast, only the largest out of the 21 deletions tested (16 bp) was detected upon visual inspection due to a conspicuous decline in the hybridization strength (sensitivity rate: 4.8%). In none of the replicate experiments was the 25 bp duplication and the seven insertions detected (adapted from my own publication Kathiravel *et al.*, 2012). Practical verification included the analysis of the impact of short versus long-range PCR amplicons on the overall assay sensitivity. To assay this, a further experiment was carried out containing exclusively long-range amplicons with a total of 51 point mutations distributed over 3 DNA pools. Of these mutations, 48 were covered by short range PCR products in the initial experiments, replicate A and B. All of these mutations were detected correctly.

	Replicate-A* (7 arrays)	Replicate-B* (7 arrays)	Replicate C[%] (3 arrays)
point mutations	153/153 (100%; 97%-100)	153/153 (100%; 97%-100%)	51/51 (100%; 97%-100%)
insertions or duplications	0/8 (0%; 0%-0.4%)	0/8 (0%; 0%-0.4%)	
Deletions	1/21 (4.8%; 0%-25.9%)	1/21 (4.8%; 0%-25.9%)	

Table 4-2:   **Analytical sensitivity of the MFSTAAD resequencing assay.**

*Seven pools of mutated PCR products were analysed with two arrays each (Replicate-A and –B). Given is the detection rate in percent and, in parenthesis are the interrogation rates in percentage with the upper and lower 95% confidence intervals calculated with Wilson score method (http://faculty.vassar.edu/lowry/prop1.html). [%]3 pools with long range PCR amplicons containing a total of 51 point mutations.

4.2.3   General performance characteristics of the MFSTAAD custom microarray of two different cohorts (retrospective and prospective)

The general performance characteristics of the MFSTAAD assay were assessed using both retrospective cohort of 36 subjects who were mutation-negative for genes *FBN1*, *TGFBR1* and *TFGRB2*, a subset of 18 were only tested for genes *FBN1* and *TGFBR2*; and a prospective cohort of 30 subjects (Table 4-3). For the total of 66 samples analyzed, an initial call-rate (i.e. fraction of the total of 106.322 bp which could be base-called) of 94.4% and "no-call" rate of 5.7% was defined using the program GSEQ 4.1 data analysis software. The number of no calls could be resolved by using the SeqC commercially available sequence data analyzer, achieving an overall For the 66 samples analysed, an overall call-rate of 99.8%. The remaining 0.2% of ambiguous nucleotide DNA positions was found to locate within GC-rich sequence regions. An average of 301 DNA variants were base called using SeqC, of which about 90% could be corrected as wild-type upon visual inspection applying the constructed statistics by the software from previous runs. About 17.6% (53/301) revealed to be false positive DNA variants upon validation of these variants using conventional Sanger sequencing reaction and which were observed to be recurrent variant anomalies (for reference please see Appendix-13). The remainder were true single nucleotide variants (26/ per sample),

of which most of them represented to be single nucleotide polymorphisms (SNPs) and 0.4of which were defined as known or potentially pathogenic mutations. Only known and novel potentially disease causing mutations were confirmed by Sanger sequencing, because the remaining DNA presented mostly recurrent SNPs.

Data are mean values ± SEM. *Percentage of base pairs called either A, C, G or T by the *GSEQ* program. °Percentage of no calls made by *GSEQ*. **Improved call rate achieved by using SeqC software. §Total number of sequence variants called as homo- or heterozygous change by the SeqC program. †Number of true single nucleotide DNA variants. $Sequence changes which were listed as SNPs (single nucleotide polymorphisms), in the NCBI, UMD

Table 4-3:   General performance characteristics of the "MFSTAAD custom-array" in the prospective and retrospective cohorts.

	Total (n=66 subjects)	retrospective cohort (n=36)	prospective cohort (n=30)
Initial call-rate (%)*	94.4±0.2	94.0±0.3	94.8±0.4
Initial no calls (%) °	5.7±0.2	6.0±0.1	5.2±0.4
Improved call-rate (%) **	99.8±0.0	99.9±0.0	99.8±0.0
called variants (n) §	301±20	327±36	269±16
retained variants (n) †	26±2	29±1.4	23±2
possibly pathogenic mutations (n)$	0.4±0.1	0.3±0.0	0.5±0.1

(Universal Mutation Database) and HGMD (Human Gene Mutation Database).

4.2.4   Mutation yield and false positive rate

A total of 26 mutations in 22 individuals were found with the MFSTAAD resequencing microarray for retrospective and prospective cohorts from Hannover and Dortmund (A schematic diagram on the topography of each known and novel DNA variants is found in the Appendix 14) (Table 4-4). The mutation yield were substantially higher (13/30) versus (9/36) in the prospective group than in the retrospective cohort. To note, individuals from the retrospective group have undergone previous genetic testing a subset of 18 were negative for

a mutation in the genes *FBN1* and *TGFBR2* and the other half was negative for a mutation in an additional gene, *TGFBR1*. A total of eleven were among the known mutations that have been previously published (Table 4-5). The remaining 15 of novel possibly disease causing DNA variants (Table 4-6) were confirmed for their pathogenicity using *in silico* BMAPs and an amino acid alignment was performed to determine the conservation of each mutation between various species (Figure 4-8). Having a definite probably pathogenic effect on protein level (4/4 biometric programs) was obtained for the mutations *FBN1* c.6821G>C), p.C2274S in PL22, *MYH11* c.2005C>T ,p.R669C in R25; *NOTCH1* c.2734C>T, p.R912W in R4 and *ACTA2* c.598C>T, p.R198C in R14, which were predicted to affect the calcium-binding epidermal growth factor (cb-EGF) domain; the actin-binding domain (AB) of the myosin head of the myosin protein, the EGF-like domain of the notch-1 protein and in the exon 2 of the *ACTA2* gene, respectively. A total of 9 including 5 missense mutations (DNA variants *COL3A1* c.217G>C, p.D73H in PD20; *FBN1* c.3715A>G, p.I1239V in PD19; *MYH11* c.5676G>C, p.E1892D in R6; *NOTCH1* c.939C>G, p.H313Q in PD19 and T*GFBR2* c.1159G>T, p.V387L in PD18 were called as probably damaging by 2 out of the 4 biometric programs. The remaining 4 DNA variants were splice site changes in the genes *MYH11* (c.4116+6T>A in PD17; c.4578+3A>G in PD9; c.4791+4C>T in R4) and *FBN1* (c.442+15G>T in R9), respectively and for the potential effect on splicing was predicted using three different splice-site prediction programs (MT, N2G and FF). Splice changes in the gene *MYH11* c.4116+6T>A and c.4578+3A>G showed a donor site increase by two splice site programs (MT and FF) and a donor site decrease was predicted by N2G. Splice variants (*MYH11* c.4791+4C>T and *FBN1* c.442+15G>T) had no potential effect on the splicing process. "Interestingly, a cardiac counterpart of *MYH11* Arginine 669, *MYH7* Arginine 663, has previously been found to be substituted by Serine in a patient suffering from hypertrophic cardiomyopathy (Richard *et al*., 2003)" (adapted from my own publication Kathiravel *et al.*, 2012). Two different mutations, one in the gene *COL3A1* p.R878H and one in the gene *SLC2A10* p.A283G were found in patient RL30 who was suspected for MFS. In terms of pathogenicity, the first mutation was defined as disease causing by one of the *in silico* programs, whereby the *SLC2A10* gene was classified as benign. Interestingly, a previously found mutation p.G822A (Eder et *al*., 2013) in the *COL3A1* gene which is located in the same triple helical domain and has been reported in a 28 year old female who had a classic form of vEDS in association with peripheral artery occlusive disease (Eder *et al.*, 2013), thus, it would be interesting to know whether our patient has the same clinical phenotype. In addition, the presence of an additional mutation in the *SLC2A10* gene (p.A283G) may not have

predisposing effect to TAAD due to the autosomal recessive nature of the ATS; it is less precedent to be a disease-causing DNA variant in our case. Another patient PD19 was a 26 year old male with an obvious appearance for classic form of MFS with thoracic aortic rupture, he was a carrier of two mutations in the gene *FBN1* p.I1239V and p.C1860R and one in the gene *NOTCH1* p.H313Q, from which the mutation *FBN1* p.C1860R was a previously known DNA variant (Attanasio *et al.*, 2008). The novel variant *FBN1* p.I1239V was assigned as probably disease causing by 3 out of 4 *in silico* programs, one of the program (PP1) could not assign a potential effect for this particular variant, and the DNA variant *NOTCH1* (p.H313Q) was assigned as probably disease causing by 2 out the 4 programs. Due to the fact, that both mutations in the *FBN1* gene have a potential effect on the fibrillin-1 protein it could be speculated that these two DNA disease causing variants alone were sufficient to cause the disease in PD19. In addition to the 15 novel mutations, eleven previously published single mutations have been detected by the array-based assay and were predicted to be disease-causing: three in the gene *ACTA2* (c.145A>G, p.M49V; c.773G>A, p.R258H; c.910G>C, p.G304R) and four in the gene *FBN1* (c.527A>C, p.Q176P; c. 217G>C; p. R1170H; c. 5578T>C, p.C1860R; c.6700G>A, p.V2334M) and two in the gene *MYH11* (c.2005C>T, p.R669H; c.4676C>T, p.T1558M) (Hoffjan *et al.*,2011; Waldmueller *et al.*, 2007; Hayward *et al.*, 1994; Robinson *et al.*, 2002, Attanasio *et al.*, 2008, Tjeldhorn *et al.*, 2006 and *HGMD* mutation database), whereby DNA variants *MYH11* p.R1669H (rs111404182), T1558M (rs11854563) have been defined as SNPs with extremely low frequency rates of 0.2% and 0.1% for both *MYH11* variants, respectively and were in reference to *in silico* programs a "probably damaging" variants. Noteworthy, the variant T1558M has been found twice in our study (PD7 and R20). Another synonymous DNA variant in the *TGFBR1* gene c.207C>T (S69S) has been listed as SNP but was predicted to have a potential effect on the splicing process. Additional variant in the *NOTCH1* gene c.3836G>A, p.R1279H has been recently classified as a single nucleotide polymorphisms and McBridge *et al*, 2008 reported this variant both in control and diseased subjects. Overall, a total of 26 of potentially pathogenic mutations were detected in 22 unrelated patients, suggesting a yield of the assay of 33%. To note the mutation yield was higher in the prospective group (13 versus 9), because the retrospective underwent pre-screening for mutation in the genes *FBN1*, and *TGFBR2*, by which part of the retrospective group from Hannover were tested for an additional gene, *TGFBR1*. The results between the two retrospective group from Hannover and Dortmund show a slight difference in the mutation yield, 4 versus 5, accordingly which was reflective of subjects from Hannover were tested negative for mutations in a total of three out of eight

target genes. In the investigated cohort, compound and digenic mutations were rare (0/66 and 3/66, respectively). False positive mutations were detected in 9 out of 66 patients, indicating a false-positive rate of 13.6% of the MFSTAAD microarray.

[&]The assay has been performed in two different laboratories (Institute for Human genetics, Hannover and in the CorTag, Dortmund). [%]Retrospective samples from Hannover are confirmed negative for mutations in the genes *FBN1*, *TGFBR1* and *TGFBR2* and from [€]Dortmund is negative for mutations in the genes *FBN1* and *TGFBR2*. *Fraction of patients carrying a possibly pathogenic mutation that was confirmed by means of conventional sequencing, in parenthesis is the result in percent with upper and lower 95% confidence limits. [§]Fraction of patients in which the software SeqC called a possibly pathogenic mutation

Table 4-4:	**Mutation yield and false positive rate of the MFSTAAD resequencing assay.**		
[&]**Laboratories**	**Retrospective/prospective and total number of samples (n)**	[*]**Mutation yield n, (%)**	[§]**False positive rate n (%)**
Hannover	[%]Retrospective (18) Prospective post-mortem (20)	4/18 (22.2%; 7.3%-48.1%) 9/20 (45%; 23.8%-68%)	3/18 (16.7%; 4.4%-42.2%) 2/20 (10%; 1.8%-33.1%)
Dortmund	[€]Retrospective (18) Prospective pre-mortem (10)	5/18 (27.8%; 10.7%-54%) 4/10 (40%; 13.7%-72.3%)	3/18 (16.7%; 4.4%-42.2%) 1/10 (10%; 0.5%-45.9%)
Hannover & Dortmund	Retrospective (36)	9/36 (25%; 12.7%-43%)	6/36 (16.7%; 0.07-33.5%)
Hannover & Dortmund	Prospective (30)	13/30 (43.3%; 26%-62.3%)	3/30 (10%; 0.03%-27.7%)
Hannover & Dortmund	Total samples (66)	22/66 (33.3%; 22.5%-46.1%)	9/66 (13.6%; 0.07%-25%)

that was shown to be false-positive upon conventional sequencing of the affected exon.

Table 4-5:	**Previously published missense mutations**		
Gene	**Mutation**	**Consequence**	**Reference**
ACTA2	c.145 A>G	p.M49V	Hoffjan *et al*. 2011
ACTA2	c.910 G>C	p.G304R	Hoffjan *et al*. 2011
ACTA2	c.773 G>A	p.R258H	Hoffjan *et al*. 2011

FBN1	c.527 A>C	p.Q176P	Waldmueller *et al*. 2007
FBN1	c.3509 G>A	p.R1170H	Hayward *et al*. 1994; Robinson *et al.* 2002
FBN1	c.5578 T>C	p.C1860R	Attanasio *et al*. 2008
FBN1[§]	c.6700 G>A	p.V2234M	Known as disease variant rs112084407 Tjeldhorn *et al*. 2006
MYH11[¥]	c.2005 C>T	p.R669H	http://www.ncbi.nlm.nih.gov/projects/SNP
MYH11[¥]	c.4673 C>T	p.T1558M	http://www.ncbi.nlm.nih.gov/projects/SNP
TGFBR1	c.207 C>T	p.S69S	Listed as SNP rs145033378 but potential effect on the splicing
NOTCH1	c.3836 G>A	p.R1279H	Mc Bridge *et al*. 2008

[§]DNA variant that has been previously described as disease causing variant in UMD-*FBN1* mutation database. [¥] DNA variants with small occurrence rate.

Table 4-6: **Affected protein domains of novel point mutation.**

Gene	Nucleotide change	Presumed Amino acid change	Affected protein domain
COL3A1	c.2633G>A	p.R878H	TH domain
COL3A1	c.217G>C	p.D73H	VWFC
FBN1	c.3715A>G	p.I1239V	cb-EGF-like (20)
FBN1	c.6821G>C	p.C2274S	cb-EGF-like (35)
FBN1[$]	c.442+15G>T	Splice change	MT: acceptor site increased N2G and FF: no change
SLC2A10	c.848C>G	p.A283G	TMD (8)

MYH11	c.2005C>T	p.R669C	AB domain, myosin head
MYH11	c.5676G>C	p.E1892D	Coiled coil domain
MYH11[$]	c.4116+6T>A	Splice change	MT: donor site increased N2G and FF: donor site decreased
MYH11[$]	c.4578+3A>G	Splice change	MT and FF: donor site increased N2G: donor site decreased
MYH11[$]	c.4791+4C>T	Splice change	MT: donor site increased N2G and FF: no change
NOTCH1	c.939C>G	p.H313Q	cb-EGF like (8)
NOTCH1	c.2734C>T	p.R912W	EGF-like (24)
ACTA2	c.592C>T	p.R198C	Natural variant
TGFBR2	c.1159G>T	p.V387L	PK domain

The online UniProt provides information on protein sequence and functional information and has been used to find which domain might be affected by the corresponding DNA variant. TH, triple helix; VWFC, van willebrand factor c; cb-EGF, calcium-binding epidermal growth factor domain; AB, acting binding; TMD, trans-membrane domain; PK, protein kinase; [$]DNA splice variants are examined for their effect on splicing changes using MT, N2G and FF.

COL3A1 c.2633G>A (p.R878H)

```
Human    P G A R G L P G P
Mutated  P G A H G L P G P
Put.     P G A R G L P G P
M.m.     P G A R G L P G P
M.m.     P G G R G L P G P
G.g.     P G A R G L P G P
```

MT: disease causing
PM: neutral
PP: benign
PP2. unknown

COL3A1 c.217G>C (p.D73H)

```
Human    D   Q E L D C P N P
Mutated  D Q E L H C P N P
Put.     D   Q E L D C P N P
M.m.     D   Q E L D C P N P
M.m      E   E P L D C P N P
G.g.     D   Q E L D C P N P
```

MT: disease causing
PM: neutral
PP: unknown
PP2: probably damaging

FBN1 c.3715A>G (p.I1239V)

```
Human    R   S C T D I D E C
Mutated  R S C T D V D E C
Put.     R   S C T D I D E C
M.m.     R   S C T D I D E C
M.m.     R   S C T D I D E C
G.g.     R   T C T D I D E C
```

MT: disease causing
PM: neutral
PP: unknown
PP2. Probably damaging

FBN1 c.6821G>C (p.C2274S)

```
Human     G T Y M C I C G P
Mutated   G T Y M S I C G P
Put.      G T Y M C I C G P
M.m.      G T Y M C I C G P
M.m.      G T Y M C I C G P
G.g.      G T Y M C I C G P
```

MT: disease causing
PM: pathogenic
PP: probably damaging
PP2: probably damaging

SLC2A10 c.848C>G (p.A283G)

```
Human     V  K V A A T L T A M
Mutated     V K V A G T L T A M
Put.      V  K V A A T L T A M
M.m.      V  K V A A T L T A M
M.m.      V  K V A A T L V A T
D.r       V  K V I A T L L A M
F.c.      V  K V L A T L T A M
```

MT: polymorphism
PM: neutral
PP: benign
PP2: benign

MYH11 c.2005C>T (p.R669C)

```
Human    M  T T L R N T T P
Mutated  M T T L C N T T P
Put.     M  T T L R N T T P
M.m.     M  T T L R N T T P
M.m.     M  T T L R N T T P
G.g.     M  T T L R N T N P
D.r.     M  T T L H N T Q P
```

MT: disease causing
PM: pathogenic
PP: probably damaging
PP2: probably damaging

MYH11 c.5676G>C (p.E1892D)

```
Human    E  A E E E S Q R I
Mutated  E A E E D S Q R I
Put.     E  A E E E S Q R I
M.m.     E  A E E E S Q R I
M.m.     E  A E E E S Q R I
G.g.     E  A E E E S Q R I
D.r.     E  S E E E S Q R I
```

MT: disease causing
PM: neutral
PP: unknown
PP2: possibly damaging

NOTCH1 c.939C>G (p.H313Q)

```
H.s.   G  GTCHNTHGG
Mutated  GGTCQNTHGG
Put   G  GTCHNTHGG
M.m.*  G  GTCHNTHGG
M.m   G  GTCHNTHGG
G.g.  G  GTCHNNHGG
D.r.  G  GTCLNTQGG
```

MT: disease causing

PM: neutral

PP: unknown

PP2: probably damaging

NOTCH1 c. 2734C>T (p.R912W)

```
Human  I  DDCRPNPC
Mutated  IDDCWPNPC
Put.  I  DDCRPNPC
M.m.*  I  DDCRPNPC
M.m.  I  DDCRPNPC
G.g.  I  DDCQPNPC
D.r.  I  NECESNPC
```

MT: disease causing

PM: pathological

PP: unknown

PP2: possibly damaging

ACTA2 c.592C>T (p.R198C)

```
Human  K  ILTERGYSFV
Mutated  KILTECGYSFV
M.m.*  K  ILTERGYSFV
M.m.  K  ILTERGYSFV
G.g.  K  ILTERGYSFV
D.r.  K  ILTERGYSFV
F.c.  K  ILTERGYSFV
```

MT: disease causing

PM: pathological

PP: unknown

PP2: probably damaging

TGFBR2 c.1159G>T (p.V387L)

```
Human  S  NILVKNDL
Mutated  SNILLKNDL
Put.  S  NILVKNDL
M.m.  S  NILVKNDL
M.m.  S  NILVKNDL
G.g.  S  NILVKNDL
D.r.  S  NILVKNDL
```

MT: disease causing

PM: neutral

PP: unknown

PP2: probably damaging

Figure 4-8:   **Amino acid alignment and *in silico* biometric analysis of novel mutations.**

Gene name and nomenclature of the mutation between two panels. Left panel represent the conservation of each novel DNA variant across different mammals. Blue script represent the amino acid sequence with the mutated residue represented as bolded, red letter; Black branded are wild type residue for that specific amino acid change. H.s. Homo sapiens; M.m*., Mus mulatta; M.m., Mus musculus; P.t., Pan troglodytes; F.c., Felis catus; G.g., Gallus gallus; D.r., Danio rerio. Right panel represent the output for amino acid substitution; MT, Mutation Taster; PM, pMut; PP, PolyPhen; PP2, PolyPhen2; and FF, FruitFly.

4.2.5 Novel SNPs found with the MFSTAAD resequencing assay

On average, SNPs are found at a frequency of 1 in every 1000 bases across human genome (Sachidanandam *et al.*, 2001). In this study, a total of 76 SNPs could be detected with the MFSTAAD microarray which were either homozygous or heterozygous SNPs (Table 4-7). A total of 69 SNPs have been listed in the GenBank SNP database (NCBI), whereby the remainder (total of 7) were novel synonymous DNA variants (Table 4-8). Majority of these SNPs listed herein, were recurrent among the 66 arrays analyzed. The novel SNPs were absent in the dbSNP database and were checked for their pathogenicity using the aforementioned BMAPs and were checked in the literature.

Table 4-7: **Number of reported and novel SNPs detected with the MFSTAAD resequencing assay**

Gene	Number of known SNPs	Number of novel SNPs
FBN1	3	-
TGFBR1	1	-
TGFBR2	2	-
COL3A1	13	-
ACTA2	2	-

MYH11	17	3
SLC2A10	2	1
NOTCH1	29	3
Total	**69**	**7**

Table 4-8: **Name and nucleotide position of all novel synonymous DNA variants found with MFSTAAD resequencing assay**

Gene	Exon	Nucleotide change
MYH11		
	17	c.2058+30G>A
	32	c.4158C>T
	34	c.4719+4C>T
SLC2A10	3	c.1305C>T
NOTCH1	17	c.2058+30C>T
	32	c.4158C>T
	34	c.4791+4C>T

4.2.6   Mutation segregation analysis of known and novel DNA variants

Mutation segregation analysis was performed in families of three decedents (PD7, PD11 and PD15) and in families of two living subjects (RL4 and RL6). Family segregation analysis of DNA variants *MYH11* c.4673C>T, p.T1158M; *FBN1* c.3509G>A, p.R1170H; *COL3A1* c.217G>C, p.D73H; NOTCH1 c.2734C>T, p.R912W and *MYH11* c.5676G>C, p.E1892D in family members of PD7, PD11, PD15, RL4 and RL6, respectively can be found in Appendix 15-19. The remaining potential pathogenic mutation could not be tested for their inheritance in parents and siblings due to the manner of recruitment. Co-segregation of the possibly disease causing mutation and the genetic disease was only observed in family 1 of PD7 for the mutation in the gene *MYH11* c.4673C>T, p. T1558M. Conventional Sanger sequencing of the father of decedent 7 confirmed the same mutation.

4.3   Results on the correlation between CMN and EF versus genetic predisposition

The exact Chi-square test was used to analyse the correlation between specific histopathological medial changes which are characteristic for TAAD, such as CMN and EF versus mutation yield found in this study. In respect of the publication by Bode-Jänisch *et al.* 2012 a grading score of ≥2 for CMN and EF were suggestive of a heritable disease of the thoracic aorta (Figure 4-9). A total of 7 subjects were carriers of a possibly disease causing mutation, but the majority of cases (10 subjects) had the same grade of medial changes, but were negative for a disease causing mutation (Table 4-9). Among the 18 decedents, one decedent had medial changes of grade 1 for both CMN and EF, and no subject was among grade 1 medial alteration with any mutation. Statistical examination showed no correlation between aortic alterations of CMN and EF versus genetic predisposition to a genetic disease of TAAD (p-value of 0.44).
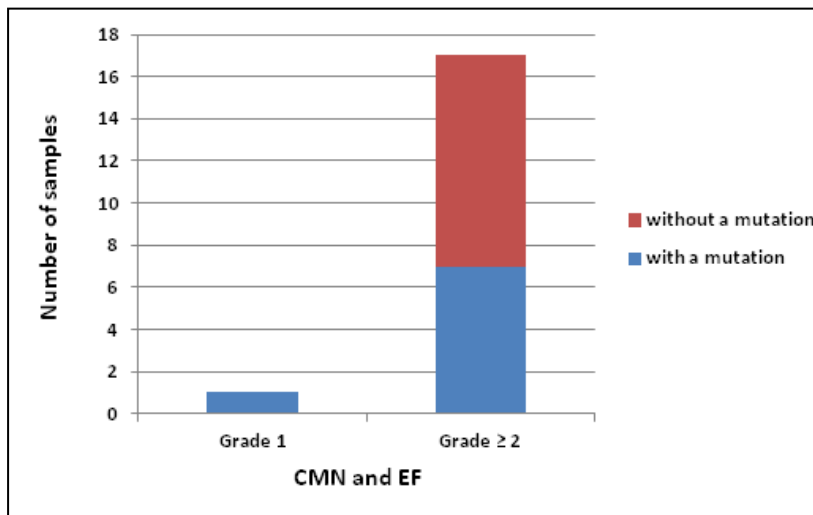
Figure 4-9: **Correlation of histopathological changes (Bode-Jänisch *et al*., 2012) and genetic findings in this study.** Chart represents medial alterations CMN and EF versus genetic mutations found in this study. CMN and EF with a medial alteration of ≥2 (Left column) are taken as an indication for possible genetic predisposition to a heritable disease of TAAD. Red column indicates a subject without a mutation and blue indicates with a mutation.

Table 4-9: **Correlation of cystic medial necrosis and elastin fragmentation versus genetic predisposition.**		
PD with **(n=18)**	**Grading scores for CMN and EF**	
	≥ grade 2	grade 1
possibly pathogenic mutation	7	1
no mutation	10	0

PD; prospective decedents, CMN; cystic medial necrosis, EF; elastin fragmentation. p-value of 0.44.

4.4   Correlation of young age versus mutation yield

Further interest of this study was to test whether there was a correlation between young age and genetic predisposition, in other words when TAAD occurred at a young age, is that phenomenon a good indicator for a genetic disease of TAAD. The mean age among 18 decedents was 55.5 years (Figure 4-10). The number of mutation per decedent was higher in the cohort ≤ 55.5 of mean age compared to >55.5 (6 versus 1), however the correlation was

not significant using the chi-squared two tailed test (p-value of 0.11). Number of no mutation was similar (5 versus 6).
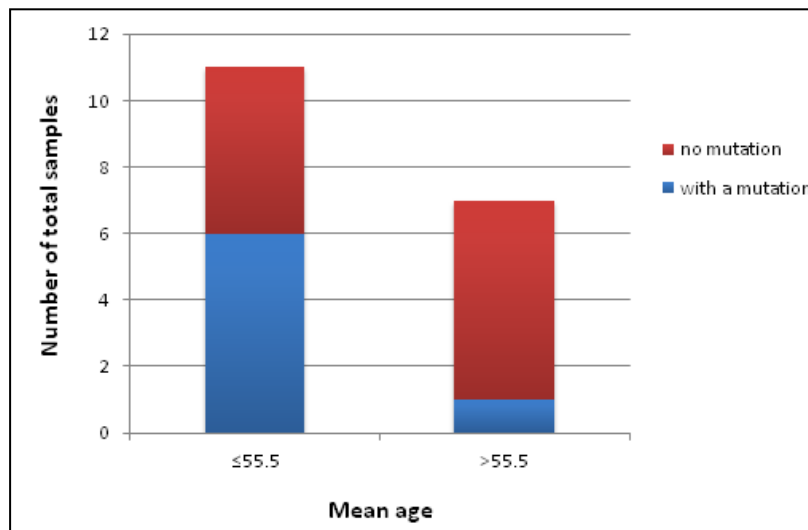
Figure 4-10: **Correlation of genetic predisposition versus age.** Chart represents age for a potential heritable TAD versus genetic predisposition. Mean age of ≤55.5 is taken as an indication of a heritable TAAD. Red column indicates subjects with no mutation and blue column are patients positive for a mutation in the TAAD candidate gene.

Table 4-10: Correlation between age and genetic predisposition of FTAAD in a total of 18 decedents.		
PD with (n=18)	**Age of decedents**	
	≤ 55.5	> 55.5
possibly pathogenic mutation	6	1
no mutation	5	6

PD; prospective decedents. P-value for one-tailed was 0.11 and for two tailed it was 0.15.

4.5   Results of conventional Sanger sequencing analysis of the SMAD3 gene

Conventional PCR reaction and Sanger sequencing reaction was performed in all retrospective and prospective samples from Hannover, since this gene have previously been reported to harbour mutations that cause an isolated form, the FTAAD. (Regalado *et al.*, 2011). This gene was not covered by the MFSTAAD resequencing microarray. A novel probably disease causing mutation c.1039 G>A, p.E347K was found in R14 (Figure 4-11) who was a carrier of a mutation in the *ACTA2* gene c.592 C>T, p.R198C using the

MFSTAAD microarray. For both DNA variants, all *in silico* biotmetric programs called these DNA variants as propably disease causing.
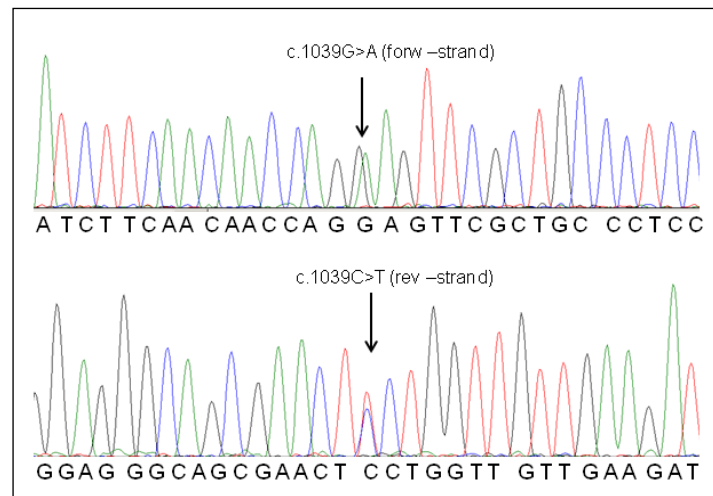
Figure 4-11: *SMAD3* **missense mutation.** A novel *SMAD3* mutation, c.1039G>A (p.E347K) detected with conventional Sanger sequencing reaction. Upper electropherogram the DNA variant on the forward strand, bottom electropherogram the same changes on the reverse strand.

4.6   Characterization of exact FBN1 gene deletion breakpoints in patients I1-I3

In our study we have identified two novel complete deletion of the *FBN1* gene each in two unrelated patients (I1 and I2) with a classic form of MFS involving the skeletal, ocular and cardiovascular system and one two-exon deletion (exons 64-65) in patient I3 by whom no clinical information were available. Both I1 and I2 met the clinical diagnostic criteria for MFS. The first heterozygous *FBN1* deletion in I1 encompassed the whole *FBN1* gene plus five consecutive genes including *DUT*, *SLC12A1*, *CTNX2*, *MYEF2* and *SLC24A5* locating upstream of the *FBN1* gene. There was no family history for MFS in patient I1. The other large deletion was found in I2 consisting of exons 6-65 of the *FBN1* gene and deleting the consecutive *DUT* gene. This patient had multiple members from the maternal side who were very tall and died of unknown heart failure. Detailed medical information of these relatives were not available, however, he had a sister with tall stature and suffered from aortic aneurysm. Patient I3 had a deletion of the exons 64-65 of the *FBN1* gene, by whom no clinical data were documented. To refine each of these deletions, we have used a 244K a-CGH e-array. Upon a-CGH, PCR and bidirectional Sanger sequencing was used to determine the exact breakpoints using the information of the probe sequences that were employed in the whole genome a-CGH analysis (Appendix 21, 22, 23). Among the complete *FBN1* deletions,

the first deletion was 674.351 bp (Figure 4-15) which resided at chromosomal location: 48.277.334-48.953.951 (676.617 bp defined by a-CGH) comprising of complete *FBN1* gene and 3' contiguous genes *DUT*, *SLC12A1*, *CTNX2*, *MYEF2* and *SLC24A5*. The second deletion was 256.593 bp (257.512 bp defined by aCGH) (Figure 4-16) in length which had encompassed exons 6 to 65 of the *FBN1* gene and the entire *DUT* gene. The smaller deletion was 9.134 bp in length (Figure 4-17) consisting of 147 bp of exon 64, intron 64, and the complete exon 65, the 3'UTR of the *FBN1* gene and 7.484 bp of the contiguous genomic sequence region (Figure 4-12-14, respectively). No deletion and duplications were found in PD1-20 in subjects who died of severe aortic rupture of unknown cause.
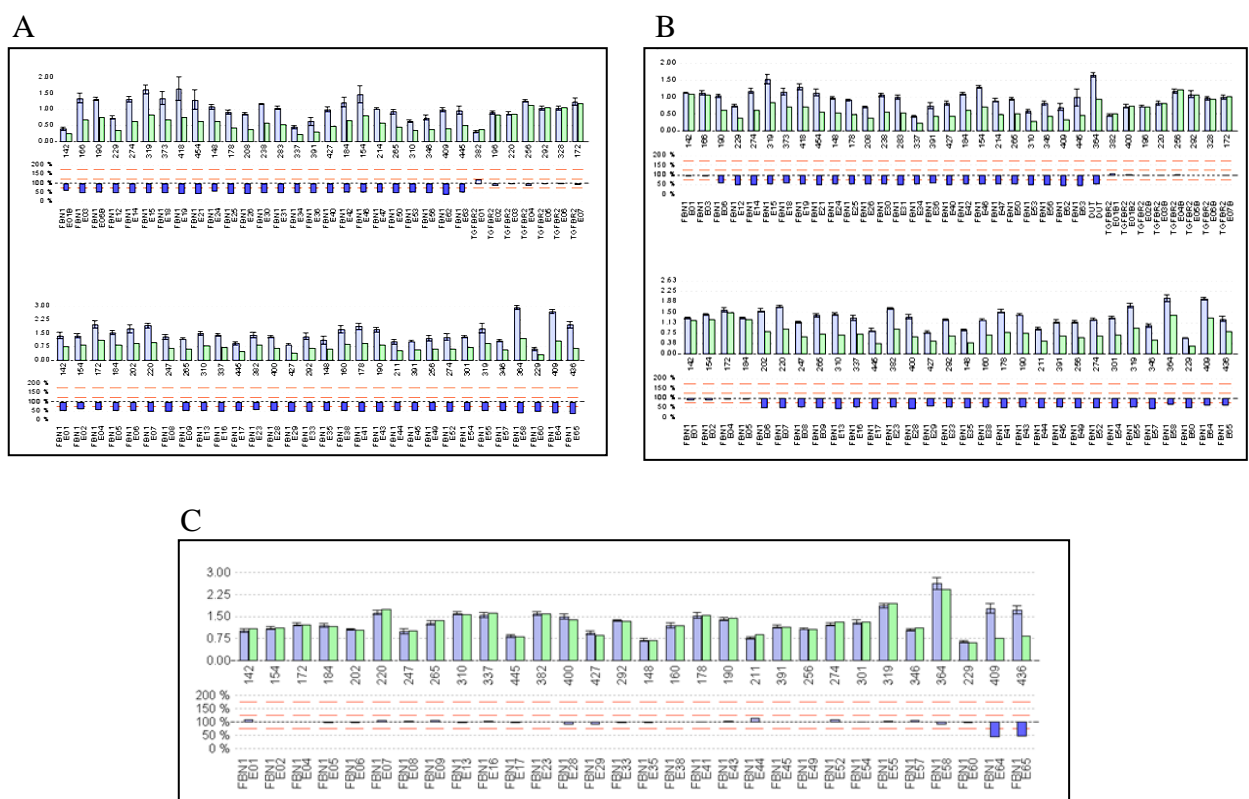
Figure 4-12: Determination of *FBN1* gene deletions using MLPA assay. (A) Deletion of exons 1-65. (B) Deletion of exons 6-65. (C) Deletion of exons 64-65. Bars below 100% represent a deletion of the corresponding exon, and bars in the upper region of 100% correspond to duplication.
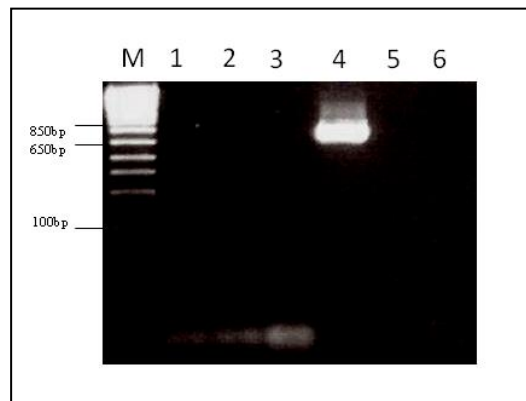
Figure 4-13: PCR amplification of the smaller deletion (exons 64-65 of the *FBN1* gene). (M) 1kb (+) DNA marker. (Lane 1-3) to be ignored. (Lane 4) Amplification of deleted region of exons 64-65 of the *FBN1* gene using primer pairs *FBN1*_65.1 F x R. (Lane 5) Control subject. (Lane 6) blank.
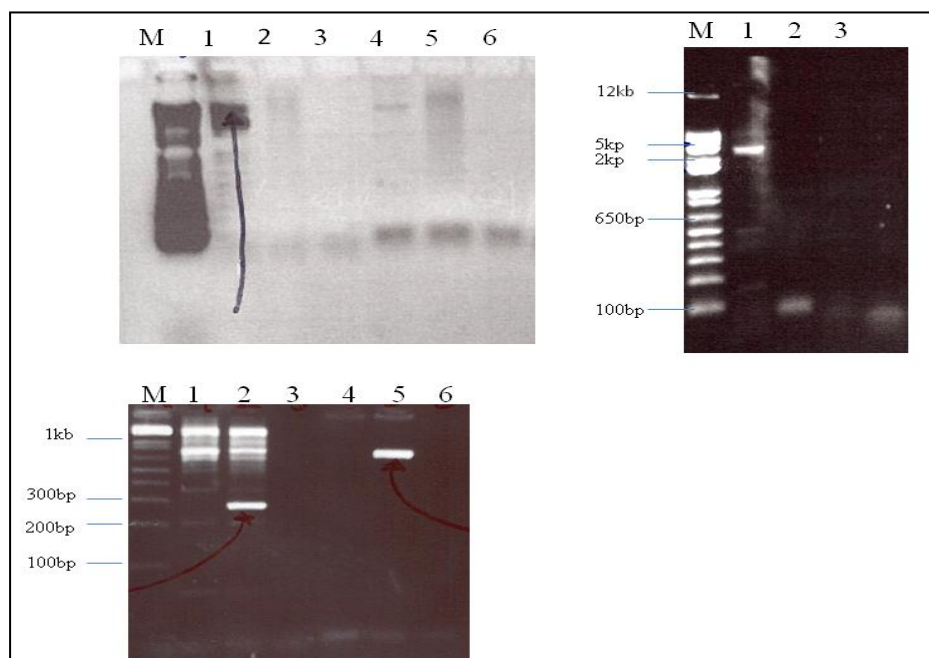
Figure 4-14: PCR amplification of large FBN1 deletions using Qiagen LongRange PCR kit. (Top left) Amplification of the largest deletion of complete *FBN1* gene. (M) 1kb (+) DNA marker. (Lane 1) Patient DNA amplification using primer pairs 1 F x R, (lane 2) control, and (lane 3) blank, (lane 4) Patient DNA amplification using primer pairs 2 F x R, (lane 5) control and (lane 6) blank. Two bands were visible in lane 1, whereby the top band had the expected band size of about 3 kb. A gel band purification was performed for lane 1 and lane 4 using Illustra GFX PCR DNA followed by a second PCR amplification step (top right); (M) marker, (lane 1) Patient DNA second amplification using primer pairs 1 F x R and (lane 3) DNA amplification using primer pairs 2 F x R following gel band purification.

Bottom picture represents the PCR amplification of the second largest deletion consisting of exons 6 to 65 of the *FBN1* gene and *DUT* gene. (M) marker, (lane 1) DNA amplification in control subject using primer pairs 3 F x R, (lane 2) patient, (lane 3) blank, (lane 4) DNA amplification in control subject using primer pairs 4 F x R, (lane 5) patient and (lane 6) blank. Arrows indicate the expected band size in patient upon deletion.
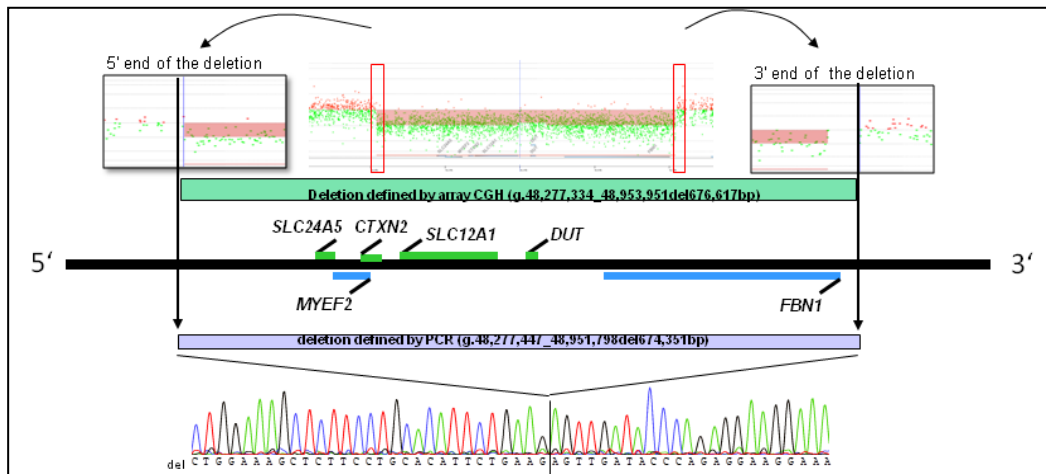
Figure 4-15:   Deletion of genes *FBN1*, *DUT*, *SLC12A1*, *CTXN2*, *MYEF2* and *SLC24A5* in I1. Deletion of 674.351 bp comprising of the complete *FBN1* gene, and the genes *DUT*, *SLC12A1*, CTXN2, *MYEF2* and *SLC24A5* located 3' of the *FBN1* gene. Flags show the direction of the corresponding gene (either found on the 5' or 3' strand). The line across the sequence (electropherogram below) indicates the deletion breakpoint determined by Sanger sequencing reaction, the left sequence is the 3' sequence of the *FBN1* gene and the right sequence starting with <u>*AGTT*</u> is the 5' sequence of the *FBN1* sequence.
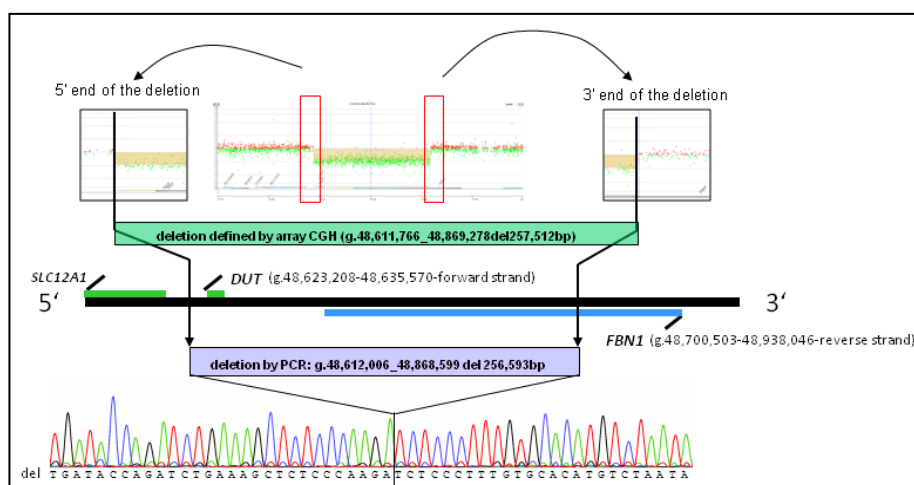
Figure 4-16:   Detection of genes *FBN1* and *DUT* in I2. *FBN1* deletion of 256.593 bp consisting of exons 6 to 65 and the *DUT* gene. The line across the sequence indicates the deletion breakpoint determined by Sanger sequencing reaction, the left sequence is the 3'

sequence of the *FBN1* gene and the right sequence starting with <u>*TCTC*</u> is the 5' sequence of the *FBN1* gene.
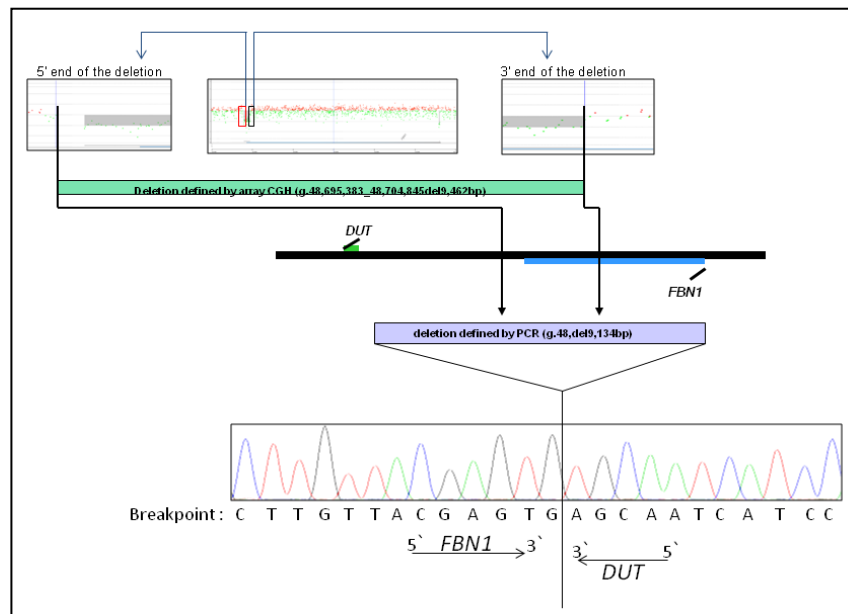
Figure 4-17: Deletion of exons 64-65 of the *FBN1* gene in I3. The smaller deletion was 9.134 bp in length consisting of 147 bp of exon 64, intron 64, and the complete exon 65 and the 3'UTR of the *FBN1* gene and 7.484 bp of the contiguous genomic sequence region.

4.7 Indirect DNA marker linkage analysis in family 1 with promiscuous skeletal features

Index patient (I6) in family 1 (Appendix 2) has been suspected for MFS with TAAD because several members of her family from her paternal side and her two borther had a conspicious Marfan habitus, and one of her uncle died of abdominal aortic rupture at the age of 65. Nonetheless, traditional sequencing and the novel MFSTAAD resequencing methodologies have revealed no mutation in eight MFS and MFS-related genes (*FBN1*, *TGFBR1*, *TGFBR2*, *COL3A1*, *MYH11*, *ACTA2*, *SLC2A10* and *NOTCH1*) and MLPA was negative for deletions and duplications in the *FBN1* and *TGFBR2* genes. Furthermore, since this family was previously tested for linkage with DNA STR markers for MFS by Dr. Rhode as an independent study and she has demonstrated a linkage of the disease and markers of *TGFBR1* and *TGFBR2*. However, no mutation was detected using conventional Sanger sequencing reaction. Herein, we analysed this family using markers for FTAAD. Only two DNA markers for each *AAT1* (D114195 and D114132) and *AAT2* (D5S626 and D5S2029) have been informative for this family (Appendix 4). None of the other FTAAD markers including

markers for TAAD locus (TAAD3/BAV) and for two TAAD genes (*ACTA2* and *MYH11*) mapped on chromosome 10q22-24 and 16p12.12-13.13, respectively have shown a linkage with the disease running in family 1 (Appendix 4 and 5).

4.8   Indirect DNA marker linkage analysis in family 2 with Marfan habitus and aortic aneurysm

In family 2, I9 had a Marfan habitus and aortic aneurysm. From his maternal side, he had an uncle with similar phenotypes, whereby his mother had only presented with a Marfan habitus. Furthermore, a twin sister of his grandmother died of aortic rupture of unknown cause, clinical data from this subject has not been available. Similarly, his cousin from the maternal side had aortic aneurysm, unfortunately we had no further clinical information for this subject either. A mutation has been found in the *ACTA2* gene c.977 C>A, p.T326N which did not segregate with the disease running in this family. Indirect DNA marker analysis for FTAAD, we have been able to find a linkage between the disease and the *TAAD3*/BAV locus which maps on chromosome 15q24-16, where the disease gene remained unknown (Figure 4-18). The haplotype 20/23/16 for TAAD3 have been carried only by the individuals who have been either had a Marfan habitus or aortic aneurysm. No further linkage was found for the remaining two FTAAD loci and the two candidate genes (*ACTA2* and *MYH11*) with the anomaly in family 2 (Appendix 6). Only two DNA markers have been informative for AAT2 locus (D5S641 and D5S626).
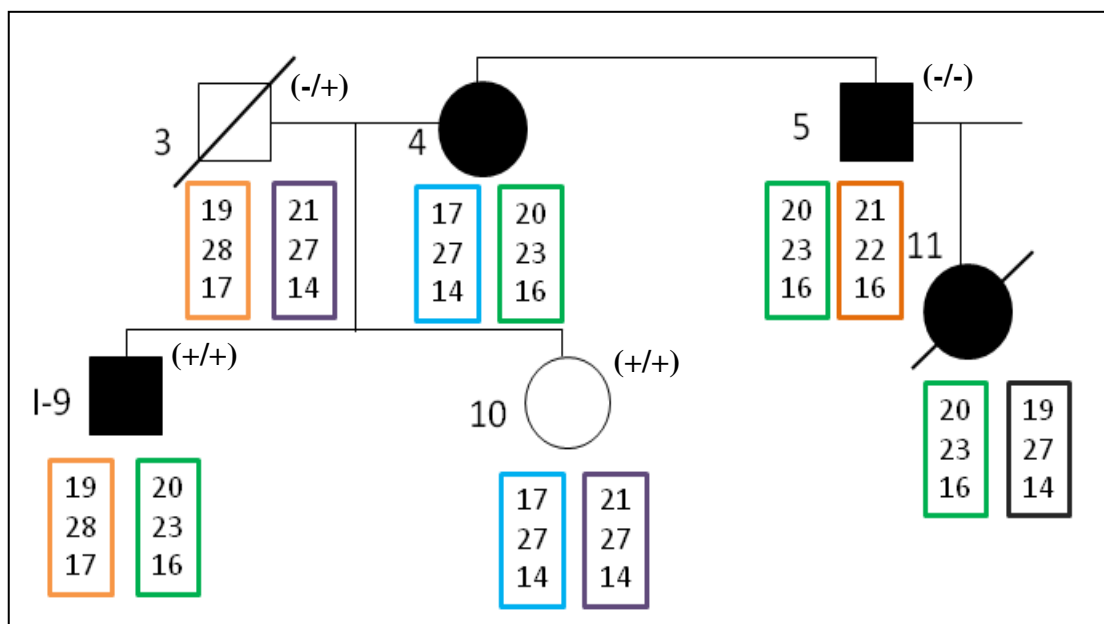
Figure 4-18:   Linkage of *TAAD3*/BAV locus and disease running in family 2. Each Subject is indicated with numbers. Squares represent male member and circles stand for

females. Affected and unaffected individuals are represented by bold and open symbols, respectively. Line across denote deceased. Haplotypes for *TAAD3*/BAV locus are shown from top to bottom in the following order D11S4132, D11S924 and D11S4195. A (+) or (-) sign in brackets stand for mutation positive or negative of previously found DNA variant *TGFBR3* c.44C>T, p.S15F and *ACTA2* c.977C>A, p.T326N. A plus sign designated mutation-positive and minus sign for mutation-negative for the respective DNA alteration.

5. *Discussion*

5.1 Design of the novel "MFSTAAD" high density oligonucleotide based resequencing microarray

Herein, we introduce the novel "MFSTAAD" high-density oligonucleotide based, a large-scale resequencing microarray which is an "efficient and economically competitive method for genetic screening of heterogeneous disease" such as TAAD by enabling the simultaneous resequencing of a large panel of candidate genes in a single experiment (text in double quotes has been adapted from Kothiyal *et al.*, 2010). This pre-screening technology will benefit in the identification of patients at-risk for TAAD, especially in those who fulfil the Ghent nosology criteria for MFS, but are non-carriers of a mutation in the *FBN1* gene, which is known to be defected in MFS patients, and in order to differentiate classic MFS from MFS related syndromic and non-syndromic genetic diseases, who present with a severe form of TAAD. Additionally, through the parallel resequencing of several candidate genes of TAAD, allows a scientist to unravel the interaction between the genes/proteins in health and disease state, these comprehensive undertaking and elucidating the molecular pathogenisis of TAAD will definetly have a benefit in the clinic to manage these genetically predisposed patients at an early stage before a severe ruptur occurs. High-density oligonucleotide based resequencing microarray is a highly reliable and sensitive in the detection of heterozygous and homozygous single nucleotide DNA variants, which accounts for the majority of mutations found in both syndromic and non-syndromic thoracic aortic diseases. A series of resequencing arrays have been so far reported such as for hypertrophic cardiomyopathy (Waldmueller *et al.*, 2008; Fokstuen *et al.*, 2008), for dilated cardiomyopathy (Zimmermann *et al.*, 2010) for child hearing loss (Kothiyal *et al.*, 2010), for inherited retinal dystrophy (Song *et al.*, 2011) and for Marfan syndrome (Ogawa *et al.*, 2011). In the interest of my own study, until date, one resequencing assay by (Ogawa *et al.*, 2011) have been reported to identify mutations in the *FBN1* gene causing Marfan syndrome, and one next generation sequencing array which has been evaluated by de Leeneer *et al, 2011* which covered the genes *FBN1*, *TGFBR1* and *TGFBR2* genes. Our MFSTAAD is the first resequencing microarary so far, that has been designed to identify mutations in a total of eight TAAD candidate genes (*FBN1*, *TGFBR1*, *TGFBR2*, *COL3A1*, *ACTA2*, *MYH11*, *SLC2A10* and *NOTCH1*) on a single platform. Mutations in the gene *SMAD3* has recently been described in the context of underlying osteoarthritis with TAAD (Regalado *et al.*, 2011), and has been not included in our MFSTAAD design.

5.1.1 Benefits of long range PCR assay for target amplification

Target generation using long range PCR assay has a further advantage over traditional short range PCR reaction, in a way that this assay allows the coverage of all coding exons plus splice site junctions of our eight target genes in fewer as 52 PCR reactions, additionally reducing the handling time and cost. Several long range PCR kits have been available and have been employed in the generation of target amplicons for resequencing microarray, such as TaKaRa LA Taq polymerase (TaKaRa Bio, Madison, WT; Kothiyal *et al.*, 2010 and Song *et al.*, 2011; GeneChip CustomSeq Resequencing array protocol, Affymetrix), Go *Taq* Flexi DNA polymerase (Promega; Waldmueller *et al.*, 2008) and LongAmp *Taq* DNA polymerase (NEB; Kathiravel *et al.*, 2013), in addition to LongAmp Taq DNA polymerase, Hannover samples have been generated using the high-fidelity Qiagen LongRange Taq DNA polymerase for target amplification after optimizing the conditions for our target amplicons (Kathiravel *et al*, 2013, paper sent to Journal of Molecular and Cellular Probes for publication).

5.1.2 Evaluation of the general performance characteristics of the MFSTAAD resequencing microarray

For the evaluation of the general performance of our novel MFSTAAD microarray, we screened a total of 66 consecutive patients and achieved an overall initial call rate of 94.4% (66 arrays: range: 93.4%-95.7%) using the *GSEQ* sequence analysis software. We performed the base-calling under the default settings as recommended by Affymetrix for diploid sample data analysis. This call rate, however, varies intensively between the custom-based microarrays that have been reported so far, 84.8% to 98.5% (Denning *et al.*, 2007; Kothiyal *et al.*, 2010, Liu *et al.*, 2007 ;Song *et al.*, 2011; Fokstuen *et al.*, 2008; Waldmueller *et al.*, 2008 and Zimmermann *et al.*, 2010). It can be speculated that the discrepancy is due to the employment of different user-specific setting of the G*SEQ* data analysis software, or it can be based on the nucleotide composition of the different genes and the mutational heterogeneity in the disease analyzed. For instance, we could achieve a better call rate with larger samples analzed in a batch (Denning *et al*., and Lebet *et al*,.). Still, we had a no call rate of ~5.7%. Most of them have been found to be located in <u>*GC*</u> rich regions and in homopolymer stretches (mainly G-stretches). Similar observations have been reported by Denning *et al*; Kothiyal *et al* and Waldmueller *et al*. Interestingly, many studies have been performed to demonstrate the performance of <u>*GC*</u> rich probes under the hybridization setting in a resequencing assay which has shown that <u>*GC*</u> rich probes, most importantly G-rich probes are eligible to cause cross

hybridization which lead to poorer base-calling for that regions (Cutler *et al.*, 2001; Zhan & Kulp 2005; Waldmueller *et al.*, 2008). This would be a limitation of the assay, if a disease-causing mutation lies within G-stretches. One way to overcome this limitation and improve the overall call rate, is to adjust the probe length of G-rich probes, and to intergrate a known variable base at either end of the probe (Southern *et al.*, 1999;Waldmueller *et al.*, 2002 and 2008), another way would be to generate a triplicate set of probes for each reference base ("triplicate design"- Zimmermann *et al.*, 2011) by which each of these probe sets contained a different position of interrogation such as positions 9,13 and 17 within the 25-mer probe. This strategy has shown to have dramatically improved the call rate. Our current study, utilizes a duplicate design without the probe modification. Furthermore, we have used a commercially availabe Sequence Pilot module SeqC software which recalculates the base-calling of "no calls" assigned by G*SEQ*. With this software we could substantially reduce the number of "no calls" and achieved a final call rate of 99.8%. The remaining 0.2% (~1.3kb of target sequence) of no base-calling was visually inspected and in the case of relevant sequence region it was resequenced using conventional Sanger sequencing reaction. These results were comparable with other algorithm software and user-defined criteria as post G*SEQ* data analysis (Kothiyal *et al*, 2010 and Song *et al*., 2011, respectively). In the study of Song *et al*, they filtered out the variants that cause "SNP nearby effect", which means that a true variant is most likely to impulse false variation calls at positions of about 10 bases on either side of the true variant. These abnormality calls has been also observed for our array samples (Figure 5-1), in most cases if it has been conspicuous for a true variant this change has been confirmed with conventional Sanger sequencing reaction. In most cases these were false positive and were recurrent, thus they have been ignored in further analysis.

5.1.3 Analytical Sensitivity of the MFSTAAD microarray

The MFSTAAD microarray has shown an analytical sensitivity of 100% (153/153) for both known and novel single nucleotide DNA variants using a duplicate tiling system. Same sensitivity has been achieved by Zimmermann *et al.,* using a triplicate probe array design with interrogation sites on positions 9, 13 and 17. However, the assay has a reduced sensitivity for insertions and deletions (4.8%; 1/21) which constitutes of ~19.5% of all known TAAD mutations, with the *FBN1* gene contributing to 17.4% (22.3% of all known *FBN1* mutations; Human Gene Mutation Database. Upon interrogation of 21 known deletions (size range: 1 to 16 bp), we could detect the largest deletion (Figure 5-2) due to a dramatic decline in the hybridization signal when comparing the same sequence frame with several other test

samples. Similar observation has been described by Fokstuen *et al*.,. Noteworthy is, that the SeqC software has failed to call this variant, thus it would have remained unseen, if it was an unknown variant. Whereby, Kothiyal *et al.*, have reported the detection of the largest deletion through a series of "no calls" and a heterozygous call within the expected deleted region. Similarly, "the DCM assay by Zimmermann *et al.* outperformed the MFSTAAD assay and other similar assays in respect to the detection of insertions and deletions (42% vs. 5% in our case) by performing a "best case/worst case" scenario. Thus, the detection rate of insertions and deletions by the MFSTAAD assay may be improved by the modification of interrogation site in the duplicate probe design (interrogation of DNA variants at different sites in the 25-probe). At present, however, the inability to detect small heterozygous insertions and deletions presents a significant limitation of the "MFSTAAD" assay. Nevertheless, in comparison to traditional methods such as conventional Sanger sequencing, the "MFSTAAD" array allows the parallel sequencing of eight TAAD candidate genes in a single experiment, which is highly preferred in the routine clinical setting due to the maxmum gain in time, labor and cost-efficiency of the assay. To date, the largest platform allows interrogation of 300 kb of target sequence, which has been reported by Booij *et al.,* for retinal disease. Certainly, new large-scale platforms such as "next generation sequencing microarray platforms" are taking their placement in the clinical diagnostic and will soon replace all the other large scale technologies, to date their main limitation lie in the data handling and are still too costly for medium sized or for disease-specific applications. Thus, we are highly convinced, that the "MFSTAAD" array, is a good pre-screening tool for the detection of single nucleotide variants due its ability to analyze a large panel of genes in a single experiment with a reasonable turn-around time and cost-efficiency. The resequencing assays for child hearing loss and dilated cardiomyopathy have shown to reduce the cost by ~50% when compared with conventional Sanger sequencing reaction (Kothiyal *et al*., 2010 and Zimmermann *et al.*, 2011). Further refinements in base-calling algorithms for indels (e.g. algorithm that detects regional drop in signal intensity indicative of possible deletions) and for DNA variants in G-rich probes will make this technology even more favourable both in research and clinical environments. In the interim, the "MFSTAAD" array is used for the detection of single nucleotide DNA variants in TAAD patients.
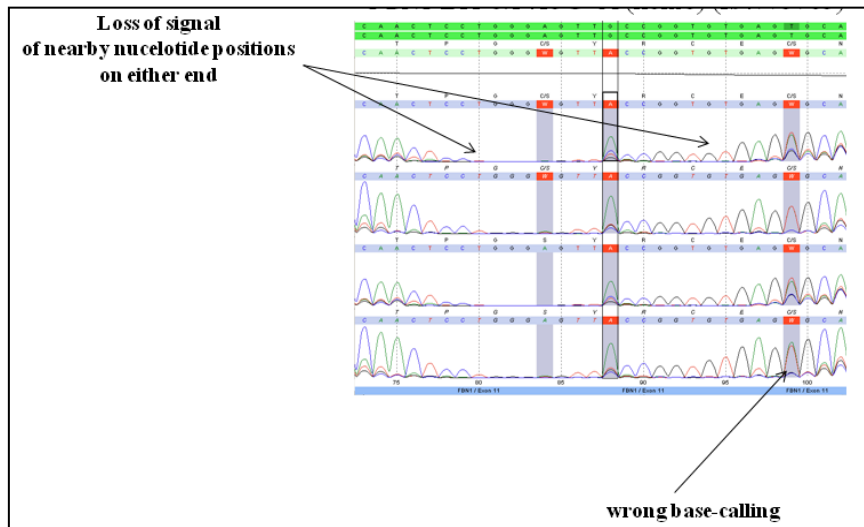
Figure 5-1:   A "*SNP* nearby effect". Single nucleotide variant in the exon 11 of the *FBN1* gene (c.1415G>A; rs4775765 decreases the signal intensity for the probes of contiguous nucleotides on either side leading to false reads or possible true variants might be missed.
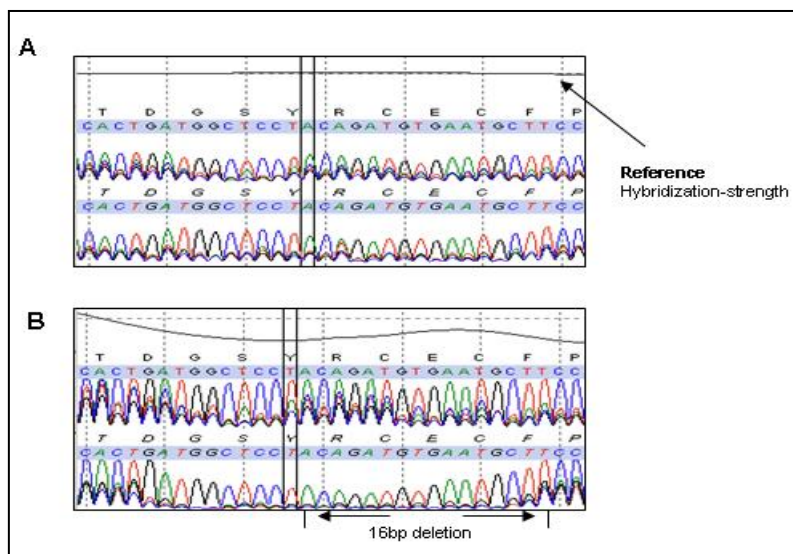
Figure 5-2:   SeqC electropherogram result of a 16 bp deletion in the *FBN1* gene. SeqC defines a position based on the signal intensity of perfect match probes for the corresponding position based on the existing chip files with same chemistry found in the database. (A) In the first diagram (control), straight line running horizontally (see arrow above) represents strong hybridization strength from a normal patient. In addition, the sequence electropherogram of this subject remains uniform throughout the region of interest. (B) The hybridization strength displays a drop (see bottom diagram) that corresponds to a weak hybridization process and an irregular flow of the sequence electropherogram is also observed in this patient (see diagram B, bottom flow), possibly caused by this 16 bp deletion.

5.1.4   Evaluation of mutation yield of the MFSTAAD microarray

Using the "MFSTAAD" resequencing array, we could detect a total of 22 mutations in 66 unrelated patients with classic MFS or diagnosed for TAAD, among these, a total of 9/22 were known and a total of 13/22 were novel DNA variants, corresponding to an overall mutation yield of ~33%. Similar mutations yield was observed by Fokstuen *et al.*, for their HCM resequencing microarray. Noteworthy, when considering the mutation yield in our prospective cohort who consisted of blinded samples who were not previously tested for mutations in any of these eight TAAD genes, the mutation yield has been 45%, higher than the detection rate observed for the retrospective group (45% versus 22.2%). Thus, the chance to detect a possibly disease causing mutation in clinical setting is ~45%. The absence of mutations in the remaining 44 samples may be due to the inability of the "MFSTAAD" array to detect indels as discussed above, or presence of mutations in the regulatory elements which are not covered in the design of the resequencing assay, mutations in other previously found TAAD such as *SMAD3* (Regalado *et al.*, 2011) and *MYLK* (Wang *et al.*, 2010) which were unknown during the "MFSTAAD" array design, or the presence of mutations in still unidentified TAAD genes, and due to the fact of sample bias. Since 36/66 samples were previously tested for MFS and LDS-specific disease genes (*FBN1*, *TGFBR1* and *TGFBR2*, respectively). The assay may have a limited application in the clinical diagnosis of TAAD patients, as indels account for ~17.4% and ~19.5% of all TAAD mutations, however, modification in the probe design and a suitable algorithm for the detection of indels using G*SEQ* data analysis software are attempted which will hopefully improve the mutation yield of the MFSTAAD assay.

5.2   Reduced penetrance and variable expression of MYH11 p.T1558M

Following the evaluation of pathogenicity of novel DNA variants using *in silico* BMAPs, we have further evaluated the pathogenic effect of novel and known DNA variants *MYH11* c.4673 C>T, p.T1558M; *FBN1* c.3509 G>A, p.R1170H; *COL3A1* c.217 G>C, p.D73H; *NOTCH1* c.2734 C>T, p.R912W and *MYH11* c.5676 G>C, p.E1892D in close relatives of PD7, PD11, PD15, RL4 and RL6, respectively. Results of mutation segregation analysis are depicted in the Appendix (Appendix 15-19). A co-segregation of a mutation and the disease has been observed in PD7 for the mutation *MYH11* (p.T1558M). This variant has been listed in the NCBI dbSNP database with a reduced occurrence rate of 0.1. Medico-legal reports of PD7 has been available, this individual has a tall stature and died of TAAD. Upon genetic screening of this decedent we have contacted close-relatives of this decedent in order to

examine the segregation of this DNA variant within the family. Medical records of the father revealed the presence of aortic aneurysm, confirming that this variant is possibly the disease-causing variant, however, showing reduced penetrance and variable expressivity in the father. Other four variants did not co-segregate in the family; however, they have been made aware of potential risk of FTAAD (Boileau *et al.*, 2005; Milewicz *et al.*, 1998).

5.3   Evaluation of correlation of histopathological changes versus genetic predispotion to TAAD

Specific histopathological features such as CMN and EF have been suggested by the group of (Bode-Jaenisch *et al.,* 2012) as indicators for MFS and other related thoracic aortic diseases. They have shown quantitative difference in the grade of CMN and EF between the group of decedents with dissecting aneurysms and group of decedents without dissecting aneurysms, with statistically significant p-value of <0.001. These results are in accordance with Schlatmann & Becker, 1977, particularly for EF upon comparing the normal aging aorta and abnormal aortas with TAAD. Whereby, Hasleton & Leonard, 1979 found local EF in the majority of patients with a dissecting aorta, but also in the control aortas. In addition, they could not determine a difference in the grade of CMN between cases with TAAD and control groups. Similar results have been found in our study with substantially higher grades for CMN and EF in the group without a mutation, and confirm that there is no correlation between CMN and EF and genetic predisposition to FTAAD (p-value of 0.44). As an evidence for a possible misinterpretation of histopathological results, we show in Figure 5-3 variable grading scores (1, 2 and 3) for CMN and EF from three different decedents (D15, 7 and 19) carrying one or more potentially pathogenic mutations. If the decisions for a genetic background of TAAD will be made solely upon histopathological grounds then D15 with grade 1 alteration for CMN and EF with a mutation in the gene *COL3A1* (c.217C>G, p.D73H) would have been missed out. In addition, D19 suspected of MFS with TAAD with two mutations in the *FBN1* gene and one mutation in the gene *NOTCH1* show only grade 2 alterations for CMN and EF, whereby grade 3 alterations for CMN and EF have been observed in D7 by which a rare DNA variant in the gene *MYH11* (c.4673C>T, p.T1558M) has been found. Therefore, we suggest that high grades for CMN and EF are not necessarily specific features of a heritable disease of the aorta and should be used in caution when these information are used for the decision whether a relative of the decedent is affected or not. And rather confirm that these changes in the aortic wall occurs with age (Schlatmann & Becker, 1977), and the deterioration of the aortic wall function may be accelerated by genetic

defects or other factors such as hypertension, hypercholestemia and smoking (Ince & Nienbar, 2007). Interestingly, Ince & Nienbar have also reported a functional role of matrix metalloproteinases (MMPs), which is a group of more than 20 zinc-dependent proteolytic enzymes in the ECM metabolic events, aortic wall remodelling, and have speculated to have a potential role in the development of aortic aneurysms and dissections. More specifically, due to a localized increase in MMP-8 and MMP-9 enzymes. A polymorphism in the MMP-9 (-8202A>G) have been reported to have a potential role in the TAA development, but the functional role of this variant remains to be examined (Chen *et al.*,). For instance, murine models without MMP-9 have shown that complete loss of MMP-9 gene (*Mmp*-9) have a delayed TAA development. Furthermore, Wilson *et al*. has reported a case with a localized increase in expression levels of MMP 8 and MMP-9 at the site of abdominal aortic rupture leading to exhilarate aortic expansion and rupture in this individual. Similar observations have been made in individuals with TAAD (Ikonomidis *et al.*, 2006). This suggests, that MMP9 may have a potential role in the TAAD development and it would be of interest to study this gene in our cohort, by whom TAAD has occurred unexpectedly. This will not only widen our understanding on the pathogenesis of TAAD, and possibly enable a targeted mecical treatment to decrease the levels of MMP-9 in patients with TAAs which may possibly rescue TAAD development.
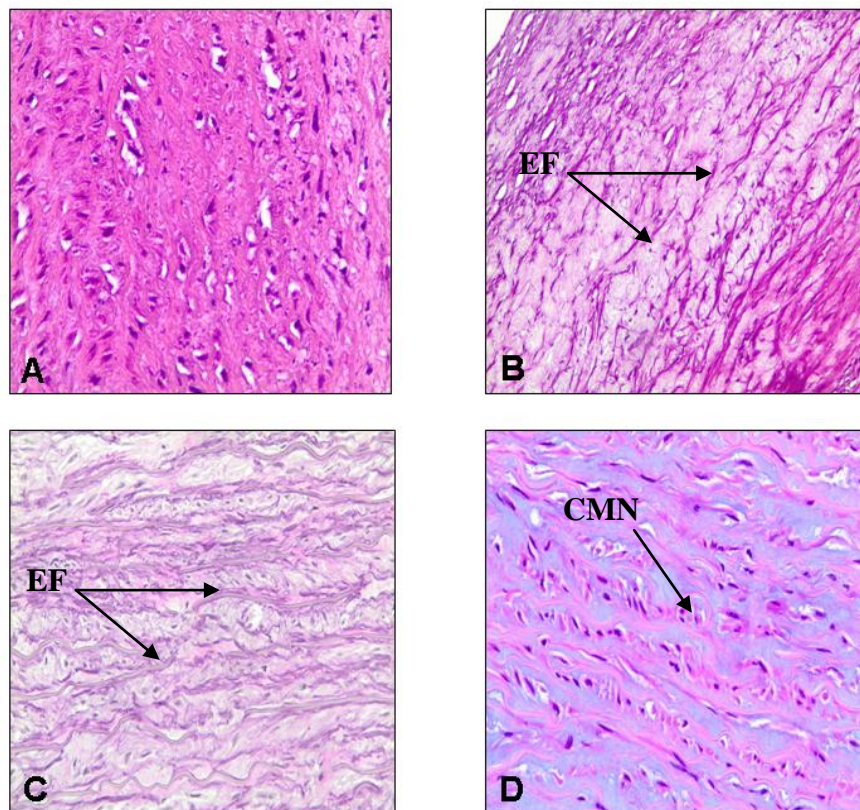
Figure 5-3: **Comparison of specific medial alteration in respect of Cystic medial necrosis (CMN) and Elastin fragmentation (EF).** Medial changes: grade 1, mild; grade 2, moderate and grade 3, severe. Upper row left (A) represents grade 1 alteration (H&E, 200:1) aortic specimen of a decedent carrying a missense mutation in the *COL3A1* gene c.217G>C, p.D73H. Upper row right (B) grade 3 alterations (H&E, 100:1), carrier of a missense mutation in the *MYH11* gene c.4673C>T, p.T1558M. Bottom row left and right (C and D) grade 2 alterations for EF (EVG, 200:1) and grade 2 alterations for CMN (AB, 200:1) in a decedent carrying a digenic mutation in the *FBN1* gene (c.3715A>G, p.I1239V; c.5578T>C, p.C1860R) and one mutation in the *NOTCH1* gene (c.939C>G, p.H313Q).

5.4 Evaluation of the correlation of age versus genetic predisposition

Nonetheless, we highly believe that TAAD occurring at young age can be considered for a syndromic or non-syndromic genetic disease of the thoracic aorta, in the absence of other risk factors such as hypertension, hypercholesterolemia and habit of smoking. Klintschar *et al,.* has reported three cases on sudden, unexpected TAAD as a result of a genetic disease and have raised the importance of a genetic screening in close-relatives of young decedent died of unexplained TAAD, due to the fact that about 20% of TAAD can present in several close-relatives. In this work we have tested the correlation between genetic predispositions versus occurrence of TAAD at different age stages (genetic changes occurring at ≤55.5 years versus

> 55.5 years). Upon testing this phenomenon, we have observed that the mutation rate, hence genetic predisposition to TAAD, was higher among the young adults compared to old generation (6 versus 1). However, the difference was not significant (p-value of 0.11). This may be explained by our large number of decedents >55.5 years of age, by which aortic dissections possibly occurred as an event of normal degeneration of the aortic wall (Larson & Edwards, 1984) or our sample size has been far to small for a correlation study, and our study include sample bias. In a case report by Klintschar *et al.*, a young adult that died of sudden aortic rupture was described to have remarkable skeletal phenotypes of MFS. Molecular testing of the *FBN1* gene, revealed a disease-causing mutation. Similarly, we describe herein a young adult who died of TAAD who is a carrier of a digenic mutation in the *FBN1* gene (c.3715A>G, p.I1239V; c.5578T>C, p.C1860R) and one mutation in the gene *NOTCH1* c.939C>G (p.H313Q). In this individual a classic MFS was suspected due to his skeletal features conspicuous for a connective tissue disorder, however, subjects with FTAAD do not present with any of the syndromic features, which makes the identification of these individuals at-risk very difficult in a clinical setting, and are generally overlooked until a tremendous complication of the aorta occurs. Thus, only way to prevent this type of complications from reoccurring, is firstly through careful documentation in the medico-legal autopsies, and to contact directly or indirectly close relatives in order to inform potential risk of FTAAD and to invite them for a genetic counseling. This approach will allow commencing a preventative management and reducing the mortality and morbidity rate associated with genetic forms of TAAD (Klintschar *et al.*, 2009; Hirani *et al.*, 2008; Ripperger *et al.*, 2009).

5.5   Classic MFS caused by true haploinsufficiency of the FBN1 gene

To date, over 2000 mutations have been described for the *FBN1* gene in the UMD-FBN1 and only a few of these are recurrent DNA variants. Missense mutations are the most prevalent DNA variants reported for the *FBN1* gene. Other mutations include frame-shift, splice-site and nonsense mutations (Faivre *et al.*, 2007) and each of these show a variable expressivity in the clinical phenotype among MFS patients (Boileau *et al.*, 2005). MFS is generally characterized into three forms including neonatal, severe and classic MFS. Specific hot spot region in the *FBN1* gene have only been described for the neonatal form of MFS (*FBN1* exons 28-32), whereby the mutations causing severe to classic form of MFS are distributed over the entire *FBN1* gene. To date, only a few large deletions encompassing single and multiple exons have been reported and have been shown to be associated with a severe form of MFS, such as a mosaic deletion of exons 13-49, deletion of a whole exon 33 (Blyth *et al.*,

2008); an in-frame deletion encompassing exons 42-43 in a case with classic MFS (Liu *et al.*, 2001) and most recently, Hilhorst-Hofstee *et al.*, 2011 reported the first series of 10 patients with a whole *FBN1* gene deletions causing a range of mild to severe form of MFS, caused purely by the true haploinsufficiency of the FBN1 protein. Five of their unrelated patients had a deletion beyond the *FBN1* gene, spanning 1-9.4 MB, deleting further 1-46 consecutive genes. Similar deletion spanning have been described by another group (Furtado *et al.*, 2011) and has been observed in our patient 1 and 2 who have a classic form of MFS, except that breakpoints, size and the position has differed among these three groups. Noteworthy is that patient 2 is a carrier of a heterozygous deletion which consits of exons 6-65 of the *FBN1* gene and the consecutive *DUT* gene. Regardless, of the deletion of additional five consecutive genes (*SLC24A5*, *MYEF2*, *CTXN2*, *SLC2A1* and *DUT*), these two patients have not exhibited any additional clinical features than seen in a classic form of MFS. Similar observations have been reported by Hilhorst-Hofstee *et al,*. in two patients who have presented with even larger deletions of 9 further genes including the *FBN1* gene. These findings not only support the hypothesis that true haploinsufficiency can lead to classical phenotype of MFS (Matyas *et al.*, 2007), but additionally that the loss of the five further genes upstream of the *FBN1* does not have an additional impact on the clinical appearance of MFS patients. Nevertheless, Hilhorst-Hofstee *et al,*. described two further patients with an extended phenotype of mental retardation and dysmorphic abnormalities in addition to classic MFS, by which one patient has shown even more severe neurological features exhibiting lack of skin and hair pigmenation (Hilhorst-Hofstee *et al.*, 2011), however. These severe phenotype have been attributed to the loss of genes Myosin 5A (*MYO5A*, MIM-160777) and RAS-associated protein (*RAB27A*, MIM-6033868) which are both located downstream of the *FBN1* gene leading to haploinsufficiency of additional two genes including *FBN1*, whereby deletions described in our study and by Furtado, *et al.*, have been found upstream of the *FBN1* gene. Several reports exists who described deletion of downstream genes, with similar psychomotor features (Faivre *et al.*, 2007; Ades *et al.*, 2006; Hutchinson *et al.*, 2003), whereby Hutchinson, *et al*. described a deletion extending further into centromeric portion of the chr. 15q. The sizes and breakpoints of these deletions remains unknown. Furthermore, within the group of whole *FBN1* gene deletion, the clinical phenotype can vary substantially from mild to severe classical form of MFS. This phenomenon has also been seen between patient 1 and 2, the first deletion encompassed the whole *FBN1* gene and five further genes, this patient exhibited a classic form of MFS with involvement of the skeletal, ocular and cardiovascular system, whereby patient 2 was a carrier of much smaller deletion compared to patient 1, by whom the

deletion started in exon 6, but had a severe form of MFS, and received a heart transplantation at young age. Hutchinson *et al*., has reported that levels of fibrillin-protein and mRNA transcripts have been significantly higher than expected for a single *FBN1* allele in a patient with whole *FBN1* gene deletion and suggested that the variable clinical phenomenon seen in MFS patients could be explained by the variable expression of the wild type fibrillin-1 protein upon comparing this results with three members in a family with a PTC mutation showing variable expression of the normal fibrillin-1 allele. Thus, it would be interesting to know whether the hypothesis of "variable phenotpyic appearance in MFS is due to variable expression of the wild-type fibrillin-1 protein", can explain the different clinical phenotpye between patients 1 and 2 in this study. But in respect of these previous work on fibrillin-1 expression, it shows that a complete loss of fibrillin-1 allele is rather compensated by normal fibrillin-1 allele than when high levels of mutant fibrillin-1 are present which may explain the severe form of MFS in patient 2. Therefore, a mRNA analysis for this patient would be a benefit of to understand the fibrillin-1 function in MFS patient with a mutant fibrillin-1 compared to those with a loss of one fibrillin-1 allele. Furthermore, we have found a two-exon mutation encompassing exons 64-65 of the *FBN1* gene in a patient by whom no clinical signs have been documented. We believe that this is the first deletion so far described to include the complete deletion of last exons of the fibrillin-1 gene, which is important for the termination of the protein synthesis. Fibroblast analysis has been performed by Dr. Keyser, institute of Human Genetics and she has found a reduction in the fibrillin-1 protein levels. In our cohorts of 20 decedents, who died of sudden, unexpected TAA has shown no larger deletions and duplication in the *FBN1* and *TGFBR2* gene using the MLPA-P065 and P066 kits. This could be due to several factors such as, these patients DNA have been obtained from tissue samples, in the MLPA analysis we have observed false positive expression levels across both *FBN1* and *TGFBR2* genes, upon repeating and comparing with reference samples, these reduction or increase in copy numbers have not been recurrent and indicative for a true copy number changes, indicating of possibel carry overs during the extraction of genomic DNA using phenol-choloform extracton method. This may be improved by using automated DNA purification kit such as the QIAamp DNA Mini QIAcube kit which has been modified for the use of DNA extraction from human tissue. Another reason may be that these patients may harbour a large DNA variant in exons 1, 11-12, 21, 23, 28, 33, 38, 40, 49 52, and 60 of the *FBN1* gene or in exon 2 of the *TGFBR2* gene, which has not been covered by the recent MLPA kit. Or these patients may harbour deletions or duplications in other genes that have been described in the context of Marfan-LDS- related syndromic and non-syndromic forms

with TAAD such as *COL3A1*, *ACTA2*, *MYH11*, *SLC2A10* and *NOTCH1* gene which are not covered by todays MLPA kits. Mosaicism and copy number rearrangements are also not covered by this assay, which seems to be one of the limitation of the assay: Nevertheless, kits containing probes for further TAAD linked genes may be a benefit to locate deletions and duplications in these genes. Further MLPA kits are avaliable for complete exons of the genes *TGFBR1* and *TGFBR2* (P-148, MRC-Holland, Netherlands), with the exception of exon 2 in the *TGFBR2*. Nonetheless, major pathogenic mutations for *TGFBR1* and *TGFBR2* have been predominantly missense or splice–site mutations (Faivre *et al.*, 2007). So far only one *de novo* 14.6 MB duplications have been localized in the *TGFBR1* gene on chromosome 9p22.32q31.2 in a 17 year old girl with dysmorphic features indicative for LDS, however, so far no deletions have been described for both *TGFBR1* and *TGFBR* 2 genes (Furtado *et al.*, 2011), which coincides with our findings that large DNA changes are very rare in the two latter genes.

5.6   Evaluation of indirect DNA marker analysis in two unrelated German families

Indirect genetic analysis with polymorphic short tandem repeat DNA markers for TAAD are useful application in families who are clinically obvious for MFS or MFS-related heritable diseases, but do not completely fulfil the Ghent nosology criteria or the index patient is negative for mutation in the *FBN1* gene using conventional Sanger sequencing or other sequencing methodologies. This is a good alternative approach of traditional sequencing methods since it reduces the impact of sequencing complete exons of all TAAD candidate genes, which can be too expensive and time consuming. Herein, we have found no linkage of TAAD markers and the disease running in family 1 (patient I6), where several members in the family have shown typical skeletal abnormality and manifestation of the cardiovascular system. Only five family members have been available for the analysis, which is a small group to get a good and reliable result. In family 2 (patient I9), a linkage has been found for the marker of TAAD3/BAV and the disease, by which the marker haplotype (20/23/16) segregated with the disease in family 2 (patient I9). Till today, the disease gene remains unknown for this locus (Elliso *et al.*, 2007). Goh *et al.*, has reported the first case on genetic linkage of TAAD3/BAV in several family members who have exhibited BAV with ascending aneurysm. Similar phenotypes have been found in multiple family members in our family. Thus, patients will benefit from the identification of the disease gene for this loci and the other two TAAD loci (AAT1 and AAT2), this could only be done by studying a panel of large families who show a strong history for TAAD and in families who do not fulfil the clinical

criteria for MFS but show features which are typical of a MFS patient or by simply sequencing this marker region where we found to segregate with the disease in family 2 (patient I9). Once the disease gene is identified, either conventional Sanger sequencing reaction or the novel MFSTAAD resequencing assay can be performed in order to look for a disease-causing mutation. Furthermore, abnormal MMPs and their inhibitors have been described in the context of aortic aneurysms (Knox *et al.*, 1997). A total of 20 metalloproteinases exists and are shown to play an important role in the ECM metabolism and aortic wall remodelling (Galis & Khatri). A gene cluster encoding several MMPs, especially *MMP1*, *MMP3*, *MMP8* and *MMP10* maps to the same chromosome 11q like the AAT1 locus. Interestingly, gene encoding MMP-8 has been reported to be upregulated in patients with abdominal aortic rupture (Wilson *et al.*, 2006), similar clinical feature have been found in family 2. Furthermore, an additional gene encoding for *MMP9* has shown to be involved in the formation of aortic aneurysms and dissections in the thoracic aorta, which is mostly described in FTAAD, and in syndromic form of TAAD such as MFS. Showing further evidence for a potential role of MMPs in the pathogenesis of the heterogenous TAAD disease. Thus, it would be worthwile to test markers spanning this MMP gene cluster on chromosome 11q2, and additional markers covering the gene *MMP9* mapping on chromosome 20q13.12 in furture family studies with TAAD, including markers of the gene *NOTCH1*, on chromosome 9q34.

5.7   Résumé

In conclusion, this study shows that MFSTAAD microarray platform is an appropriate, rapid and cost-effective mutation analysis tools by which it allows parallel mutation analysis of all target genes in a single experiment. The microarray facility allows a custom array design in which all sequence positions of interest can be interrogated by specific short oligonucleotide probe sets. Through the parallel sequencing of candidate genes that encode for proteins which may play a role in the pathogenesis of TAAD allows scientists to gain a better understanding on the interaction among the proteins that maintain normal aortic function and under a disease status. Such genetic testing with MFSTAAD microarray is definitely a golden standard tool, by which it may help to identify at-risk relatives of patients with FTAAD; still a follow-up sequencing test is required to rule out the presence of large gene deletions and insertions, such as MLPA and/ or a-CGH.

6. *Appendix*

ID	1	§2
Gender	F	M
Age	23	22
Skeletal	pectus carniatum, reduced US/LS, wrist/thumb signs, protrusion acetabuli, PES planus	general joint laxity, tall, scoliosis
Cardiac	mitral valve prolapsed without mitral valve insufficiency, dilatation of the pulmonary artery	mitral valve prolapsed with mitral valve insufficiency, severe aortic aneurysm, achieved a heart transplantation,
Ophthalmologic	ectopia lentis	lens luxation
Craniofacial	Palate anomaly, microretrognathie	arched mouth causing problems with teeth
Family history for MFS/TAAD	Unknown	Yes

Appendix 1: Clinical signs of two individuals with classical MFS. § This patient has a sister who is tall and has an enlarged aorta, several close relatives from his maternal side are tall people and several people died of unknown heart failure. Clinical data of the relatives were not available.
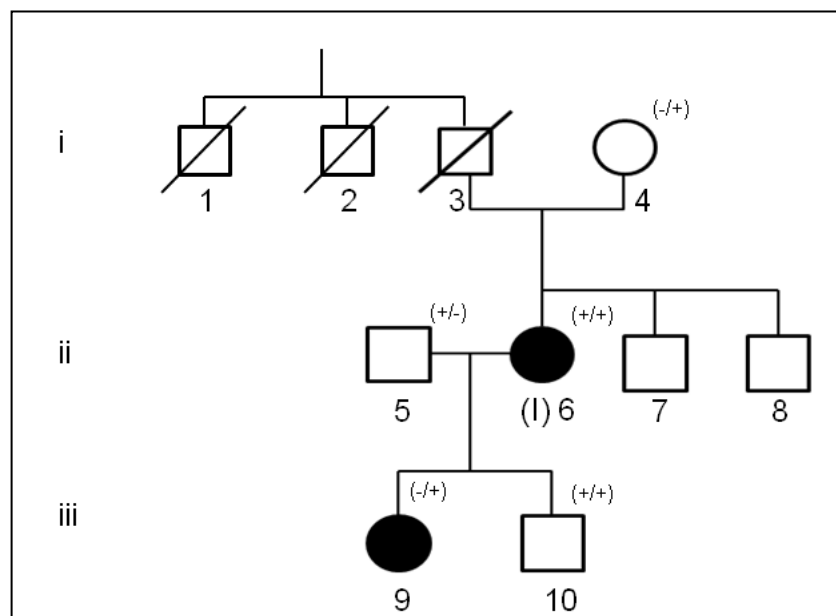
Appendix 2: Familiy pedigree 1 with Marfan syndrome with/ without aortic aneurysms carrying two non-synonymour DNA variants in the *TGFBR3* gene (c.44C>T, p.S15F and c.55A>G, p.T19A). Round symbols indicate females; square symbols indicate males.

Symbols with a line across represent a deceased subject. Round bolded symbols represent individuals affected by MFS. (I6) is the index patient in this family. From the paternal side of the index patient, one of her uncle (I2) was a tall (190 cm) and thin person who died of abdominal aortic rupture at the age of 65. Her father (I3) was also a tall person (190 cm) and died of lung disease at the age of 80. The index patient has a normal height (168 cm) compared to her father and two brothers (7 and 8, both 190cm tall). Both of her brothers have pectus excavatum and her daughter (I9) is highly suspected for MFS. No mutations have been found in the genes *FBN1*, *TGFBR1* and *TGFBR2*, but two variants were detected by Singh *et al.,* 2012, which did not co-segregate with the disease. A (+) or (-) sign in brackets stand for mutation positive or negative of previously found DNA variant *TGFBR3* c.44C>T, p.S15F and c.55A>G, p.T19A. A plus sign designate mutation-positive and minus sign for mutation-negative for the respective DNA alteration.
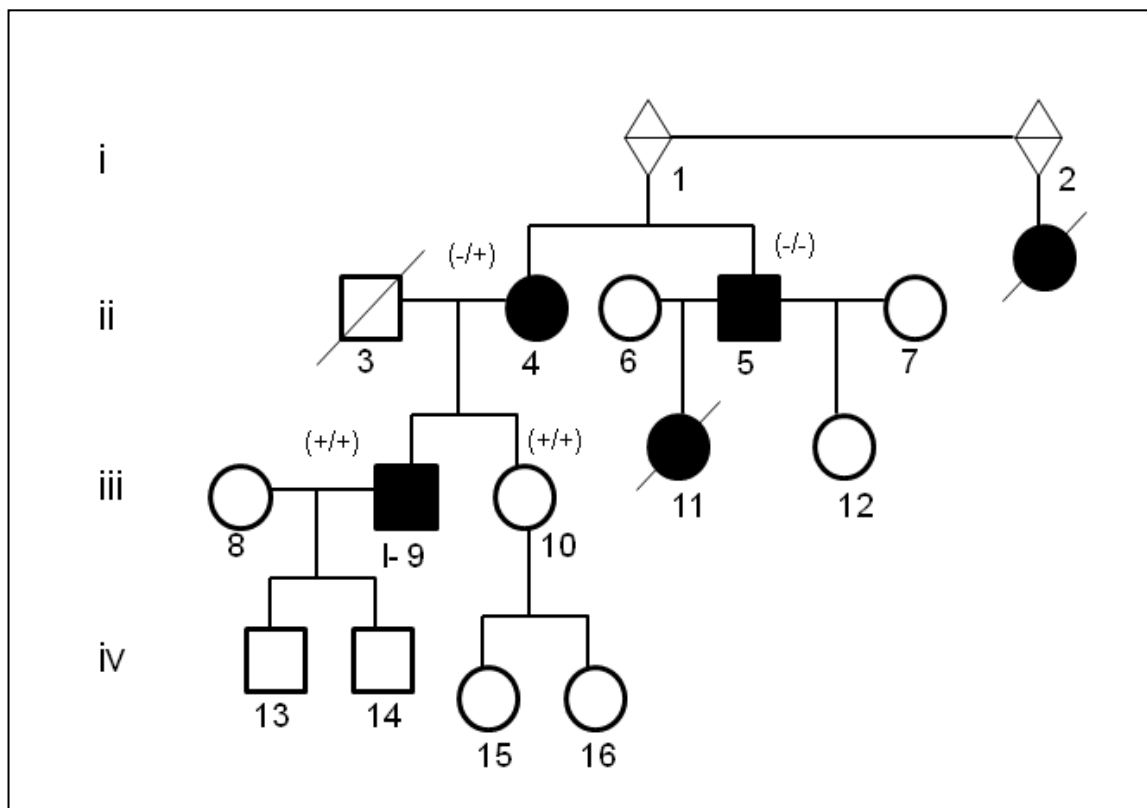
Appendix 3: Family pedigree 2 with Marfan habitus and aortic aneurysms/rupture with one non-synonymous DNA variant c.55A>G (p.T19A) in the *TGFBR3* gene and one disease-causing mutation in the *ACTA2* gene c.977C>A (p.T326N). Round symbols indicate female and square symbols stand for male. Line across indicate deceased subjects. Filled symbols indicate affected individuals. Index patient (I9) has a Marfan habitus with aortic rupture. His sister (10) is a normal subject. From the maternal side of the index patient, his uncle (5) shows similar clinical feature, and his mother has only a Marfan habitus. Aunt

(2) of the mother of the index patient died of aortic aneurysm at the age of 33 years of unknown cause. Father of the index patient (3) died of lymphoma. A (+) or (-) sign in brackets stand for mutation positive or negative of previously found DNA variant in the *TGFBR3* gene c.44C>T, p.S15F and *ACTA2* gene c.977C>A, p.T326N. A plus sign designate Mutation positive and minus sign for mutation-negative for the respective DNA alteration.
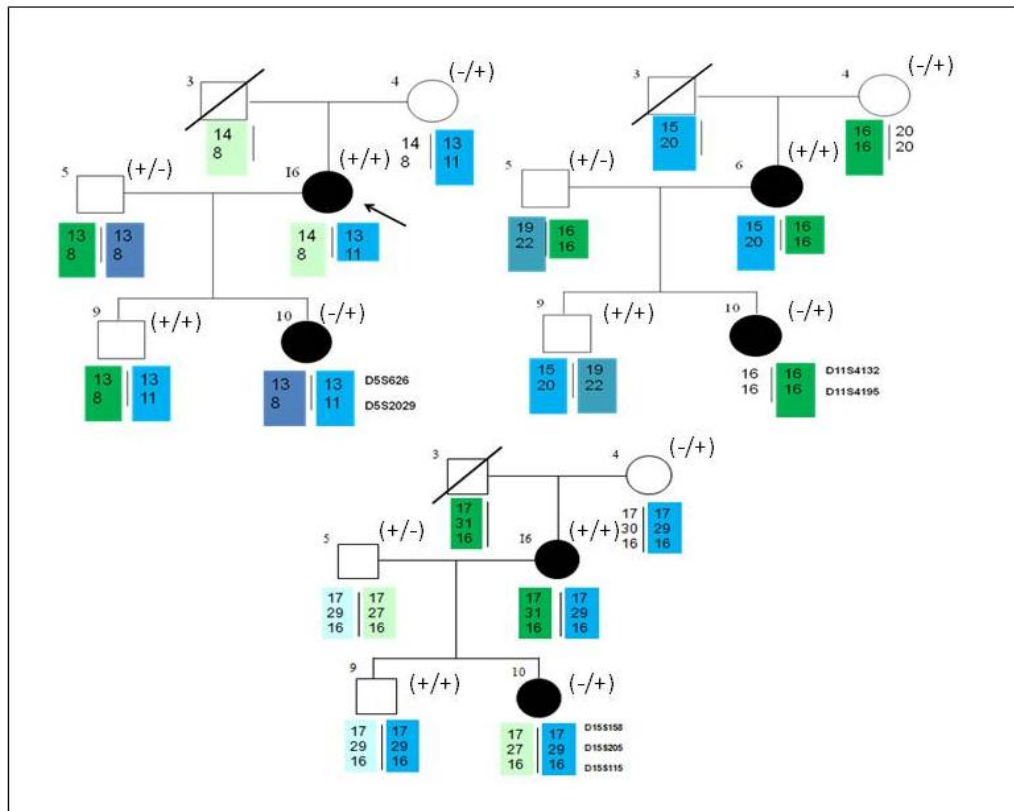
Appendix 4: Indirect marker analysis for FTAAD in family 1 using markers for TAAD loci. The numbering correlates with the family pedigree in appendix 2. Squares represent male member and circles stand for females. Affected and unaffected individuals are represented by black bold and open symbols, respectively. Line across denote deceased. A (+) or (-) sign in brackets stand for mutation positive or negative of previously found DNA variants in the *TGFBR3* gene, c.44C>T, p.S15F and c.55A>G, p.T19A. A plus sign designate mutation-positive and minus sign for mutation-negative for the respective DNA alteration. Top left are haplotypes for *TAAD1* locus (top to bottom D5S626 and D5S2029). Haplotypes for *AAT1* locus (top to bottom D11S4132 and D11S4195) are shown on the top, right panel. Bottom right are the haplotypes for *TAAD3*/BAV locus (top to bottom D15S158, D15S205 and D15S115, respectively). The haplotype analysis was performed for each subject.
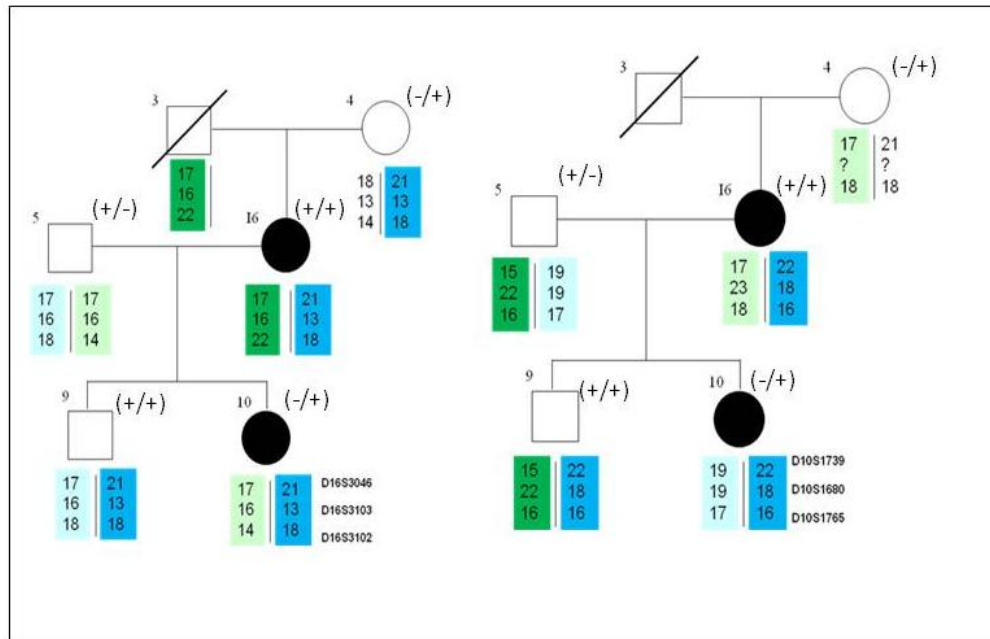
Appendix 5: Indirect marker analysis for FTAAD in family 1 using markers for TAAD candidate genes *ACTA2* and *MYH11*. The generation and subject number correlate with the original pedigree numbering in the appendix 2. Squares represent male member and circles stand for females. Affected and unaffected individuals are represented by bold and open symbols, respectively. Line across denote deceased. A (+) or (-) sign in brackets stand for mutation positive or negative of previously found DNA variant *TGFBR3* c.44C>T, p.S15F and c.55A>G, p.T19A. Left panel are haplotypes for the *MYH11* candidate gene (*MYH11* locus) from top to bottom D16S3046, D16S3103 and D16S3102, respectively. Right panel are haplotypes for *ACTA2* candidate gene of TAAD (*ACTA2* locus; right panel) from top to bottom D10S1739, D10S1680 and D10S1765, respectively.
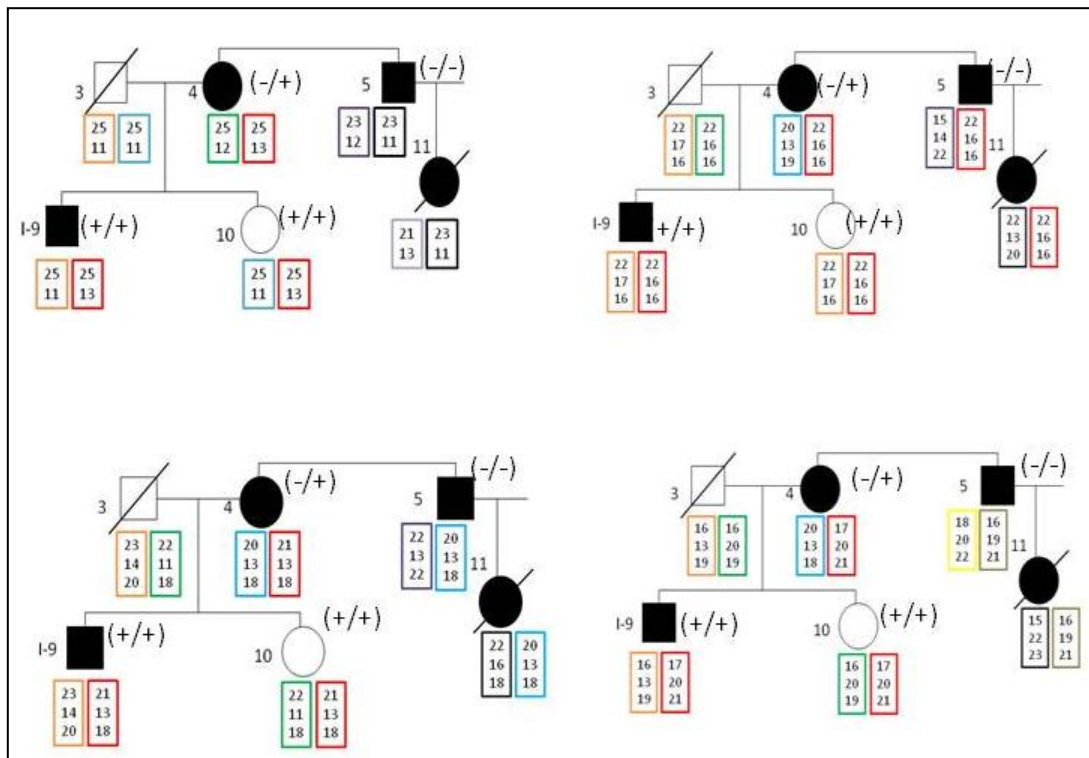
Appendix 6: Indirect marker analysis for FTAAD in family 2 using markers for candidate genes *ACTA2* and *MYH11*. Subject numbers are indicated with numbers. Squares represent male member and circles stand for females. Affected and unaffected individuals are represented by bold and open symbols, respectively. Line across denote deceased. A (+) or (-) sign in brackets stand for mutation positive or negative of previously found DNA variant *TGFBR3* gene c.44C>T, p.S15F and *ACTA2* gene c.977C>A, p.T326N. A plus sign designate mutation-positive and minus sign for mutation-negative for the respective DNA alteration. Left panel are haplotypes of *AAT2* locus (top to bottom D5S641 and D5S626) shown below each respective individual. Haplotypes for *AAT1* locus (top to bottom D11S4132, D11S924 and D11S4195) are shown on the top, right panel. Bottom left panel are haplotypes for the *MYH11* candidate gene (*MYH11* locus) from top to bottom D16S3046, D16S3103 and D16S3102, respectively. Bottom right panel, are the haplotypes for *ACTA2* candidate gene of TAAD (*ACTA2* locus; right panel) (from top to bottom D10S1739, D10S1680 and D10S1765).

Appendix 7:	Primer sequence flanking genetic markers.			
Marker	Primer forward (fluorescently-tagged) 5'-(6-FAM…-3'	Primer reverse 5'-3'	PCR product size (bp)	Number of CA_n repeats
D5S626	ACCTGCACATGTACTCTCTGA	CATGGAAGGAGCCTGTATAA	100	13
D5S641	AGTTGTGTATTGGAGAATGTTATCA	AGGGACAGTCCACTTCCAGT	265	22
D5S2029	AAGAATTGCACAGTGATGGC	CCATTGACTTTAAATGTCACCATAC	129	18
D11S4132	GTGCAAGTTTTGGCTTCGTC	ACTCCAGCCTGGGTGAAA	206	23
D11S924	TAGAGTGAGACTCTGTCTCAAACA	GAGGGATGGACTAGCCTAAA	119	17
D11S4195	GTGGCCCAGGCTGTTC	GCTGCTAAATGTCACACTGAGA	275	17
D15S158	CAGGAGACCTCCAAACACA	TTTCAGCCAAGAAGCACG	87	20
D15S205	CTTAATGGTTTGGCAGGATA	AGCTTAAAANCAAAATCTCCC	160	31
D15S115	TACACAAATGGTACACTTTCCA	TGGCTGGGTCTCTACATTTA	115	18
D16S3046	CCCAGAATAAACTGCGTG	TTCATGGACCCCCTATTG	233	22
D16S3103	GCTTTGAGTCTCCACATCTATGA	GGCCAGCAGGTCTTCCTA	102	14
D16S3102	CATGGGGACTCTGGCTAAC	ATCGTGTAATGACTGCCACAA	170	18
D10S1739	CTGGAAAAACAACAGAGGTG	GCTGTCTAAATCAAGGAATGTC	239	17
D10S1680	AGCCTGAGCAACATATCGAA	TCCCGAAGCAGAGAGTACCT	217	25
D10S1765	ACACTTACATAGTGCTTTCTGCG	CAGCCTCCCAAAGTTGC	180	23

Appendix 8:	Primer pair for fibrillin-1 (*FBN1*) Gene	
Primer description	Primer sequence (5'⟹ 3')	PCR product size (bp)
FBN1_E1F	ACGAAGGAGGGGGTGTCATTTTCTT	1,373
FBN1_E1R	TGGGGACTAAACAACCCTAGCACCT	
FBN1_E2F	CTGATGGGCCATATGCATAGGTGATA	3,329
FBN1_E3R	GGGGTGCATTTTCTTACAGGACAAAA	
FBN1_E4F	TTTTGTATTTTTAGTAGGGACGGGGTTC	4,362
FBN1_E5R	GAAGTAGCCATGCAGACCCAATGTC	
FBN1_E6F	GTTCCTCTGCATGATGGTTCCTGCTTT	11,951
FBN1_E8R	TCTTTTATGGGAGGCAAAACGTCTCCA	
FBN1_E9F	GAGGTGTGAGTTAATCCTGCCGTAGCC	10,956
FBN1_E13R	AGACCCCTGATATTGAAACTGCAATGG	
FBN1_E14F	CATGCACATGCCAAAACTCAAGAACT	11,964

FBN1_E18R	GAGAATGGCTCAGAATCTCTGCATCTT	
FBN1_E19F	AAACCAGGTCAAGCCTCTGTTTTCC	4,083
FBN1_E23R	CCCTATCGGACATGCTGAATTTTGGAG	
FBN1_E24F	GCAGTGGAAGCCGTGTGGCTCTATTTA	4,834
FBN1_E29R	GACTCCAAAGCCTGGGCCCTAAA	
FBN1_E30F	AGACTTTTAAGCAGGTGTGGACGTTGC	10,109
FBN1_E33R	AGGTCTCCCTAATTGACCTGGTTCCAA	
FBN1_E34F	TGTATTTCTCTCCAACAGGCCATCATC	3,163
FBN1_E35R	TCTTCTGTGACGGCCCTTGTGTAG	
FBN1_E36F	GATTGGGCCCTGTTCTTTTATG	3,605
FBN1_E39R	CTCCATGTAGATGAAAACCATGGCTCA	
FBN1_E40F	ATCAGGCCATTCCAAAATGTGAAGTTT	11,793
FBN1_44R	CGAGCAGACAGGCAAATAGCAAATCTA	
FBN1_E45F	ATAACAGTGGCATCCCGGACACAT	3,464
FBN1_E46R	GGGGGTCTCAGAATGTATCCCTCAC	
FBN1_E47F	TTGGGTAGCAGCTGACCTTGGATAA	4,858
FBN1_E49R	GTAGCTCAACTTCCCCCAGGCTTT	
FBN1_E50F	TTGCTGTGGTCCTGAGAGGAGAACATA	5,298
FBN1_E54R	CCCCCGTATTGTCCACGGACTATTTAT	
FBN1_E55F	GAAGAGGTCATCAGTTGATTAGGGAGCA	5,860
FBN1_E59R	CTTCCTCCACAATCTCCCTGGCTTTAG	
FBN1_E60F	CTTGCCTTTTGCTGTGGCTTCTTTCTA	11,424
FBN1_E65R	CACATGAGAAGCCTGAGAAAGTGGTTG	

Primer pair forTransforming growth factor beta receptor- 1 (*TGFBR1*) Gene		
Primer description	Primer sequence (5' ⟹ 3')	PCR product size (bp)
TGFBR1_E1F	AAAGAGACTCACACAGACACACCCATC	1,085
TGFBR1_E1R	GACTCCCACTGGACGAAGCCCTAGA	
TGFBR1_E2F	TCACACATTGCTTCTCAAAGGAGGA	4,691
TGFBR1_E3R	AATGGGTTAGCTGCAGATCATGTGAAT	
TGFBR1_E4F	CTTCTGTGTTTCAGCGTTCACATCC	12,401
TGFBR1_E9R	GCAATCCACTCCTTTGCCCTTAAA	

Primer pair for transforming growth factor beta receptor- 2 (*TGFBR2*) Gene		
Primer description	Primer sequence (5' ⟹ 3')	PCR product size (bp)
TGFBR2_E1F	GAGCGAGGAACTCCTGAGTGGTGT	779
TGFBR2_E1R	AAAACTCACAATCCCTGCAGCTACG	
TGFBR2_E2F	ACCCCTCACCACGGTACAATGGATTT	6,016
TGFBR2_E3R	CCACCACAGGAGGAATGTGCTCTATGA	

TGFBR2_E4F	TGAAAAGAGGAATGTTGGGTGGATG	3,534
TGFBR2_E5R	CCCCAAATAGTTCTGGGATGGTTGT	
TGFBR2_E6F	TACTTCTCTAGCCCTTCCCAACCA	3,573
TGFBR2_E7R	CCCTGCTGCTGTTGTTTCTGCTTAT	

Primer pair for actin, alpha 2, smooth muscle, aorta (*ACTA2*) Gene		
Primer description	Primer sequence (5'⟹3')	PCR product size (bp)
ACTA2_E1F	TGTTAGACTGAACGACAGGCTCAAG	5,707
ACTA2_E3R	CCCAGCAGTAGTGTGGTGTTCTGTA	
ACTA2_E4F	TCAAGTAGCTTCTGGTCCCTTTTTG	8,982
ACTA2_E9R	GGGTGAGGTCAACCTAACAAATGGT	

Primer pair for myosin heavy chain 11, smooth muscle (*MYH11*) Gene		
Primer description	Primer sequence (5'⟹3')	PCR product size (bp)
MYH11_E1F	GTTCTCAAGCATCCCGCACAGAC	654
MYH11_E1R	GCACCCCCAAAATGGTACTTCTC	
MYH11_E2F	CCTTTGGGTGGTCTCTGTTCTTTGA	752
MYH11_E2R	ACCACCACCCTTGGCTACTTTTTGT	
MYH11_E3F	GTGACAGAGTGAGACCCCATCTCAAA	614
MYH11_E3R	GTGACAGAGTGAGACCCCATCTCAAA	
MYH11_E4F	GGCCAGCATGGAGAAGCTTTAGAAT	275
MYH11_E4R	AGAGGCACTTGGAACCATGAACAAA	
MYH11_E5F	CTCTGGGAAATGGTGGTGATGATC	11,165
MYH11_E9R	TGCCCCTGCAAATTCCTTATAAAAC	
MYH11_E10F	GTGTAAGGCTGGCAGTGGTTGGTG	12,569
MYH11_E13R	GAGAACGATGGCGGGAGATCAGAC	
MYH11_E14F	GGGGCTCCTTGTCTTCTGACTTCAT	5,014
MYH11_E16R	CACAGAGCTAGGAGGTGGCAGAGAC	
MYH11_E17F	AGGTGCTCTCAGGATTTCCCCAATA	3,163
MYH11_E20R	TCCACGATGAGAACCCAGGTCTAAA	
MYH11_E21F	GAGCCCTGGGTCTTCCTTGTCC	10,217
MYH11_E27R	GCGGCCAGGAAGGTAAATGCAC	
MYH11_E28F	GAGGGGTGGTGATGAGGACTGC	8,818
MYH11_E32R	CGCCCAAGACAAGATAAGACAGC	
MYH11_E33F	CACCTGCACCTCAATACATTCAGC	8,703
MYH11_E41R	CAGGGTTTCGGCATTCACATCCAG	
MYH11_E42F	CAGCCTGGGTGACAGAGACTATC	5,163
MYH11_E43R	TGTGAGGGGTGTCTGTGATATTTG	

Primer pair for collagen type III, alpha 1 (*COL3A1*) Gene		
Primer description	Primer sequence (5'⟹ 3')	PCR product size (bp)
COL3A1_E1F	CAGATGCATACAAACTCCAGATGTGCT	724
COL3A1_E1R	CTTCCAGACTGCCTGGGGAAGTATT	
COL3A1_E2F	TCCCATCTGCTGTTAAGGCAAAGAA	10885
COL3A1_E21R	GCCAGGAAAGTTGTTGAACAGAGGA	
COL3A1_E22F	AAATGTTTCAGCAACACACGAACCC	9,602
COL3A1_E40R	CTCAGTGACTCTGGATGGCAAAGG	
COL3A1_E41F	TCCATCCATTCAAGTCATCTTGCAC	2,354
COL3A1_E44R	CCTGAACACGCTGGAAAATAAAATA	
COL3A1_E45F	GTCCAAAATGAAAACAACCACAGAAAC	4,772
COLA1_E51R	TGCAGATGGGCTAGGATTCAAAGAA	

Primer pair for solute carrier family 2, member 10 (*SLC2A10*) Gene		
Primer description	Primer sequence (5'⟹3')	PCR product size (bp)
SLC2A10_E1F	CCAGACAAGTGTGGACCAGTGATTG	806
SLC2A10_E1R	CGAATCGATGAACTGCTTTGCTTCT	
SLC2A10_E2F	TGATGGATGGTTGGGTGAATTAAGG	2,051
SLCA10_E2R	GAGGAGCAACTGCAGGTAAGTGAGG	
SLC2A10_E3F	CCTTAAAGCCCGGATAGCTCACAAC	7,528
SLC2A10_E5R	AGAGATGTGCAAGTCAATGGGGAAA	

Primer pair for notch 1 (*NOTCH1*) Gene		
Primer description	Primer sequence (5'⟹ 3')	PCR product size (bp)
NOTCH1_E1F	GGCGGGGGCGGAGCGCACCTCGACTCT	2,309
NOTCH1_E2R	CCCCGGAGCCTGAGGTGGCCCACGGAG	
NOTCH1_E3F	AGCTTGTTCCCCAAGTTAGCAGTCA	1,771
NOTCH1_E4R	GGCGTCCTACAGCTCGAATGTGAGT	
NOTCH1_E5F	GCTCTTGTGTCCAGAGCAGTGTGTC	2,809
NOTCH1_E9R	CTCCCATCCACTCATGAGGCAAAAC	
NOTCH1_E10F	CCACTGTAGCCATAGCAACCCAGTC	2,035
NOTCH1_E13R	CTGCTGGGTGTGGACTGTAGTCTGA	
NOTCH1_E14F	AAAGGACTCTGCGAGTCTGAGTGGA	3,276
NOTCH1_E17R	GCCATCCTCGGCTCAGTGAAGAG	
NOTCH1_E18F	GAGAGAGACCCCAAGCACAGGAGAC	3,771
NOTCH1_E24R	AAGACATCAGGGTGAGGAGGAGGAT	
NOTCH1_E25F	GGTTAGCAGCTTGCATCAATTTCACTC	5,233
NOTCH1_E30R	TGGCGGGCAACTGCTTCCTGACCTGCCCA	

| NOTCH1_E31F | GTCCTCTTTTTCCTGGGTGGATTTTG | 5,327 |
| NOTCH1_E34R | GGAAAACCCTGGCTCTCAGAACTTG | |

Appendix 9:   KOD XL DNA polymerase, Novagen

Reaction mix of KOD XL Long-range kit (Novagen)

Components	Volume in each reaction (µL)	Final Concentration
PCR Buffer (10x)	5	1x
dNTPs (10mM each)	5	200 µM (each)
Primer F (10µM)	2	0.4 µM
Primer R (10µM)	2	0.4 µM
KOD XL DNA polymerase	1	2.5 U/µL
Template	10	10 ng/µL
DMSO	1	3%
H_2O	23.5	Final volume of 50 µL

Initial Denaturation	94ºC	60s	
Denaturation	94ºC	30s	
Annealing	**58, 60, 62 ºC**	**10s**	**30 cycles**
Extension	72ºC	360s	
Final extension	72ºC	600s	
Holding	10ºC	∞	

Thermal Cycling Condition of KOD XL <8kb. Two different thermal cycling conditions were applied for target fragment size <6kb and >6kb.

Appendix 10:   GoTaq Flexi DNA polymerase, Promega

Reaction mix of GoTaq® Flexi DNA Polymerase

Components	Volume in each reaction (µL)	Final Concentration
GoTaq® Flexi Buffer (5x)	10	1x

108

dNTP mix (10mM each)	1	200 μM (each)
Primer F (10μM)	2	0.3 μM
Primer R (10μM)	2	0.3 μM
GoTaq® Flexi DNA polymerase	0.5	5 U/μL
Template	15	10 ng/μL
MgCl$_2$ (25mM)	6	3 mM
H$_2$O	28.5	Final volume of 50 μL

Initial Denaturation	95ºC	120s	
Denaturation	95ºC	30s	
Annealing	**58,62ºC**	**30s**	**30 cycles**
Extension	72ºC	480s	
Final extension	72ºC	300s	
Holding	4ºC	∞	

Thermal Cycling Condition of GoTaq Flexi Long Range < 8 kb.

Appendix 11:   Expand LongRange dNTPack, Roche

Reaction mix of Expand Long-range dNTPack		
Components	**Volume in each reaction (μL)**	**Final Concentration**
Expand Buffer (5x)	10	1x
dNTP mix (10mM each)	2.5	500 μM (each)
Primer F (10μM)	1.5	0.3 μM
Primer R (10μM)	1.5	0.3 μM
Enzyme	0.7	5 U/μL
Template	10	10 ng/μL
MgCl$_2$ (25mM)	4	2 Mm
H$_2$O	19.8	Final volume of 50 μL

First Cycling	92ºC	120s	
Second Cycling			
Denaturation	92ºC	10s	
Annealing	58, 60, 62ºC	15s	10 cycles
Extension	68ºC	780s	
Third Cycling			
Denaturation	92ºC	10s	
Annealing	58, 60, 62ºC	15s	20 cycles
¥Extension	68ºC	780s	
Final Elongation	68ºC	420s	
Holding	4ºC	∞	

Thermal Cycling Condition for Expand dNTPack Long-Range < 8 kb

First Cycling	92ºC	120s	
Second Cycling			
Denaturation	92ºC	10s	
Annealing	60 ,62, 64ºC	15s	10 cycles
Extension	68ºC	780s	
Third Cycling			
Denaturation	92ºC	10s	
Annealing	60 ,62, 64ºC	15s	20 cycles
¥Extension	68ºC	780s	
Final Elongation	68ºC	420s	
Holding	4ºC	∞	

Thermal Cycling Condition for Expand dNTPack Long-Range >8kb

Appendix 12: Qiagen LongRange PCR, Qiagen

Reaction mix of one 50µL long range PCR reaction.*Q-soltution was not added for PCR fragments >5kb.

Components	Volume in Each Reaction (µL)	Final Concentration
PCR Buffer (10x)	5	1x
dNTPs (10mM each)	2.5	500 µM
Primer F (10µM)	2	0.4 µM
Primer R (10µM)	2	0.4 µM
LongRange PCR Enzyme Mix	0.4	2 U/50µL
Template	5	10 ng/µL
*Q-solution (5x)	10	1x
RNAse free water		
23.1µL (with Q-solution) OR 33.1 µL (without Q-solution)		
to a final volume of 50 µL		

Initial Denaturation	93ºC	180s	
Denaturation	93ºC	30s	
Annealing	58,64ºC	30s	35 cycles
Extension	68ºC	30s	
Final extension	68ºC	480s	
Holding	4ºC	∞	

Thermal Cycling Condition for Qiagen LongRange PCR (fragments <5kb)

First Cycling	93ºC	180s	
Second Cycling			
Denaturation	92ºC	30s	
Annealing	62ºC	30s	10 cycles
Extension	68ºC	780s	

Third Cycling			
Denaturation	92ºC	30s	
Annealing	62ºC	30s	28 cycles
¥Extension	72ºC	780s + increment of 20s in each cycle	
Holding	4ºC	∞	

Thermal Cycling Condition for Qiagen LongRange PCR (fragments > 5 kb). [¥]Three system of thermal cycling condition

Appendix 13: False variants seen with the "MSFTAAD" resequencing assay.		
COL3A1		
6	c.539G>C	GC stretch
8	c.645A>T	
	c.637-16A>T	
20	c.1348-16C>T	T stretch
22	c.1546G>T	
31	c.2134C>A	
43	c.3115C>A	
44	c.3213C>T	
48	c.3531C>A	
50	c.4059T>G	wrong primer sequence
Number of variants	**10**	
FBN1		
8	c.867T>G	
14	c.1719G>T	
11	c.1415G>A	wrong ENSEMBL sequence
23	c.2729-8C>T	
	c.3589+31T>C	Tstretch
31	c.3839-19T>N	
	c.3829-20A>N	
51	c.6348G>A	
65	c.*33A>G	AG stretch
Number of variants	**9**	
TGFBR1		
4	c.805+29A>N	T stretch
9	c.1387-14A>N	Poly A tail
Number of variants	**2**	
MYH11		
1	c.-110-6G>A	

		homozygous change in the
15	c.1744G>C	neighbouring position
21	C stretch	
24	c.2997+29C>T	
31	c.4116+6T>A	
38	c.5172-11C>A	

Number of variants	**5**

NOTCH1		
1	c.-76-26C>A	
	c.-76-5A>C	
3	c.335G>A	
4	c.682C>A	
6	c.1027G>A	
10	c.1556-12C>G	
	c.1604C>G	
11	c.1840C>A	
	c.1845G>A	
13	c.2063A>G	
	c.2064C>G	
	c.2081A>T	
15	c.2467+30G>A	primer sequence wrong?
18	c.2761T>A	
	c.2876A>C	
19	c.2996T>A	
	c.3137C>G	primer sequence wrong?
	c.3476T>A	
	c.3171+36G>T	
21	c.3476C>A	
22	c.3579G>C	
29	c.5472+39A>T	
34	c.6549C>T	
	c.6844A>T	
	c.6862T>A	

Number of variants	**25**

SLC2A10	
1	c.-177G>T
2	c.170G>T

Number of variants	**2**

Total number of variants	**53**
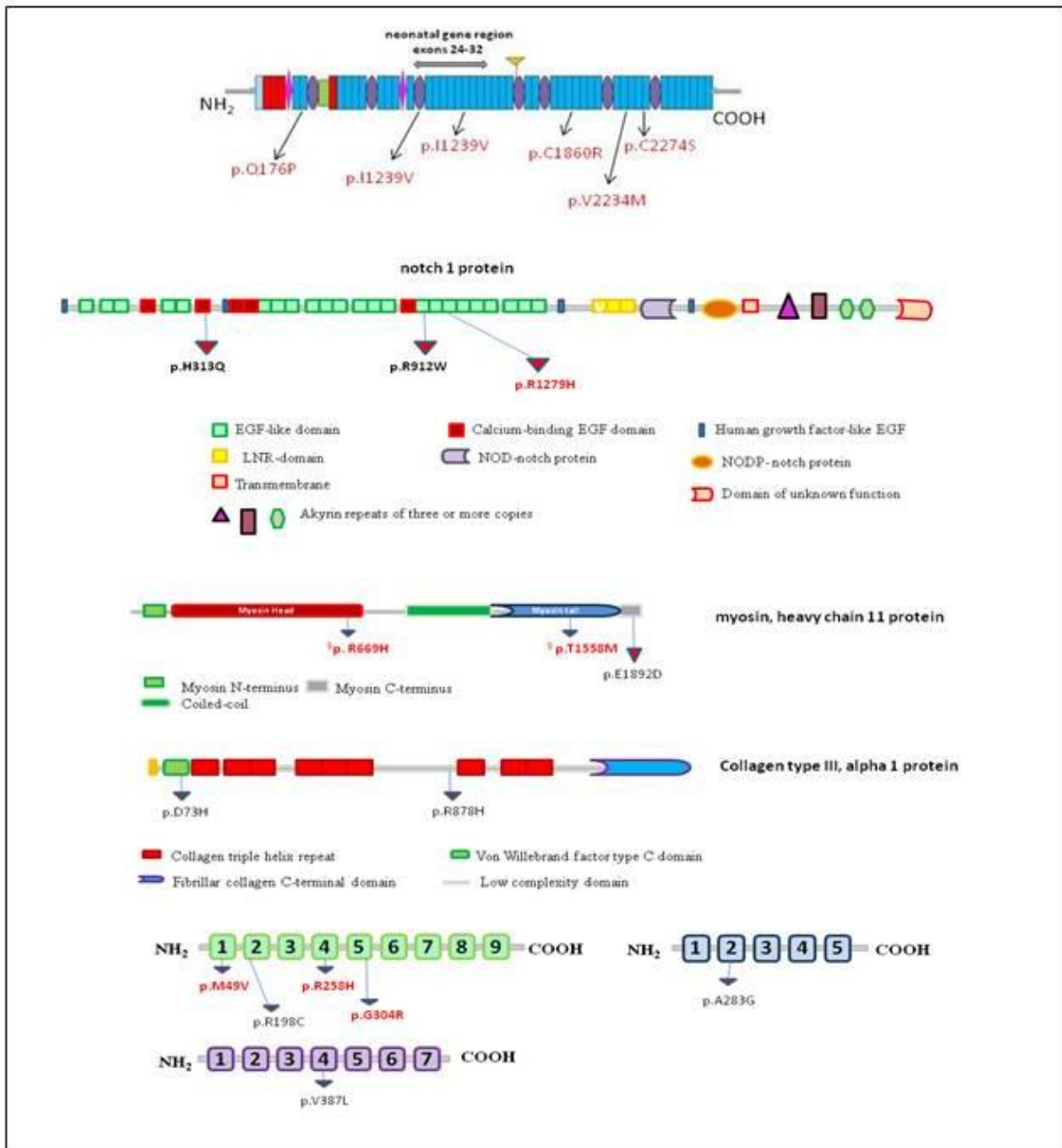
Appendix 14: Topography of known and novel point mutations found with MFSTAAD resequencing assay. Schematic representation of proteins *fibrillin-1*, *notch1*, *myosin alpha, heavy chain 11*, *collagen type III*, *alpha 1*, *and genes ACTA2* (top left) *SLC2A10* (top right) *and TGFBR2* (bottom left) with the location of point mutations. [§]DNA variants with very low occurrence rate (http://www.ncbi.nlm.nih.gov/projects/SNP).
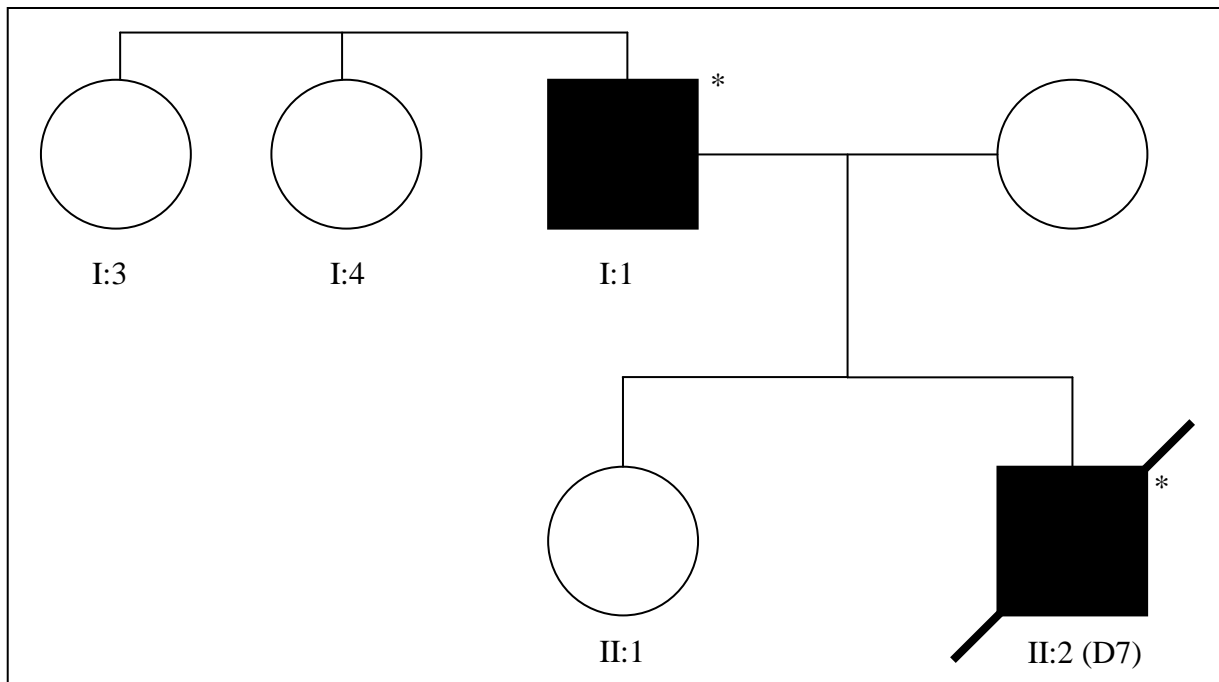
Appendix 15: Segregation analysis of DNA variant *MYH11* c.4673C>T, p.T1158M with family members of PD7. Round symbols indicate females and square symbols indicate males. Blackened symbols indicate affected individuals (determined solely by clinical information). Black symbols with crossed line indicate a deceased subject. A star beside a square or round symbol resembles carriers of this mutation.II:2 PD7 was a 32 years old young male who died of sudden and unexplained TAAD. There was no previous clinical history reported in the medico-legal autopsy. But the cause of TAAD was highly suspected of a heritable disease due to the occurrence of TAAD at young age. Upon mutational analysis of TAAD associated genes, a PDC mutation in the gene *MYH11* c.4673C>T, p.T1158M was found. Two out of three biometric programs such as Pmut and PP2 assigned this DNA substitution as possibly damaging with p-scores of 0.65 and 0.90, respectively, whereby MT called this change as a polymorphism with a p-score of 0.89. The same mutation was found in the father (I:1) of the deceased subject upon mutation segregation analysis. The clinical history of the living father suggested the presence of aortic aneurysm, thus indicating that this PDC mutation may possibly be the disease-causing sequence alteration in PD7 that caused TAAD.
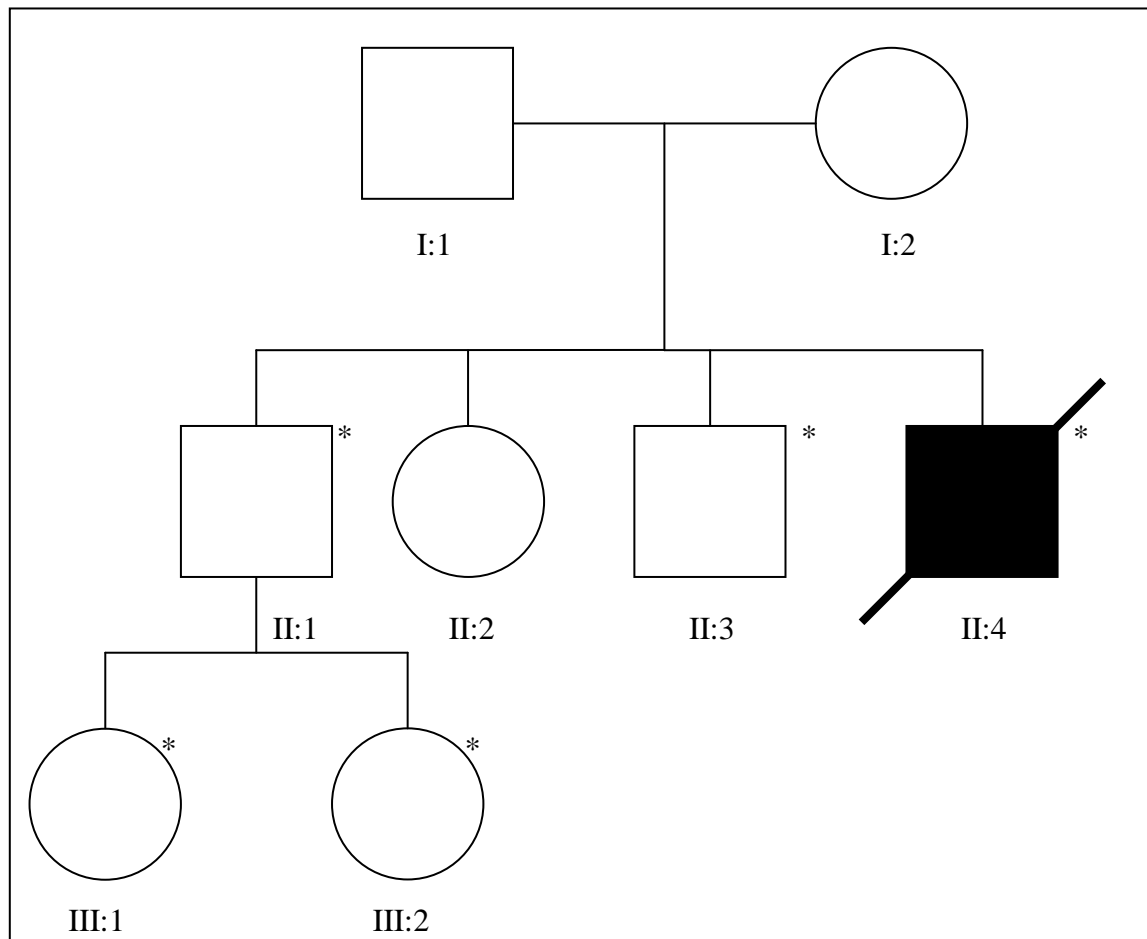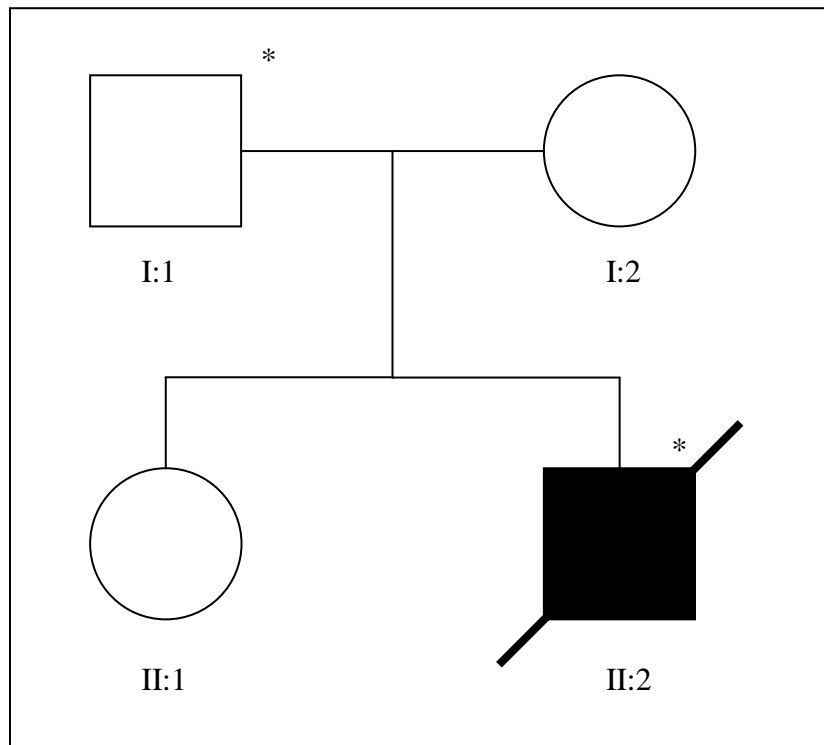
Appendix 16: Segregation analysis of DNA variant *FBN1* c.3509G>A, p.R1170H in family members of PD11. Round symbols indicate females and square symbols indicate males. Black symbols indicate affected individuals. Black symbols with crossed line indicate a deceased subject. A star beside a square or round symbol resembles carriers of this mutation. This DNA variant was firstly described by Hayward *et al.,* 1994 who presented two related subjects with marfanoid phenotype who did not fulfil the clinical criteria for MFS. Only skeletal abnormality more specifically arachnodactyly was observed. Similar observations were described in the study of Robinson *et al.,* The same mutation was found in PD11, but solely presented with TAAD, a major cardiovascular manifestation of MFS. Clinical pre-history included only longstanding hypertension. This sequence alteration was assigned as disease-causing by Pmut and MT with p-scores of 0.63 and 0.56, respectively, whereby PP2 called this change as benign giving a p-score of 0.01. Co-segregation analysis of this PDC mutation and disease was not observed since several family members such as I: 1, II:1, 3, 4 and III:1 and 2 appeared normal. Therefore, the mutation in the gene *FBN1* c.3509G>A, p.R1170H was possibly not the particular sequence alteration that caused TAAD in PD11.
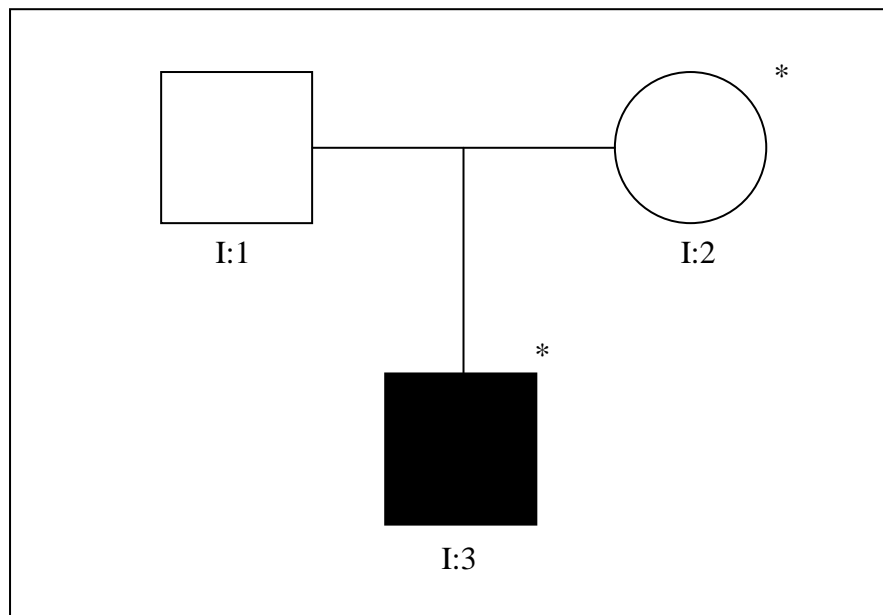
Appendix 17: Segregation analysis of DNA variant *COL3A1* c.217G>C, p.D73H in family members of PD15. Round symbols indicate females and square symbols indicate males. Black symbols indicate affected individuals. Black symbols with crossed line indicate a deceased subject. A star beside a square or round symbol resembles carriers of this mutation. A possibly novel disease-causing mutation in the gene *COL3A1* c.217G>C, p.D73H was detected in PD15, a 42 years old male by whom no previous clinical history was recorded. A phenomenon of mild scoliosis was observed in the medico-legal investigation, a classic skeletal abnormality seen in MFS patients. This individual died of sudden, unexplained TAAD of the ascending aorta. The same genetic change *COL3A1* p.D73H (c.217G>C) was observed in the father (I: 1), but he had no clinical history for thoracic aortic aneurysms. Thus, indicating that this mutation may not be the causative change for TAAD in PD15. Whereby, two biometric mutation analysis programs MT and PP2 called the mutation *COL3A1* p.D73H (c.217G>C) as probably damaging with high scores (p-scores of 0.91 (MT) and 0.98 (PP2)).

Appendix 18: Segregation of DNA variant *NOTCH1* c.2734C>T, p.R912W in family members of RL4. Round symbols indicate females and square symbols indicate males. Blackened symbols indicate affected individuals. Blackened symbols with crossed line indicate a deceased subject. *Resembles carriers of this mutation. A novel PDC mutation in the gene *NOTCH1* c.2734C>T, p.R912W has been found in the living Proband RL4. This individual was suspected for MFS, because of his classic skeletal abnormality of MFS including dolichostenomelia, mild scoliosis and his body height (212cm). Clinical records indicated the occurrence of spontaneous pneumothorax twice. The routine genetic testing was negative for mutations in the genes *FBN1*, *TGFBR1* and *TGFBR2* using the conventional Sanger sequencing. Upon subsequent mutation analysis of additional TAAD associated genes, a PDC mutation in the gene *NOTCH1* c.2734C>T, p.R912W has been found using the *MFSTAAD* resequencing protocol. All three biometric programs showed a severity score close to 1 including Pmut (p-score of 0.90), MT (p-score of 0.70) and PP2 (p-score of 0.85). Same mutation was detected in the mother (I:2) of RL4, by whom no clinical signs were described except for longstanding hypertension (I:2). Whereby, the father (I:1) of RL4 who had multiple close relatives with skeletal abnormality for classic MFS was rather negative for mutations in all nine candidate genes of MFS and FTAAD.
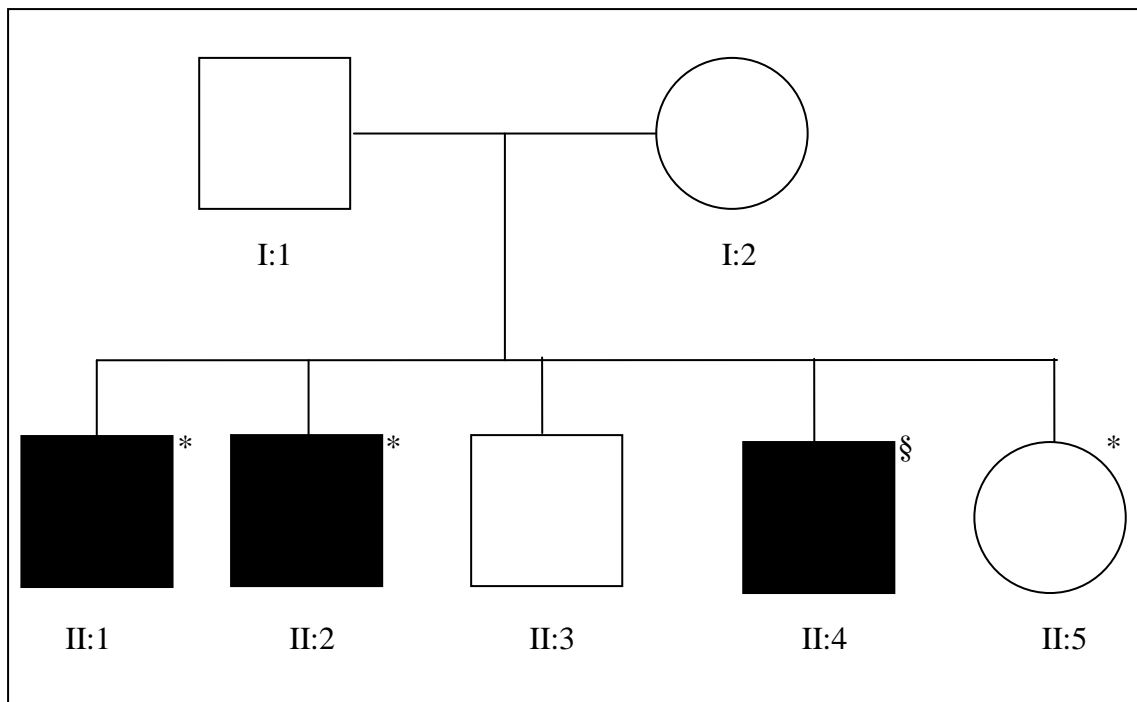
Appendix 19: Segregation analysis of DNA variant *MYH11* c.5676G>C, p.E1892D in family members of RL6. Round symbols indicate females and square symbols indicate males. Blackened symbols indicate affected individuals. *Resembles carriers of this mutation. Marfan syndrome was suspected in II:1, however no mutation was detected in the gene *FBN1*, including *TGFBR1* and *TGFBR2* genes using conventional Sanger sequencing. Subsequent mutation analysis of eight TAAD candidate genes, the PDC mutation in the gene *MYH11* c.5676G>C, p.E1892D was found in RL6. Two biometric mutation analysis programs MT and PP2 called the mutation *MYH11* c.5676G>C, p.E1892D as probably damaging with convincing severity scores (p-scores of 1.00 (MT) and 0.77 (PP2)). Similarly, II:2 and II:4 were also highly suspected for MFS with TAAD. Both of these individuals presented skeletal abnormalities and cardiovascular manifestations such as dilatation of the aortic root and aortic valve insufficiency. However, the dilatation remained within the normal diameter of 4.7cm. Furthermore, individuals II:3 and II:5, had prolonged hypertension, by which II:5 carried the PDC mutation, by which no clinical phenotypes for MFS and/or TAAD were described. These results indicate that this particular PDC mutation is possibly not the only DNA variant that has caused TAAD in RL6.
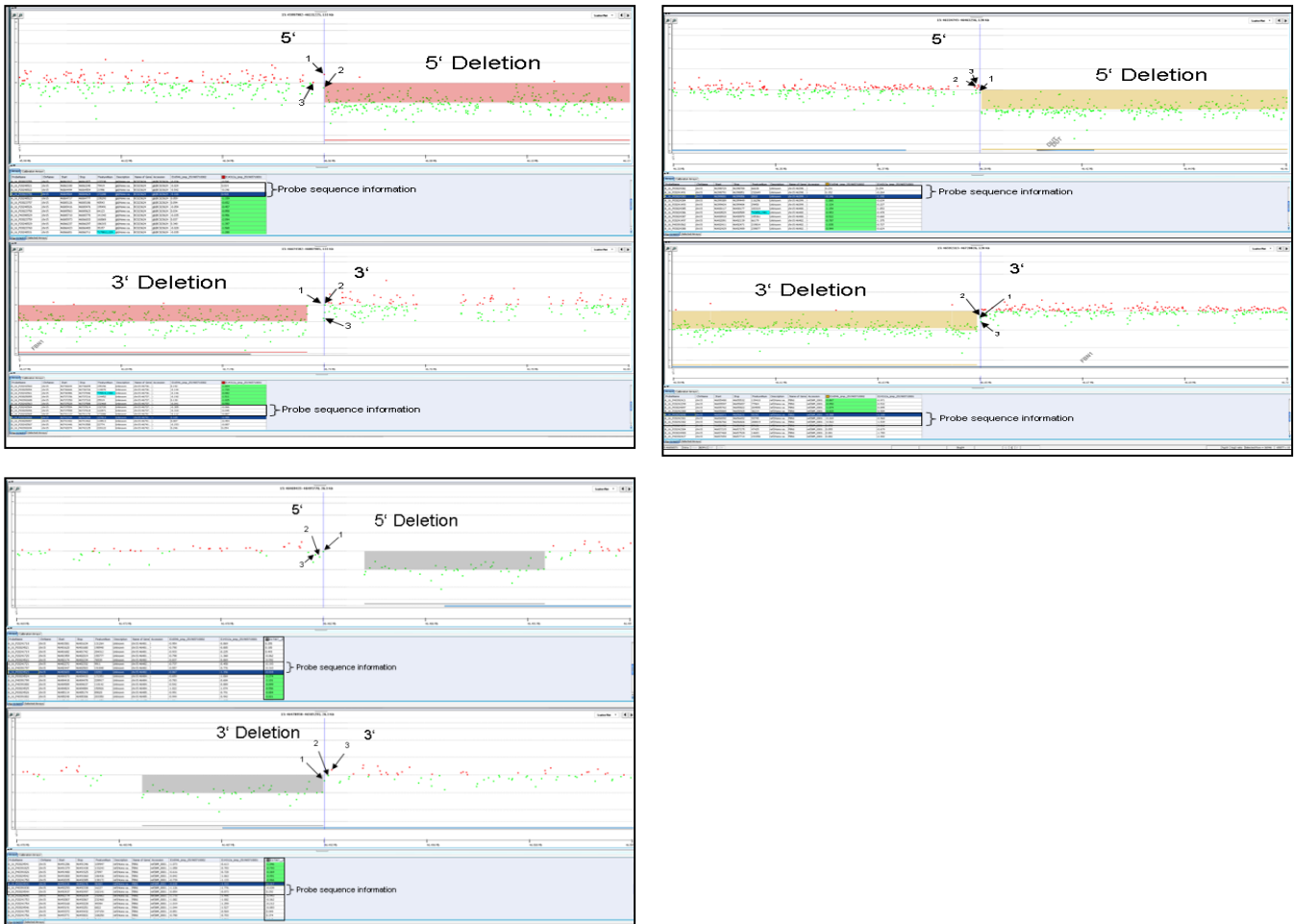
Appendix 20: Deletion breakpoint characterization by Array CGH. (Top left) Breakpoint characterization of deletion Exons 1-65 of the *FBN1* Gene, and genes *DUT*, *SLC12A1*, *CTXN2*, *MYE2* and *SLC24A5*. (Top right) Breakpoint characterization of Exons 6-65 of the *FBN1* gene and *DUT* gene. (bottom left) Breakpoint characterization of deletion Exons 64-65 of the *FBN1* gene. The final data of aCGH was then used as a reference point to derive genomic sequence of three of 60-mer oligonucleotide probes from the UCSC genome browser. Two of which encompassing the deleted region in the 3' and 5' direction and one probe positioned on the suspected breaking site of the unique deletion by aCGH. The chromosomal location of each of these probes has been used to design primer pairs for PCR amplification and conventional Sanger sequencing reaction which allowed determining the exact breakpoints.

Appendix 21: Probe information of deletion Exons 1-65 of the gene *FBN1*, genes *DUT*, *SLC12A1*,*CTXN2*, *MYE2* and *SLC24A5*

Probe	Chromosomal position (2008hg16/2009hg18)	Sequence	Direction
-1	46,064,717-46,064,777 48,277,425-48,277,484	AGTTATTCTATCACTGTGTGCCCAG GAACCAGAACAGTGCCTGGTATGT GGCAAAGGGTCA	5'
+1	46,064,564-46,064,624 48,277,272-48,277,332	TCCATGAGGCTTATGGACATGATA AACACTGATAATTTGCATTGAATG CCATTGTGGACAG	5'
+2	46,064,494-46,064,554 48,277,202-48,277,262	AACATGAGGCAGAATCTTAGCACA TGCTCTAGCCAGCTGCTTTCAGCTC TTACCCACCTCT	5'
-1	46,737,528-46,737,588 49,950,236-48,950,284	CCCAATTCCATATTGCCACTGCAA ATCTCTGTATTTAATACGCTGCTTT	
+1	46,741,244-46,741,294 48,953,952-48,954,002	CTGAGAATTTCAAGAATTGTTTAG TCTGCTGCTTTTTGCTGTTTCTTTCC A	3'
+2	46,741,402-46,741,462 48,954,110-48,954,170	CTCAATTTGAGCCTCCTTGGCCTCC ACAAACTCTAATCTGTATCTTTTCA AATCACAAATA	3'

Appendix 22: Probe information of deletion Exons 6-65 of the gene *FBN1* and *DUT* gene

Probe	Chromosomal position (2008hg16/2009hg18)	Sequence	Direction
-1	46,399,389-46,399,449 48,612,097-48,612,157	AAAGGGGTAAAATTACCCAAATCA CCAATAATTCATCTCAATATCTTCT TCCACCTATTCT	5'
+1	46,399,424-46,399,484 48,612,132-48,612,192	TCTCAATATCTTCTTCCACCTATTC TACCCTATTTCCATATCAAATTGAC TTACTGAGCCA	5'
+2	46,400,117-46,400,176 48,612,825-48,612,884	GCTTCTTAGTCTCCACGTCATCTTA GAAAATCTCATTCCACTAAACTCTT GTCAAATATT	5'

-1	46,655,865-46,655,925 48,868,573-48,868,633	AAATGTTTTTTTCCCCCTCTACTCT GATCTCCCTTTGTGCACATGTCTAA TATAGCATTAT	3'
+1	46,656,571-46,656,631 48,869,279-48,869,339	ATGCCCAACATCAATTGGACTATA AATCTGTCATATACTACTACTCGTT TAGGTCTCTCCA	3'
+2	46,656,592-46,656,652 48,869,300-48,869,360	ATAAATCTGTCATATACTACTACTC GTTTAGGTCTCTCCAAGTTATAACC CATGTGGTCCA	3'

Appendix 23: Probe information of Exons 64-65 deletion of the *FBN1* gene

Probe	Chromosomal position	Sequence	Direction
-1	46,484,373-46,484,433	TTGGATTTCAGAGTAAGTTTCATTT AAATATAGAAATTTAACTTTAAAA ATGAACTCACCA	5'
+1	46,482,603-46,482,663 48,695,311-46,695,371	AATTAAATGGTGGATTTCCCCAAG AAAACACCCTCATCTGTGTTATCTA AAGATTTAGAAA	5'
+2	46,482,447-46,482,503 48,695,155-49,695,211	CCTCACTGCTGCTTAATTCTTGTCT ACTGATGACATGCCGCAAAACTCC AGTAAAAA	5'
-1	46,492,035-46,492,085 48,704,743-48,704,743	GGAGAAACTAACTTCTGACCCACC TCGATATTGGAGGCATCAGTTTCG TTT	3'
+1	46,492,126-46,492,176 48,704,834-46,704,884	TCTTACACTCGTAACAAGCCTCTG GGGAGAGTGAATTGTCATCCATTT CAC	3'
+2	46,492,293-46,492,338 48,705,001-46,705,46	CAAGAGTTCTGGTGAAGCCTGTTC CTTGCAGTTGTGAGATACAGCC	3'

Appendix 24: Primer pairs used for deletion breakpoint characterization				
Deletion	**Primer Name**	**Forward Sequence 5'-3'**	**Reverse Sequence 5'-3'**	**Product size (bp)**
Deletion 1	MFS_De1_1	ATGGTCATTTGGGCCAATTCCAT TTTT	TTGTCCTTGGAGATTTCTGCTGT ATCC	4178
	MFS_Del_2	GCTAGGTTACAGTTCATCCACAA GGACTCA	CCTCCTCCTCTAGCCCACAAAG ACAGA	4935
	MFS_Del_3	GTAAGTCCATCCCTGGGGACACT CAGA	CATCTATCTCTCCCTCCCTCCCA CCTT	456
Deletion 2	MFS_Del_4	TACTGCGCTTTGGCAATCATTTG TCAT	CAGAGACCCCTCCTCCAAGATC CCTTA	959
	MFS_Del_5	TAAAGGTTGTTTCACCAGGGCAG AATG	AAATCAATCATGTGGTGCCAGC TGAGG	2695
Deletion 3	DEL.65-1	AAAACTTCTAGGGAGGCATATGA AAGG	TTTCAGTTATCAAAGCCAAGTT ACGGA	3437

7.   *References*

Ades LC, Holman KJ Brett MS, Edwards MJ, Bennets B. 2004. Ectopia lentis phenotypes and the FBN1 gene. *Am J Med Genet* 126: 284-289.

Ades LC, Sullivan K, Bigging A. 2006. FBN1, TGFBR1 and the Marfan-craniosynostosis/mental retardation disorders revisited. *Am J Med Genet A* 140:1047-1058.

Aldred MA. 2006. BMPR2 gene rearrangements account for a significant proportion of mutations in familial and idiopathic pulmonary arterial hypertension. *Hum Mutat* 2:212-213.

Ammash NM, Sundt TM, Connolly HM. 2008. Marfan syndrome- diagnosis and management. *Curr Probl in Cardiol* 33:7-39.

Arbustini E, Grasso, M, Ansaldi S, Malattia C, Pilotto A, Porcu E, et al. 2005. Identification of sixty-two novel and twelve known FBN1 mutations in eighty-one unrelated probands with Marfan syndrome and other fibrillinopathies. *Hum Mutat* 26:494.

Aretz S, Stienen D, Uhlhaas S, Stollte M, Entius MM, Loff S, et al. 2007. High proportion of large genomic deletions and a genotype phenotype update in 80 unrelated families with juvenile polyposis syndrome. *J Med Genet* 44:702-709.

Avidan N, Tran-Fadulu V, Chen J, Yuan J, Braverman A, Yu R, Shete S, Milewicz DM. Mapping a third locus for famililal TAAD (TAAD3) using samples from a single family with multiple affected indiviuals and determining the contribution of this locus to familial disease. *Am Soc Hum Genet Annu Mtg abstract* 1515.

Bartlett SJ, Stirling D. 2003. "A short History of the Polymerase Chain Reaction". *PCR Protocols* 226:3-6.

Beetz C, Nygren AO, Schickel J, Auer-Grumbach M, Bürk K, et al. 2006. High frequency of partial SPAST deletions in autosomal dominant hereditary spastic paraplegia. *Neurol* 67:1926-1930.

Biddinger A, Rocklin M, Coselli J, Milewicz DM. 1997. Familial thoracic aortic dilatations and dissections: a case control study. *J Vasc Surg 25*:506-511.

Biggin A, Holman K, Brett M, Bennetts B, Ades L. 2004. Detection of thirty novel FBN1 mutations in patients with Marfan syndrome or a related fibrillinopathy. *Hum Mut* 23:99

Blyth M, Foulds N, Turner C, Bunyan D. 2008. Severe Marfan syndrome due to FBN1 Exon deletions. 2008. *Am J Med Genet* 146.1320-1324.

Bode-Jaenisch S, Schmidt A, Guenther D, Stuhrmann M, Fieguth A. 2012. Aortic dissecting aneurysms-histopathologican findings. *Forensic Sci Int* 214,.13-7.

Boileau C, Jondeau G, Babron MC, Coulon M, Alexander JA, Sakai L, et al. 1993. Autosomal dominant Marfan-like connective tissue disorder with aortic dilatation and skeletal anomalies not linked to the fibrillin genes. *Am J Hum Genet* 53:46-54.

Boileau C, Jondeau G, Mizuguchi T, Matsumoto N. 2005. Molecular genetics of Marfan syndrome. *Curr Opin Cardiol* 20:194-200.

Booij JC, Bakker A, Kulumbetova J, Moutaoukil Y, Smeets B, Verheij J, et al. 2011. Simultaneous mutation detection in 90 retinal disease genes in multiple patients using a custom-designed 300-kb retinal resequencing chip. *Ophthalmol* 118:160-167.

Bowne SJ, Sullivan LS, Koboldt DC. 2011. Identification of disease-causing mutations in autosomal dominant retinitis pigmentosa (adRP) using next generation DNA sequencing. *Invest Ophthalmol Vis Sci* 52:1135-1145.

Chaudhri SS. 2007. Fibrillin-1 regulates the bioavailability of TGFbeta1. *J Cell Biol* 176:355-367.

Chen L, Wang X, Canter SA, Shen YH, Bartsch HR, Thompson RW, et al. 2006. A single nucleotide polymorphism in the matrix metalloproteinases 9 gene (-8202 A/G) is associated with thoracic aortic aneurysms and thoracic aortic dissection. *J Thorac Cardiovasc Surg* 131:1045-1052.

Chomoczynski P, Sacchi N. 1987. Single-step method of RNA isolation by acid guanidinium thiocyanate-phenol-chloroform extraction. *Analytic Biochem* 162:156-159.

Coady MA, Davies RR, Roberts M, Goldstein LJ, Rogalski MJ, Rizzo JA, et al. 1999. Familial patterns of thoracic aortic aneurysms. *Arch Surg* 134:361-367.

Coady MA, Rizzo JA, Goldstein LJ, Elefteriadesq JA. 1999. Natural history, pathogenesis, and etiology of thoracic aortic aneurysms and dissections. *Cardiol Clin* 17:615-635.

Coady MA, Rizzo JA, Hammond GL, Mandapati D, Darr U, Kopf GS, et al. 1997. What is the appropriate size criterion for resection of thoracic aortic aneurysms. *J Thorac Cardiovasc Surg* 113:476-491.

Cohen MM. 2003. TGF beta/Smad signaling system and its pathological correlates. *Am J Med Genet A* 116:1-10.

Collod G, Babron MC, Jondeau G, Coulon M, Weissenbach J, Dubourg O, et al. 1994. A second locus for Marfan syndrome maps to chromosome 3p24.2-p25. *Nat Genet* 8:264-268.

Collod-Beroud G, Beroud C, Ades L, Black C, Boxer M, Brock DJ. 1998. Marfan database (third edition): new mutations and new mutations for the software. *Nuc Acids* 26:229-232.

Collod-Beroud G, Le Bourdelles S, Ades L, Ala-Kokko L, Booms P, Boxer M, et al. 2003. Update of the UMD-FBN1 mutation database and creation of an FBN1 polymorphism database. *Hum Mutat* 22:199-208.

Comeglio P, Evans AL, Brice G, Cooling RJ, Child AH. 2002. Identification of FBN1 gene mutations in patients with ectopia lentis and marfanoid habitus. *Br J Ophthalmol* 86:1359-1362.

Cutler DJ, Zwick ME, Carrasquilo MM, Yohn CT, Tobin KP, Kashuk C, et al. 2001. High-throughput variation detection and genotyping using microarrays. *Genom Res* 11:1913-1925.

Daily PO, Trueblood HW, Stinson EB, Wuerflein RD, Shumway NE. 1970. Management of acute aortic dissections. *Ann Thorac Surg* 10:237-247.

De Leeneer K, De Schrijver J, Clement L, Baetens M. 2011. Practical tools to implement massive parallel pyrsequencing of PCR products in next generation molecular diagnostics. *PLoS ONE* 6:1-7.

De Paepe A, Devereux RB, Dietz HC, Hennekam RC, Pyeritz RE. 1996. Revised diagnostic criteria for the Marfan syndrome. *Am J Med Genet* 62:417-426.

Dean JC. 2007. Marfan syndrome: clinical diagnosis and management. *Eur J Hum Genet,* 15:724-733.

DeBakey ME, Henley WS, Cooley DA, Morris GC, Crawford ES, Beall AC. 1965. Surgical treatment of dissecting aneurysm of the aorta. *J Thorac Cardiovasc Surg* 49:130-149.

References

Denning L, Anderson JA, Davis R, Gregg JP, Kuzdenyi J, Maselli RA. 2007. High throughput genetic analysis of congenital myastenic syndromes using resequencing microarrays. *PLoS ONE* 2:918.

Derynck R, Akhurst RJ, Balmain A. 2001. TGF-beta signaling in tumor suppression and cancer progression. *Nat Genet* 29:117-129.

Desai AN, Jere A. 2012. Next-generation sequencing:ready for the clinics? *Clin Genet* 81:503-510.

Dietz HC, Cutting GR, Pyeritz RE, Maslen CL, Sakai LY. 1991. Marfan syndrome caused by a recurrent de novo missense mutation in the fibrillin-1 gene. *Nat* 352:337-339.

Downing AK, Knott V, Werner JM, Cardy CM, Campbell ID, Handford PA. 1996. Solution structure of a pair of calcium-binding epidermal growth factor-like domains:implications for the Marfan syndrome and other genetic disorders. *Cell* 85:597-605.

Eder J, Laccone F, Rohrbach M, Giunta C, Aumayr K, Reichel C, et al. 2013. A new COL3A1 mutation in Ehlers-Danlos syndrome type IV. *Exp Dermatol* 3:231-4.

El-Hamamsy I, Yacoub MH. 2009. A measured approach to managing the aortic root in patients with bicuspid aortic valve disease. *Curr Cardiol Rep* 11:94-100.

El-Hamamsy I, Yacoub MH. 2009. Cellular and Molecular mechanisms of thoracic aortic aneurysms. *Nat Rev Cardiol* 6:771-786.

Ellison JW, Yagubyan M, Majumdar R, Sarkar G, Bolander ME. 2007. Evidence of genetic locus heterogeneity for familial bicuspid aortic valve. *J Surg Res* 142:23-31.

Faivre L, Collod-Beroud G, Loeys BL. 2007. Effect of mutation type and location on clinical outcome in 1013 probands with Marfan syndrome or related phenotypes and FBN1 mutations: an international study. *Am J Hum Genet* 81:454-466.

Faivre L, Gorlin RJ, Writz MK, Godfrey M, Dagoneau N, Samples JR. 2003. In frame fibrillin-1 gene deletion in autosomal dominant Weil-Marschesani syndrome. *J Med Genet* 40:34-36.

Fokstuen S, Lyle R, Munoz A, Gehrig C, Lerch R, Perrot A, et al. 2008. A DNA resequencing array for pathogenic mutations detection in hypertrophic cardiomyopathy. *Hum Mutat* 29:879-885.

Francke U, Berg MA, Tynan K, Brenn T, Liu W, Aoyama T, et al. 1995. A Gly1127Ser mutation in an EGF-like domain of the fibrillin-1 gene is a risk factor for ascending aortic aneurysm and dissection. *Am J Hum Genet* 40:34-36.

Furtado LV, Wooderchak-Donahue W, Rope AF, Yetman AT, Lewis T, Plant P, et al. 2011. Characterization of large genomic deletions in the FBN1 gene using multiplex ligation-dependent probe amplification. *BMC Med Genet* 12:1-7.

Galis ZS, Khatri JJ. 2002. Matrix metalloproteinases in vascular remodelling and atherogenesis: the good, the bad, and the ugly. *Circ Res* 90:251-262.

Garg V, Muth AN, Ransom JF. 2005. Mutations in NOTCH1 cause aortic valve disease. *Nat* 437:270-274.

Gelb BD. 2006. Marfan's syndrome and related disorders: more tight connected than we thought. *N Engl J Med* 355:841-844.

Guo D, Hasham S, Kuang S, Vaugham CJ, Boerwinkel E, Chen H, et al. 2001. Familial thoracic aortic aneurysms and dissections genetic heterogeneity with a major locus mapping to 5q13-14. *Circulat* 103:2461-2468.

Guo D, Pannu H, Tran-Fadulu V, Papke CL, Yu RK, Avidan N, et al. 2007. Mutations in smooth muscle alpha-actin (ACTA2) lead to thoracic aortic aneurysms and dissections. *Nat Genet* .

Hacia JG. 1999. Resequencing and mutational analysis using oligonucleotide microarrays. *Nat Genet* 21 (1 Suppl):42-47.

Hasham SN, Willing D, Guo D, Muilenburg A, He R, Tran VT, et al. 2003. Mapping a locus for familial thoracic aortic aneurysms and dissections (TAAD2) to 3p24-25. *Circulat* 107:3184-3190.

Hasham S, Lewin MR, Tran VT, Pannu H, Muilenburg A, Willing M, et al. 2004. Nonsyndromic genetic predisposition to aortic dissection:A newly recognized, diagnosable, and preventable occurrence in families. *Ann Emerg Med* 43:79-82.

Hasleton PS, Leonard JC. 1979. Dissecting aortic aneurysms: a clinicopathological study II. Histopathological study of the aorta. *Q J Med* 48:63-67.

Hilhorst-Hofstee Y, Hamel BJ, Verheij JB, Rijlaarsdam ME, Mancini GM. 2011. The clinical spectrum of complete FBN1 allele deletions. *Eur J Hum Genet* 19:247-252.

Hirani R, Koszyca B, Byard RW. 2008. Marfan syndrome and sudden death within a family-aetiologic, molecular and diagnostic issues at autopsy. *J Forensc Leg Med* 15:205-209.

Hoffjan S, Waldmueller S, Blankenfeldt W, Kötting J, Gehle P, Binner P, et al. 2011. Three novel mutations in the ACTA2 gene in German patients with thoracic aortic aneurysms and dissections. *Eur J Hum Genet* 19:520-524.

Huntington K, Hunter AG, Chan KL. 1997. A prospective study to assess the frequency of familial clustering of conmgenital bicuspid aortic valve. *J Am Coll Cardiol* 30: 1809-1812.

Hutchinson S, Furger A, Halliday D, et al. 2003. Allelic variation in normal human FBN1 expression in a family with Marfan syndrome: a potential modifier of phenotype? *Hum Mol Genet* 12:2269-2276.

Ikonomidis JS, Jones JA, Barbour JR, Stroud RE, Clark LL, et al. 2006. Expression of matrix metalloproteinases and endogeneous inhibitors within ascending aortic aneurysms of patients with Marfan syndrome. *Circulat* 114 (1 Suppl):365-370.

Ince H, Nienbar CA. 2007. Etiology, pathogenesis and management of thoracic aortic aneurysm. *Nat Clin Pract* 4:418-427.

Iserin L, Jondeau G, Sidi D, Kachaner J. 1997. Marfan syndrome. Cardiovascular manifesstations and therapeutic indications. *Arch Mal Coeur Vaiss* 90:1701-5.

Isselbacher, E. M. 2004. Diseases of the aorta. In E. In Braunwald, D. P. Zipes, P. Libby, & R. O. Bonow, *Braunwald's Heart Disease: A textbook of Cardiovascular Medicine.* (7th Ausg.). WB Saunders, Philadelphia.

Isselbacher EM. 2005. Thoracic and abdominal aortic aneurysms. *Circulat* 111:816-828.

Johnston KW, Rutherford RB, Tilson MD, Shah DM, Hollier L, Stanley JC. 1991. Suggested standards for reporting on arterial aneurysms: Subcommittee on reporting standards for arterial aneurysms, Ad Hoc Committee on reporting standards, society for vascular surgery and North American Chapter, Internat. societ. for cardiovasc. surg. *J Vasc Surg* 13:452-458.

Judge DP, Dietz HC. 2005. Marfan's syndrome. *Lancet* 366:1965-1976.

References

Kainulainen K, Karttunen L, Puhakka L, Sakai L, Peltonen L. 1994. Mutations in the fibrillin gene responsible for dominant ectopia lentis and neonatal Marfan syndrome. *Nat Genet* 6:64-69.

Kakko S, Räisänen T, Tamminen M, Airaksinen J, Grounstroem K. 2003. Candidate locus analysis of familial ascending aortic aneurysms and dissections confirms the linkage to the chromosome 5q13-14 in Finnish families. *J Thorac Cardiovasc Surg* 126:106-113.

Kanno, J, Hutchin T, Kamada F, Narisawa A, Aoki Y, Matsubara Y, Kure S. 2007. Genomic deletion with GLDC is a major cause of non-ketotic hyperglycinaemia. *J Med Genet* 44:1-9.

Karnik SK. 2003. A critical role for elastin signaling in vascular morphogenesis and disease. *Develop* 130:411-423.

Kathiravel U, Keyser B, Hoffjan B, Judith K, Mueller M, Sugirthan S, et al. 2013. High-density oligonucleotide-based resequencing assay for mutations causing syndromic and non-syndromic forms of thoracic aortic anerurysms and dissections. *Mol Cell Probes* 27:103-108.

Katzke S, Booms P, Tiecke F, Palz M, Pletschacher A, Turkmen S, et al. 2002. TGGE screening of the entire FBN1 coding sequence in 126 individuals with Marfan syndrome and related fibrillinopathies. *Hum Mutat* 20:197-208.

Keane MG, Pyeritz RE. 2008. Medical management of Marfan syndrome. *Circulat* 117:2802-2813.

Khau-Van-Kien P, Mathieu F, Zhu , Lalande A, Betard C, Lathrop M, Brunotte F, Wolf JE, Jeunemaitre X. 2005. Mapping of famial thoracic aortic aneurysm/dissection with patent ductus arteriosus to 16p12.12-13.13. *Circulat* 112:200-206.

Kielty CM, Sherrat MJ, Shuttleworth CA. 2002. Elastic fibres. *J Cell Sci* 115:2817-2828.

Klintschar M, Bilkenroth U, Arslan-Kirchner M, Schmidtke J., Stiller D. 2009. Marfan syndrome: clinical consequences resulting from a medico-legal autopsy of a case of sudden death due to aortic rupture. *Int J Legal Med* 123:55-58.

Kluwe L, Nygren AO, Errani A, Heinrich B, Matthies C, Tatagiba M, Mautner V. 2005. Screening for large mutations of the NF2 gene. *Genes Chromosomes Canc* 42:384-391.

Knox JB, Sukhova GK, Whittemore AD. 1997. Evidence for altered balance between matrix metalloproteinases and their inhibitors in human aortic disease. *Circulat* 95:205-212.

Kothiyal P, Cox S, Ebert J, Husami A, Kenna MA, Greinwald JH, et al. 2010. High-throughput detection of mutations responsible for childhood hearing loss using resequencing microarrays. *BMC Biotechnol* 10:1-11.

Larson EW, Edwards WD. 1984. Risk fators for aortic dissections: A necropsy study of 161 cases. *Am J Cardiol* 53:849-855.

Lederle FA, Wilson SE. Johnson GR, Reinke DB, Littooy FN, Acher CW, et al. 2002. Immediate repair compared with surveillance of small abdominal aortic aneurysms. *New Engl J Med* 346:1437-1444.

Lee B, Godfrey M, Vitale E, Hori H, Mattei MG, Sarfarazi M, et al. 1991. Linkage of Marfan syndrome and a phenotypically related disorder to two different fibrillin genes. *Nat* 352:330-334.

Liu C, Bruce J, Anil G, Wang N, Miethke A, Mourya R. 2007. Novel resequencing chip customized to diagnose mutations in patients with inherited syndromes of intrahepatic cholestasis. *Gastroenterol* 132:119-126.

LiuW, Schrijver I, Brenn T, Furthmayr H, Francke U. 2001. Multi-exon deletion of the FBN1 gene in Marfan syndrome. *BMC Med Genet* 2:11-19.

Loeys BL, Chen J, Neptune ER, Judge DP, Podowski M, Holm T, et al. 2005. A syndrome of altered cardiovascular, craniofacial, neurocognitive and skeletal development caused by mutations in TGFBR1 and TGFBR2. *Nat Genet* 37:275-281.

Loeys BL, De Backer J, Van Acker P, Wettinck, K, Pals G, et al. 2004. Comprehensive molecular screening of the FBN1 gene favors locus homogeneity of classical Marfan syndrome. *Hum Mutat* 24:140-146.

Loeys BL, Dietz HC, Braverman AC, Callewaert BL, De Backer J, Devereux RB, et al. 2010. The revised Ghent nosology criteria for the Marfan syndrome. *J Med Genet 47*:476-485.

Loeys BL, Schwarze U, Holm T, Callewaert BL, Thomas GH, Pannu H. 2006. Aneurysm syndromes caused by mutations in the TGF-beta receptor. *J Med Genet* 355:788-98.

Loeys B, De Backer J, Van Acker P, Wettinck K, Pals G, et al. 2004. Comprehensive molecular screening of the FBN1 gene favors locus homogeneity of classical Marfan syndrome. *Hum Mutat* 24:140-146.

Loeys B, Nuytinck L, Delvaux I, De Bie S, De Paepe A. 2001. Genotype and phenotype analysis of 171 patients referred for molecular study of the fibrillin-1 gene FBN1 because of suspected Marfan syndrome. *Arch Intern Med* 161:2447-2454.

Marfan AB. 1896. Un cas de deformation congenitale des quatre membres plus prononcee aux extremites characterisee par l'allongment des os avec un certain degre d'amincissement. *Bull Mem Soc Med Hop Paris* 13:220-1.

Massague J, Blain SW, Lo RS. 2000. TGF-beta signaling in growth control, cancer and heritable disorders. *Cell* 103:295-309.

Matyas G, Alonso S, Patrignani A, Marti M, Arnold E, Magyar I, et al. 2007. Large genomic fibrillin-1 (FBN1) gene deletions provide evidence for true haploinsufficiency in Marfan syndrome. *Hum Genet* 1:23-32.

Meszaros I, Morocz J, Szlavi J, Schmidt J, Tornoci L, Nagy L, et al. 2000. Epidemiology and clinocopathology of aortic dissection. *Chest* 117:1271-1278.

Michils G, Teijpar S, Thoelen R, van Cutsem, Vermeesch JR, et al. 2005. Large deletions of the APC gene in 15% of mutation-negative patients with classical polyposis (FAP): a Belgian study. *Hum Mutat* 25:125-134.

Milewicz DM, Regalado E. 2003. Thoracic aortic aneurysms and aortic dissections. GeneReviews (http://www.ncbi.nlm.nih.gov/books/NBK1120/)

Milewicz DM, Chen H, Park ES, Petty EM, Zaghi H, Shashidhar G. 1998. Reduced penetrance and variable expressivity of familial thoracic aortic aneurysms/dissections. *Am J Cardiol* 82:474-9.

Milewicz DM, Guo DC, Tran-Fadulu V. 2008. Genetic basis of thoracic aortic aneurysms and dissections: focus on smooth muscle contractile dysfunction. *Ann Rev Genom Hum Genet* 9:283-302.

Milewicz DM, Kwartler CS, Papke CL, Regalado ES, Cao J, Reid AJ. 2010. Genetic variants promoting smooth muscle cell proliferation can result in diffuse and diverse vascular disease: evidence for a hyperplastic vasculomyopathy. *Genet Med* 12:196-203.

Milewicz DM, Michael K, Fisher N, Coselli JS, Markello T, Biddinger A. 1996. Fibrillin-1 (FBN1) mutations in patients with thoracic aortic aneruysms. *Circulat* 94:2708-2711.

Mizuguchi T, Collod-Beroud G, Akiyama T, Abifadel M, Harada N, Morisaki T, et al. 2004. Heterozygous TGFBR2 mutations in Marfan syndrome. *Nat Genet* 36:855-860.

Morse PR, Rockenmacher S, Pyeritz ER. 1990. Diagnosis and management of infantile marfan syndrome. *Pediat* 86:888-895.

MRC- Holland - SALSA MLPA kit P065 Marfan Syndrome-1. Von http://www.mlpa.com/WebForms/WebFormProductDetails.aspx?Tag=tz2fAPIAupLo0TRBqt iGHA%7C%7C&ProductOID=dLvyQjydEjk%7C.

MRC- Holland - SALSA MLPA kit P148 TGFBR. Von http://www.mlpa.com/WebForms/WebFormProductDetails.aspx?Tag=tz2fAPIAupKyMjaDF %5CE%5Ct9bmuxqlhe/Lgqfk8Hkjuss%7C&ProductOID=DTHYpQR%5CkEU%7C.

MRC-Holland- SALSA MLPA kit P066 Marfan Syndrome-2. Von http://www.mlpa.com/WebForms/WebFormProductDetails.aspx?Tag=tz2fAPIAupKyMjaDF %5CE%5Ct9bmuxqlhe/Lgqfk8Hkjuss%7C&ProductOID=9qMCkc7Xu6c%7C.

Nicod P, Bloor C, Godfrey M, Hollister D, Pyeritz RE, Dittrich H. 1989. Familial aortic dissecting aneurysm. *J Am Coll Caridiol* 13:811-19.

Ogawa N, Imai Y, Takahashi Y, Nawata K, Hara K, Nishimura H. 2011. Evaluation of japanese patients with the Marfan syndrome using high-throughput microarray-based mutational analysis of fibrillin-1 gene. *Am J Cardiol* 108:1801-1807.

Olsson C, Thelin S, Stahle E, Ekbom A, Granath F. 2006. Thoracic aortic aneurysm and dissection. Increased prevalence and improved reported in a nationwide population-based study of more than 14 000 cases from 1987 to 2002. *Circulat* 114:2611-2618.

Pannu H, Fadulu V, Chang , Lafont A, Hasham SN, Sparks E. 2005. Mutations in transforming growth factor-beta receptor type II cause familial thoracic aortic aneurysms and dissections. *Circulat* 112:513-20.

Pannu H, Guo DC, Tran-Fadulu V, Milewicz DM. 2005. Genetic basis of thoracic aortic aneurysms and dissections. *Am J Med Genet* 139:10-16.

Pearson GD. 2008. Report of the National Heart, Lung and Blood Institute and National Marfan Foundation Working Group on Research in Marfan syndrome and related disorders. *Circulat* 118:785-791.

References

Pedak PW, de Sa MP, Nili N, Kazemian P, Butany J, Strauss BH, et al. 2003. Vascular matrix remodelling in patients with bicuspid aortic valve malformations: implications for aortic dilatation. *J Thorac Cardiovasc Surg* 126:797-806.

Ramirez F, Dietz HC. 2007. Fibrillin-rich microfibrils:structural determinants of morphogenetic and homeostatic events. *J Cell Physiol* 213:326-330.

Redeker EJ, de Visser AS, Bergen AA, Mannens MM. 2008. Multiplex ligation dependent probe amplification (MLPA) enhances the molecular diagnosis of aniridia and related disorders. *Mol Vis* 14:836-840.

Regalado ES, Guo D, Villamizar C, Avidan N, Gilchrist D, McGillivray B, et al. 2011. Exome sequencing identifies SMAD3 mutations as a cause of familial thoracic aortic aneurysm and dissection with intracranial and other arterial aneurysms. *Circ Res* 109:680-686

Ripperger T, Tröger HD, Schmidtke J. 2009. The genetic message of a sudden, unexpected death due to thoracic aortic dissection. *Forensic Sci Int* 187:1-5.

Robinson PN, Booms P. 2001. The molecular pathogenesis of the Marfan syndrome. *Cell Mol Life Sci* 58:1698-1707.

Robinson PN, Godfrey M. 2000. The molecular genetics of Marfan syndrome and related microfibrillopathies. *J Med Genet* 37:9-25.

Robinson PN, Arteaga-Solis E, Baldock C, Collod-Beroud G, Booms P, De Paepe A, et al. 2006. The molecular genetics of Marfan syndrome and related disorders. *J Med Genet* 43:769-787.

Rommel K, Karck M, Haverich A, Schmidtke J, Arslan-Kirchner M. 2002. Mutation screening of the fibrillin-1 (FBN1) gene in 76 unrelated patients with Marfan syndrome or Marfanoid features leads to the identification of 11 novel and three previously reported mutations. *Hum Mutat* 20:406-407.

Rommel K, Karck M, Haverich A, von Kodolitsch Y, Rybczynski M, Muller G, et al. 2005. Identification of 29 novel and nine recurrent fibrillin-1 (FBN1) mutations and genotype-phenotype correlations in 76 patients with Marfan syndrome. *Hum Mutat* 26:529-539.

Sachidanandam R, Weissman D, Schmidt SC, Kakol JM, Stein LD. 2001. A map of human genome sequence variation containing 1.42 million single nucleotide polymorphisms. *Nat* 409:928-933.

Schlatmann TJ, Becker AE. 1977. Histologic changes in the normal aging aorta: Implications for dissecting aortic aneurysms. *Am J Cardiol* 39:13-20.

Schrijver I, Liu W, Odom R, Brenn T, Oefner P, et al. 2002. Premature termination mutations in FBN1: distinct effects on differential allelic expressions and on protein and clinical phenotypes. *Am J Hum Genet* 71:223-237.

Singh KK, Schmidtke J, Keyser B, Arslan-Kirchner M. 2012. TGFBR3 variation is not a common cause of Marfan-like syndrome and Loeys-Dietz-like syndrome. *J Neg Res Biomed* 11:1-5.

Song J, Smaoui N, Ayyagari R, Stiles D, Benhamed S, MacDonald IM, et al. 2011. High-throughput retina array for screening 93 genes involved in inherited retinal dystrophy. *Invest Ophthalmol Vis Sci* 52:9053-9060.

Sood S, Eldadah ZA, Krause WL, McIntosh I, Dietz HC. 1996. Mutation in fibrillin-1 and the Marfanoid-craniosynostosis (Shprintzen-Goldberg) syndrome. *Nat Genet* 12:209-211.

Southern E, Mir K, Shchepinov M. 1999. Molecular interactions on microarrays. *Nat Genet* 21:5-9.

Takahashi Y, Seki N, Ishiura H, Mitsui J, Matsukawa T, Kishino A. 2008. Development of a high throughput microarray-based resequencing system for neurological disorders and its application to molecular genetics of amyotrophic lateral sclerosis. *Arch Neurol* 10:1326-1332.

ten Dijke P, Miyazono K, Heldin CH. 1996. Signaling via hetero-oligomeric complexes of type I and type II serine/threonine kinase receptors. *Curr Opin Cell Biol* 8:139-145.

Tiecke F, Katzke S, Booms P, Robinson PN, Neumann L, Godfrey M, et al. 2001. Classic, atypically severe and neonatal Marfan syndrome: Twelve mutations and genotype-phenotype correlations in the FBN1 gene. *Eur J Hum Genet* 9:13-21.

Turaclar N, Vural HC. 2011. Evaluation and optimization of genomic DNA isolation protocols from human solid tissues. *J of App Biol Sc* 5:41-43.

Tynan K, Comeau K, Pearson M, Wilgenbus P, Levitt D, Gasner C, et al. 1993. Mutation screening of complete fibrillin-1 coding sequence: report of five new mutations, including two in 8-cysteine domains. *Hum Mol Genet* 2:1813-1821.

van de Laar IM, Oldenburg RA, Pals G, Roos-Hesselink JW, de Graaf BM, Verhagen JM, et. al.. 2011. Mutations in SMAD3 causes a syndromic form of aortic aneuryms and dissections with early-onset osteoarthritis. *Nat Genet* 43:121-126.

Vaugham CJ, Casey M, He J, Veugelers M, Henderson K, Guo D. 2001. Identification of a chromosome 11q23.2-q24 locus for familial aortic aneurysm disease, a genetically heterogenous disease. *Circulat* 103:2469-75.

Waldmueller S, Mueller M, Rackebrandt K, Binner P, Poths S, Bonin M, et al. 2008. Array-based resequencing assay for mutations causing Hypertrophic Cardiomyopathy. *Clin Chem* 54:682-687.

Wang L, Guo DC, Gong L, Kamm KE, Regalado E, Li L, et al. 2010. Mutations in myosin light chain kinase chause familial aortic dissections. *Am J Hum Genet* 87:701-7.

Wieser R, Wrana JL, Massague J. 1995. GS domain mutations that constitutively activate T-beta R-I, the downstream signaling component in the TGF-beta receptor complex. *EMBO J* 14:2199-2208.

Williams A, Davies S, Stuart AG, Wilson DG, Fraser AG. 2008. Medical treatment of Marfan syndrome: a time for change. *Heart* 94:414-421.

Wilson WR. Matrix metalloproteinase-8 and -9 are increased at the site of abdominal aortic aneurysm rupture. *Circulat* 113:438-445.

Wolinski H, Glagov S. 1967. A lamellar unit of aortic medial structure and function in mammals. *Circulat* 20:99-111.

Wrana JL, Attisano L, Wieser R, Ventura F, Massague J. 1994. Mechanism of activation of the TGF-beta receptor. *Nat* 370:341-347.

Yetman AT, Bornemeier, RA, McCrindle BW. 2003. Long-term outcome in patients with Marfan syndrome: is aortic dissection the only cause of sudden death? *J of Am Coll Cardiol* 41:329-332.

Yuan S, Jing H. 2010. Marfan's syndrome: an overview. *Sao Paulo Med Journal* 128:360-366.

Zhan Y, Kulp D. 2005. Model-P: basecalling method for resequencing microarrays of diplod samples. *Bioinformat* 21:182-189.

Zhu L, Vranckx R, Khau VK. 2006. Mutations in myosin heavy chain 11 cause a syndrome associating thoracic aortic aneurysms/aortic dissections and patent ductus arteriosus. *Nat Genet* 38:343-349.

Zimmermann RS, Cox S, Lakdawaia NK, Cirino A, Mancini-DiNardo D, Clark E. 2010. A novel custom resequencing array for dilated cardiomyopathy. *Genet Med* 12:268-278.

Curriculum vitae

Personal details

Name	Kathiravel Ushanthine
Date of birth- and place	24.08.1982 in Sri-Lanka
Marital status	unmarried

School career

2000-2001	Märkisches Gymnasium, Hamm, Germany A-level's- moved to United Kingdom
1993-2000	Realschule Heessen, Hamm-Heessen, Nordrhein Westfalen, Germany
1989-1993	Stephanus Grundschule, Hamm-Heessen, Nordrhein Westfalen, Germany

Academic career

2008-2012	Leibniz university, Hannover, Germany Ph.D in Human Genetics
2006-2007	University of Nottingham, Nottingham, UK Master of Science (*M.Sc.*) in Molecular Diagnostics
2002-2006	Universität Durham, Stockton-on-Tees, Thornaby, UK Batchelor of Science (*B.Sc.*) in Biomedical Sciences
2001-2002	Uxbridge College, Uxbridge, England GCSE's and AS level, Foundation Programme

Publications

1.   **Kathiravel U**, Keyser B, Hoffjan S, Koetting J, Mueller M, Sivalingam S, Bonin M, Arslna-Kirchner M, von Kodolitsch Y, Binner P, Scheffold T, Stuhrmann M, Waldmueller S. 2013. **High density oligonucleotide-based resequencing assay for syndromic and non-syndromic forms of thoracic aortic aneurysms and dissections.** *Mol Cell Probes* 103-108.

2.   **Kathiravel U**, Bode-Jaenisch S, Guenther D, Schmidt A, Jonigk D, Keyser B, Waldmueller S, Arslan-Kirchner M, Schmidt J, Stuhrmann. **Genetic testing in young adults died of unexplained thoracic aortic aneurysm and dissection.** *Mol Cell Probes* submitted 2013.

Poster presentations

20. GfH Meeting

Aachen, Germany, 01.-03. April 2009

Breakpoint characterization of large deletions in FBN1 in patients with Marfan syndrome.

Kathiravel U, Steinemann D, Föhse L, Stuhrmann M, Schmidtke J, Arslan-Kirchner M, Schlegelberger B, Rhode B.

21. GfH Meeting

Hamburg, Germany, 02.-04. March, 2010

Characterization of a novel deletion in the FBN1 gene in a patient with Marfan syndrome.

Kathiravel U, Keyser B, Steinemann, Rybcynski M, Schlegelberger B, Schmidtke J, von Kodolitsch Y, Stuhrmann M.

ESHG Conference

Nürnberg, Germany, 23.-26. June 2012

Mutational analysis of thoracic aortic aneurysm and dissection (TAAD) using a custom resequencing array.

Kathiravel U, Keyser B, Hoffjan S, Kötting M, Sivalingam S, Bonin M, Arslan-Kirchner M, von Kodolitsch Y, Binner P, Scheffold T, Suhrmann M, Waldmüller S.

Official speech

Niedersächsisches Human Genetic Meeting, Göttingen, Germany, 12. November 2011.

Marfan/TAAD resequencing microarray as a diagnostic tool for patients with familial thoracic aortic aneurysm and/or dissection (FTAAD).